ORGANIC-INORGANIC HYBRIDS: PREPARATION, CHARACTERIZATION AND APPLICATIONS IN ADHESIVES AND COATINGS

Thesis submitted to the

UNIVERSITY OF PUNE

For the degree of

DOCTOR OF PHILOSOPHY

In

CHEMICAL ENGINEERING

By

VIVEK VITTHALRAO KODGIRE

DR. M. V. BADIGER
(Research Guide)

Polymer Science and Engineering Division
National Chemical Laboratory
PUNE-411 008

September, 2012

ॐ

।।श्री शङ्कर।।

या वेदोपनिषस्तवनादिसमयाद् मूलं बिभर्ति स्वकम् ।
या रामायणभारतादिषु हिता प्राज्ञैः समाख्यापिता ।।
या वै व्यष्टिसमष्टिमङ्गलकरी सम्पूर्णताबोधिनी ।
तां वन्दे विनयेन तत्परतया श्री भारतीसंस्कृतिम् ।।

राष्ट्रीय रासायनिक प्रयोगशाला
(वैज्ञानिक तथा औद्योगिक अनुसंधान परिषद)
डॉ. होमी भाभा मार्ग पुणे - 411 008. भारत
NATIONAL CHEMICAL LABORATORY
(Council of Scientific & Industrial Research)
Dr. Homi Bhabha Road, Pune - 411 008. India.

CERTIFICATE OF THE GUIDE

It is certified that the work incorporated in the thesis entitled **"Organic-Inorganic Hybrids: Preparation, Characterization and Applications in Adhesives and Coatings"**, submitted by **Mr. Vivek V. Kodgire** was carried out under my supervision/guidance. Such material as obtained from other sources has been duly acknowledged in the thesis.

September 2012
Pune

Dr. M. V. Badiger
(Research Guide)

Communication Channels
+91-20-2590 2000
+91-20-2590 (DID)
FAX
+91-20-2590 2601(DIR)
+91-20-2590 2660 (COA)
WEBSITE
www.ncl-india.org

DECLARATION

I hereby declare that all the experiments embodied in the thesis entitled **"Organic-Inorganic Hybrids: Preparation, Characterization and Applications in Adhesives and Coatings",** submitted for the degree of Doctor of Philosophy in Chemical Engineering, to the University of Pune has been carried out by me at the Polymer Science and Engineering Division, National Chemical Laboratory, Pune – 411008, India under the supervision of Dr. Manohar V. Badiger. The work is original and has not been submitted in part or fully by me, for any degree or diploma to this or to any other University.

September 2012

Pune

Mr. Vivek V. Kodgire

Senior Research Fellow
Polymer Science and Engineering
Division

National Chemical Laboratory,
Pune - 411008

Acknowledgement

This is an opportunity to express my gratitude for all the people who helped to drive the 0work towards the success.

My sincere thanks to my mentor, Dr. Manohar V. Badiger for his enthusiastic involvement, patient supervision with friendly and sporty spirit. Throughout the process, he has been a great philosopher and a friend. Many times he went out of the way to take care of me. His integrity, humanity, tenderness and foresight have made a deep impression on me. He encouraged me not only to grow as an experimentalist but as an independent researcher. I consider myself fortunate for having a chance of working with a person like him, who is a rare blend of many unique qualities. For everything you have done for me, Dr. Manohar V. Badiger, I will be highly obliged.

I am deeply indebted to my advisors Dr. Kundalik G. Raut and Dr. Prakash P. Wadgaonkar, for their stimulating and untiring suggestions and constant encouragement. I could not have completed this work successfully without this help. The doors were always open to me for discussion. I am really touched upon by their efforts, inputs and humanity. Plain "Thanks" cannot express my gratitude for them. My sincere thanks to Dr. S. Sivaram and Dr. Sourav Pal Directors, N.C.L., Dr. B.D. Kulkarni and Dr. Vivek V. Ranade Assistant Director and Dr. M. G. Kulkarni, Head, Polymer Science and Engineering Division, for allowing me to work in this prestigious Institute and for providing access to the facilities in the division.

I owe special thanks to Mrs. D.A. Dhoble, Dr. J.P. Jog and Dr. C. Ramesh for allowing me to use the instruments without questioning. I am very much grateful to Dr. A.K. Lele, Dr. K. Guruswamy, for teaching me during course work. I am very much thankful to Dr. C. V. Avdhani, Mr. A. S. Patil, Mr. S.K. Menon, Dr. R.A. Kulkarni, Dr. R.P. Singh, Dr. P.G. Shukla, Dr. A. S. Jadhav, Dr. B.B. Idage, Dr. S. B. Idage, Dr. N.N. Chavan, Dr. V. Garnaik, Mr. Gaikwad, Mr. Deendayalan, Mr. V.V. Borkar and Mr. H.Pol for their co-operation. I also wish to thank Mrs. Neelima Bulakh, Mr. Sarojkumar, Mrs. Purvi Purohit and Mr.

Rajendra for instrumental training. I am thankful to the NMR group, Glass blowing group, DIRC group and Workshop group for their timely help. I also wish to thank Library, Administrative and other supporting staff for their co-operation. I am grateful to Vikram, Jine, Kakade, Jadhav,More and Shelar for their co-operation. I am also thankful to staff members at University of Pune.

My friends made the process very much enjoyable. I owe deeply to ever-trustful friends for always being with me. I sincerely thank them for all their affection and help. Specifically, I thank Rajeshwari, Omkar, Vijay, Asheesh, Pratheep, Ashwini and Yogesh for the discussions and suggestions (both scientific and nonscientific) in shaping my career as professionally and personally. Many thanks to Nivika, Arti, Suresha, Anumon, Arun, Shubhangi, Sunil, Arun Kulkarni, Arvind, Pandurang, Dyaneshwar, Vijay, Prakash, Mahesh, Anil, Sandip, Savita, Parimal, Kishor, Sharad, Shraddha, Deepshikha, Bhausaheb and Indravadan. Thanks for all the parties, celebrations, fun and pleasant atmosphere. I could really work peacefully because of the support from you all. I am also thankful to Mallikarjun, Bhoje, Smitha, Mahesh, Ravi, Sandeep, Santosh Hire, Santosh Wanjale, Chetan, Prashant, Dhanlakshmi, Sameer, Mohanraj, and Ghanashyam, for the help.

I share this happy moment with my whole family Father, Mother, Brothers and Vahinees. They rendered me enormous support during the whole tenure of my research. My soul mate, my wife Shilpa allowed me to fully concentrate on research with no complaints. Innocent smile of three kids Vedika, Sharang and Sharv provided me an enormous energy, enthusiasm and encouragement. I am more than thankful to God for placing me in such a healthy environment.

Finally, I would like to thank the Council of Scientific and Industrial Research for the award of Senior Research Fellowship.

Vivek V Kodgire

Abstract

The present thesis comprises of two parts, the first part is related to the water borne coatings addressing the scratch and abrasion resistance of glossy coatings and second part deals with epoxy resin based adhesives modified with reactive liquid polymers (RLP) and the important issues like, adhesion strength at room temperature as well as at elevated temperature along with the study of curing kinetics of epoxy resins in the presence of RLPs.

Water borne coatings

Due to environmental concern, water borne coatings based on polyurethanes are attracting increasing attention lately. Therefore, there is a great scope in designing and developing new and improved polyurethane dispersion with excellent coating properties such as, gloss, scratch, and abrasion resistance.

In the first part of waterborne coatings, the following three approaches were made:

1. Preparation of coatings from the blends of polyurethane dispersion (PUD) and acrylic emulsion
2. Preparation of coatings from the dispersions obtained by reacting two polyols (polyester polyol and acrylate polyol) simultaneously with diisocyanate
3. Preparation of organic-inorganic hybrid coatings from PUD and silica nano particles

In the first approach stable dispersions of the blends of two polymers namely, polyurethane dispersion (PUD) and acrylic emulsion (AE) were successfully prepared by combination of both in different ratios. It was observed that, the physical mixing of PUD and AE did not show synergistic effect in the scratch and abrasion resistance of coatings. However, all the blends gave smooth glossy finish coatings.

In order to improve the scratch and abrasion resistance of coatings, a new approach of making PUDs by reacting mixtures of polyols i.e. polyester polyol (PEP) and acrylic polyol (ACP) with diisocyanate was studied. Synergistic effect was observed at equal

equivalent ratios of PEP/ACP and the films exhibited maximum tensile strength. The scratch resistance of the coatings increased with increase in ACP content which was attributed to increase in the modulus of the films contributed from the acrylic hard segment in the polymer.

The combination of organic and inorganic moieties on a molecular scale to achieve synergistic properties in coatings is another important approach. In this work water-borne organic-inorganic hybrid coatings were prepared from PUDs, nano silica and amino silane modified silica (G-silica). It was observed that, upon increasing the silica loading to the PU matrix the scratch and abrasion resistance of coatings were improved due to reinforcing effect. But the gloss values of coatings reduced due to roughening of surface as a result of densification of silica particles with the increase in silica content. The hybrid coating with modified silica (G-silica) exhibited improved scratch and solvent scrub resistance over PUD coating while the gloss and abrasion resistance remained unaffected. The hybrid films also showed higher tensile strength with the incorporation G-silica which attributed to the better reinforcement of modified silica (G-silica) with PU matrix. Thus, these organic-inorganic hybrid systems show promising applications in glossy scratch and abrasion resistant coatings.

Epoxy resin based adhesives

Epoxy resins have been extensively used for formulating structural adhesives because of their properties such as, good wetting and formation of strong bond with many polar high energy substrates, superior mechanical strength and environmental stability. However, epoxy resins are found to be brittle and catastrophic failure at adhesive joints. Therefore, toughening of epoxies has become a necessity to ensure the feasibility of these materials for practical applications.

In this section, we have studied the influence of CTBN and ATBN incorporation on the room temperature and elevated temperature (150°C) adhesion strength and curing kinetics of an epoxy (DGEBA) adhesive cured with a cycloaliphatic hardener namely 3,3´-dimethyl-4,4´-diaminodicyclohexylmethane. It was seen that, significant enhancement in the LSS was obtained at room temperature as well as at 150°C upon

incorporation CTBN and ATBN. However, the optimum values of LSS were obtained for the composition containing 15% CTBN and 20% ATBN. The LSS of adhesive composition containing 20% ATBN was found to be higher than with 15% of CTBN. This was attributed to the more reactivity of amine functional groups in ATBN with epoxy matrix which in turn increases the crosslinking and better mixing with the matrix as compared to CTBN which is evidenced by SEM analysis. The increase in LSS with the increase in RLPs was attributed to the cavitation of rubber phase with the inclusion of RLPs and chemical bond formation between the RLPs and the epoxy resin.

The analysis of curing kinetics was done by Coats-Redfern method (*n*th order kinetic model) using non-isothermal mode of differential scanning calorimeter (DSC). It was observed that there was an increase in activation energy (E_a) and frequency factor (A) with an increase in CTBN content. The extent of reaction decreased after attaining the gelation. This can be attributed to the phase separation of rubber from the epoxy matrix towards the end of gelation. The reaction kinetics was found to be faster with ATBN since the amine functional groups can readily react with the epoxy resin.

Table of Contents

List of figures

List of tables

Glossary

ACP	Acrylic polyol
AE	Acrylic emulsion
AN	Acrylonitrile
APTES	Aminopropyl triethoxy silane
ATBN	Amine terminated butadiene acrylonitrile
CTBN	Carboxyl terminated butadiene acrylonitrile
DGEBA	Diglycidyl ether of bisphenol A
DMA	Dynamic mechanical analysis
DMPA	Dimethylolpropionic acid
DSC	Differential scanning calorimeter
ETBN	Epoxy terminated butadiene acrylonitrile
IPDI	Isophorone diisocyanate
LSS	Lap shear strength
PEP	Polyester polyol
PUD	Polyurethane dispersion
RLP	Reactive liquid polymer
SEM	Scanning electron microscopy
TEM	Transmission electron microscopy
TGA	Thermogravimetric analysis
TPP	Triphenylphosphine
VTBN	Vinyl terminated butadiene acrylonitrile
VOC	Volatile organic compound
NMP	N-Methylpyrrolidone

1.1 Introduction to Coatings

Coatings are found everywhere, for example, there are coatings on wall, refrigerator, TV cabinets, furniture, on the wire of electrical motors, printed circuit boards, cassette tapes, video tapes and compact discs. Exterior coatings are seen on the house and cars etc. Most coatings are used for decorative, protective, and/or a functional purpose on variety of surfaces. Therefore, the functional and decorative requirements of coatings span around a very broad spectrum.

Traditionally, coatings changed slowly in an evolutionary response to new performance requirements, new raw materials and competitive pressures. An important reason for the slow rate of change was the difficulty in predicting product performance. However, since 1965, the pace of technical change has increased dramatically with a major driving force to reduce volatile organic components (VOC) emission to atmosphere causing extreme air pollution. Therefore, various approaches particularly to reduce VOC emissions are being pursued globally to meet the new requirements. The use of waterborne coatings has increased substantially and has surpassed the volume of solvent borne coatings. Latex paints have become important these days in architectural coatings and have less VOC than traditional solvent-borne paints. Another growing area has been the use of powder coatings for industrial purposes. In many applications, the use of powder coatings permits complete elimination of solvent emissions. Radiation curable coatings, particularly UV-cured coatings, have also grown for clear coatings on heat sensitive substrates. These are solvent free and require very low levels of energy for curing.

Coatings may be described by their appearance (e.g. clear, pigmented, metallic or glossy) and by their functions (e.g. corrosion protective, abrasion protective, skid resistant, decorative or photosensitive). Coatings can be distinguished as organic or inorganic, although there could be some overlap. For example, many coatings consist of inorganic pigments or fillers in organic matrix (the binder). Often coatings and paints are used interchangeably. The three broad categories of coatings are: (i) architectural coatings, (ii) product coatings sold to original equipment manufacturers (OEMs) and (iii) special purpose coatings.

Architectural coatings include the familiar paints and varnishes (transparent coating) used to decorate and protect buildings outside and inside. Product coatings, also commonly called industrial coatings or industrial finishes are applied in factories on products such as automobiles, appliances, furniture, metal cans, etc. special purpose coatings include coatings for cars and trucks that are applied outside OEM factory (usually in body repair shops), coatings for ships and air crafts and the familiar strips of coatings on highways and parking lots.

1.1.1 Film formation

Most coatings are applied as liquids and converted to solid films after evaporation of solvent. Powder coatings are applied as solid particles, fused to a liquid, then forming a solid film. A useful definition of a solid film is that it does not flow significantly under the pressures to which it is subjected during testing or use (it is reported that a film is dry-to-touch if the viscosity is greater than about 10^6 mPa.s [1]).

A way to form films is to dissolve a polymer in solvent(s) at a concentration needed for application, apply the coating, and allow the solvent to evaporate. In the first stage of solvent evaporation, the rate of evaporation is essentially independent of the presence of the polymer. As solvent evaporates, viscosity increases, T_g increases, free volume decreases, and the rate of loss of solvent become dependent on how rapidly solvent molecules can diffuse to the surface of a film.

Less solvent is needed for a coating based on solutions of lower molecular weight thermosetting resins. After application, the solvent evaporates, and chemical reactions cause cross-linking. The number-average functionality has to be over 2, and the amount of monofunctional resin should be minimal for good properties. A problem with thermosetting systems is the relationship between stability during storage and time and temperature required to cure a film after application. Generally, it is desirable to store a coating for many months without a significant increase in viscosity. After application, one would like to have the cross-linking reaction proceed rapidly at the lowest possible temperature.

Another important group of coatings utilizes vehicles in which the polymer or resin is not in solution but rather present as a dispersion of insoluble particles. After application and loss of volatile components, the particles coalesce (fuse) to form a continuous film. Latex is a dispersion of high molecular weight polymer particles in water.

The largest volume of such coatings uses latexes as binder. Coalescing solvents have been necessary to formulate latex coatings to form films at low temperatures while resisting blocking at higher temperatures. The lowest temperature at which coalescence occurs to form a continuous film is called its *minimum film-formation temperature* (MFFT). A major factor controlling MFFT is the T_g of the polymer particles. The MFFT of latex particles can be affected by water, which can act as a plasticizer [2]. Most latex paints contain volatile plasticizers, coalescing solvents to reduce MFFT. The mechanism of film formation from latexes has been extensively studied and various theories associated with it are explained in the literature[3-6]. Film formation occurs by three overlapping steps: (i) evaporation of water and water-soluble solvents that leads to a close packed layer of latex particles; (ii) deformation of the particles leading to a continuous, but weak, film; and (iii) interdiffusion, a slow process in which the polymer molecules cross the particle boundaries and entangle, strengthening the film. A review paper discusses factors affecting development of cohesive strength of films from latex particles [3].

Thermoplastic polymers, dissolved in organic solvents were widely used in coatings for automobiles, wood furniture, and as corrosion protection coatings. Such coatings, which dry by solvent evaporation alone, are generally called lacquers.

To minimize the temperature required for curing while maintaining adequate storage stability, it is desirable to select cross linking reactions for which the rate depends strongly on temperature.

1.1.2 Composition of a coating

Organic coatings are complex mixtures of chemical substances that can be broadly classified into: (i) binders (ii) volatile components (iii) pigments/fillers and (iv) additives.

Binders are the materials which form the continuous film that adheres to the "substrate" on one side, binds together the other constituents in the coatings to form a film, and presents an adequately hard surface to the outside. The binders of coatings in general are organic polymers. *Volatile components* are liquids that make the coating fluid enough for coating application and undergo evaporation during the film formation. Most of the volatile components are organic solvents that dissolve the binder. The combinations of binder and the volatile component are usually termed as "vehicle". Pigments are finely divided insoluble solids that are dispersed inside the vehicle and remain suspended in the binder after film formation. Generally, the primary purpose of pigments is to provide color and opacity to the coating film. Additives are the materials that are included in small quantities to modify some properties of the coatings. Examples are catalyst for polymerization reactions, stabilizers, wetting and dispersing agents, flow modifiers, driers, foam control agents, etc.

1.1.3 Polyurethane coatings

In the past, solvent-borne polyurethane (PU) coating systems have been extensively used in the coating industry due to their excellent solvent and chemical resistance properties along with good weather stability [4-6]. With the ease of formulating both clear coats and pigmented top coats, the film also exhibit high gloss finish and very good mechanical properties. The wide applicability of PU coatings is due to versatility in the selection of monomeric raw materials from a huge list of macrodiols, diisocyanates and chain extenders. The chemical structure of PU consists of a soft segment and a hard segment which can be controlled to tailor-make properties to suit end applications.

Besides several advantages of solvent borne PU coatings, environmental concerns have driven the coatings researches to explore new and efficient organic coatings with minimum volatile organic components. In view of this, water-borne coatings are becoming increasingly important. Particularly, aqueous polyurethane dispersions (PUDs) have become prominent [7-9].

The polyurethane dispersions (PUD) are binary colloidal systems having PU particles (size 0.01-1μm) dispersed in continuous aqueous phase. In order to enhance the

dispersibility in aqueous media, ionic groups are introduced along the polymer chain by using hydrophilic monomers or hydrophilic internal emulsifiers. The dispersions obtained using internal emulsifier, such as dimethylol propionic acid (DMPA) have fine particle size, better stability and give films with good water resistance. Most of the work on aqueous PUDs has been done in industrial laboratories and is patented. These patents have been well revised and documented by Dieterich [10], Rosthauser and Nachtkamp [11]. These dispersions can be formulated into coatings and adhesives containing little or no solvent and can be applied on to plastics or other substrates, which are sensitive to solvent attack. The viscosity of dispersion is independent of molecular weight of the polyurethane but dependent on average particle size, particle size distribution and solids content. Therefore, PUDs can be prepared at high molecular weight with low viscosity and can be easily coated on to the substrates. The coating properties of PUDs such as gloss, water resistance are comparable to those of conventional solvent-borne polyurethane lacquers and two component polyurethane coatings [12-15]. The basic building blocks used for the preparation of aqueous PUDs are the same as those used for conventional solvent borne polyurethanes.

Polymeric/organic clear coats have gained widespread usage as the final coat in many diverse manufactured goods, car bodies, mobile phones, furniture lacquers, safety helmets, writing pens, etc., just to mention a few [16]. However, their aesthetic appearance and durability is rapidly impaired through constant use. Therefore, the first objective of this research work was to prepare water-borne coatings with improved scratch and abrasion resistant properties using organic-organic/inorganic hybrid approach, where polyurethane and acrylates are organic polymers and nano silica is inorganic filler. These new waterborne systems are expected to have improved coating properties like scratch resistance and abrasion resistance to fulfill the property profile of similar solvent-borne systems.

1.1.4 Organic-inorganic Hybrids

The fundamental concept behind the development of organic-inorganic hybrid materials is the combination of organic and inorganic moieties on a molecular scale to achieve synergistic properties of both the constituents. The possibility of gaining improved

performance by combining organic and inorganic components in coatings and adhesives is well known and largely practiced. For example, inorganic pigment or fillers are dispersed in organic component/binders (solvent, surfactants, polymers etc.) to improve optical, mechanical and thermal properties of coatings. This is attributed to the synergistic reaction between their components with the possible uniform distribution of the inorganic particles into the organic matrix. In fact, it is well known in the literature that the addition of silicate nano particles such as, montmorillonite, sepiolite and kaolin, can enhance significantly the thermal, mechanical and surface properties of the organic-inorganic hybrid systems [17-25].

Nano fillers have been incorporated in to thermoplastic and thermosetting polymers to improve various mechanical, thermal and chemical properties such as, tensile strength and fracture toughness, barrier to diffusion of solvents and chemicals and dimensional stability against thermal fluctuations at high temperatures. Graphite nanoparticles have rendered semiconductor nature in *in-situ* polymerized nylon 6 [26] and smectite clay particles have been successfully incorporated in polypropylene to augment the properties[27].

High performance thermoplastic polymers such as polyethersulphone (PES), polyphenylene ether (PPE), polyether etherketone (PEEK) and polyimide exhibit superior thermal stability and strong mechanical properties but, some of them lack proper resistance to attack by solvents and chemicals and do not provide adequate dimensional stability for high temperatures application. However, upon nanofiller incorporation, they can significantly augment these properties.

Fumed silica is a very useful reinforcement for thermoplastic and thermosetting polymers and finds use as component material for electric packaging [28], thickners for paints and coatings [29], reinforcement of silicones, PVC and acrylics for various sealing and structural applications [30-34] and reinforcement of vulcanized rubber [35] .

PU nano composites with aluminosilicate fillers have been reported to exhibit enhanced tensile strength and elongation at break [36, 37].

Nanosized silica and alumina particles were used as fillers for polymer reinforcement and scratch resistant coatings. For favorable embedding of filler in the polymer matrix, the surface of the filler was chemically modified by reaction with methacryloxypropyl trimethoxy silane. The formation of covalent Si(Al)-O-Si-C bonds between functional groups from silane and –OH groups from silica and alumina was demonstrated by means of FTIR and MASS NMR spectroscopy [38] .

Scratch and abrasion resistant coatings were prepared by in-situ grafting methacryloxy functionalized silanes on commercial nanoglobular silica polymerization active silico-organic nanoparticles [39].

Reinforced clear coats were prepared using nanosized silica and alumina particles in UV/EB curable acrylate formulations [40]. The filler particles were modified by polymerization-active trialkoxysilanes, i.e. methacryloxypropyl trimethoxy silane and vinyl trimethoxy silane. The cured nanocomposite clear coats showed improved scratch and abrasion resistance.

Transparent reinforced polyacrylates were prepared using nanosized filler particles with radiation curable acrylates. To improve the dispersion of nanofiller within the acrylate matrix, the filler surface was chemically modified by trimethoxy silanes having methacryloxypropyl (MEMO), vinyl (VTMO) and n-propyl (PTMO) functionalities [41]. The silane modified silica surfaces were characterized by mass spectroscopy and atomic force microscopy (AFM) [42] .

Clays have long been used as fillers in polymer systems because of low cost and improved mechanical properties of the resulting polymer composite. The enhanced properties of polymer nanocomposite strongly depend on the efficient dispersion of clay into polymer matrix [43]. In the past, clay particles could only be dispersed on micro scale. However, in the early 1990s, Toyota researchers [44] discovered that the treatment of montmorillonite clay with amino acids allowed the dispersion of individual 1 nm thick silicate layers of the clay on a molecular scale in nylon 6 polymer. Their hybrid material

showed major improvements in physical and mechanical properties even at very low clay content (1.6 vol %).

Many naturally occurring clays are hydrophilic in nature and incompatible with the polymers which are hydrophobic. Therefore, in order to have good compatibility between the clay and polymers, surface modification of clay with organic moieties is performed. Such modified clays are commonly referred to as organoclay [45, 46].

There are essentially three different approaches to synthesize polymer-clay nanocomposites: melt intercalation, solution and in-situ polymerization. The melt intercalation process was invented relatively recently by Vaia et al. [47]. A thermoplastic polymer is mechanically mixed with organophilic clay at elevated temperature. The polymer chains are then intercalated between the individual silicate layers of the clay. The proposed driving force of this mechanism is the enthalpic contribution of the polymer/organoclay interactions. This method is becoming increasingly popular since the resulting thermoplastic nanocomposites may be processed by conventional methods, such as extrusion and injection moulding.

In the solution method, the organoclay, as well as the polymer, are dissolved in a polar organic solvent [48]. The entropy gained by the desorption of solvent molecules allows the polymer chains to diffuse between the clay layers, compensating for their decrease in conformational entropy [43]. The evaporation of the solvent results in an intercalated nanocomposite. This strategy can be used to synthesize epoxy-clay nanocomposites [49]. However, the large amount of solvent required is a major disadvantage.

An in-situ polymerization approach was the first strategy used to synthesize polymer-clay nanocomposites and is a convenient method for thermoset-clay nanocomposites [50]. It is similar to the solution method except that the role of the solvent is replaced by a polar monomer solution. Once the organoclay is swollen in the monomer, the curing agent is added and complete exfoliation occurs in favorable cases. The polymerization is believed to be the indirect driving force of the exfoliation [51]. The clay, due to its high surface energy, attracts polar monomer molecules in the clay galleries until equilibrium is reached. The polymerization reactions occurring between the layers lower the polarity of

the intercalated molecules and displace the equilibrium. This allows new polar species to diffuse between the layers and progressively exfoliate the clay. Therefore, the nature of the curing agent as well as the curing conditions is expected to play a role in the exfoliation process.

1.2 Adhesives

Adhesive surround us in nature, and have become significant part of human lives. Adhesives are used virtually in every business, industry, and home. Applications abound from Post-it Notes to automotive safety glass to clothing and footwear to food and pharmaceutical packaging to bodily implant to aerospace structures. Major industries, market segments that support the adhesive industry are indicated in **Table 1.1**

Table 1.1 *Major market types and applications of adhesives*

Major Market	Typical applications	Adhesives
Construction	Roofing and flooring	Epoxy
	Wood adhesive	PVA, Casein
	Electrical and masking tape	Melamine formaldehyde
Transportation	Auto trim	Epoxy
	Auto body patch	Polyurethane
	Auto assembly	Acrylic
	Aircraft/aerospace	Nitrile
	Marine	Polyester
Packaging	Corrugated cartons	Acrylic
	Labels, signs, decals	Polyurethane
	Envelopes	Ethylene vinyl acetate
	Food/pharmaceuticals	Casein
	Laminates	Starch and dextrin
	Pressure sensitive tapes	Polyolefins
Medical	Medical devices	Cyanoacrylate
	Skin applied treatments	Silicone
	Dental	Epoxy
	Internal implants	Polyurethane
Apparel	Shoes	Polyurethane
	Textiles	Ethylene vinyl acetate
	Laminates	Polyolefins
	Fabric repair	Acrylic
		Neoprene

1.2.1 Definition of adhesive

An adhesive is a substance capable of holding at least two surfaces together in a strong and permanent manner.

The primary function of an adhesive as per the definition is to hold substrates together for the life of the product. However, adhesives are also useful for providing secondary functions. In addition to performing mechanical fastening operation, an adhesive may also be used as a sealant, vibration damper, insulator, and gap filler all in the same

application. Many designers feel that, multifunctionality is one of the most valuable characteristics of an adhesive.

Because adhesives are viscoelastic materials, they can act as vibration dampers to reduce the noise and oscillation encountered in some assemblies. In the automotive industry, for example, adhesives are used in combination with spot welding for joining trunk assemblies. This combination provides sound deadening and sealing in addition to a strong joint. Adhesives can sometimes be used to perform sealing functions, offering a barrier to the passage of fluids and gases.

Another property of adhesive that is often advantageous is their ability to function as electrical and thermal insulators in a joint. The degree of insulation can be varied with different adhesive formulations and fillers. Adhesive can even be made electrically and thermally conductive with silver and boron nitride fillers, respectively. Since adhesives usually do not conduct electricity, they prevent galvanic corrosion when dissimilar metals are bonded.

There are advantages to combining adhesive bonding with mechanical fastening. The combination can provide properties that are superior to either singular method. It is also possible to reduce the number of mechanical fastening steps without sacrificing the strength.

Adhesives and sealants are often considered together because they both adhere and seal, both must be resistant to their operating environments, and their properties are highly dependent on how they are applied and processed.

Modern adhesives are generally manufactured by compounding (or formulating) a base resinous material with filler, pigments, stabilizers, and other additives to yield product with desired characteristics at acceptable cost. Adhesives are broadly classified into structural adhesives and non-structural adhesives. Structural adhesives have high shear strength (>1000 psi) and good environmental resistance. Structural adhesives are generally made from formulations where the main component is a thermoset polymeric resin such as epoxy, phenolics etc.

Non-structural adhesives are adhesives with much lower shear strength and performance. They are generally used for temporary fastening or to bond weak substrates. These adhesives are generally made from formulations where the main component is thermoplastic resin such as acrylic, polyvinyl acetate or cellulosics.

1.2.2 Inert molecular forces for adhesion

As mentioned earlier, adhesives function primarily by the property of adhesion. Adhesion is the attraction of two different substances resulting from intermolecular forces between the substances. Adhesive or cohesive forces can be attributed to either short or long range molecular interaction. These are also referred to as primary or secondary bonds. A general goal is to have the adhesive strength sufficiently high as to cause cohesive failure of the adhesive or adherent when the joint is stressed to its ultimate. The following table (**Table 1.2**) indicates the type of molecular forces and the bond energies involved in these forces.

Table 1.2 *Forces at the interface or within the bulk of the material*

Type of forces	Source of force	Bond length (nm)	Bond energy (KJ/mol)	Description
Chemical: Primary or short range forces	Covalent	0.1 – 0.2	150-950	Diamond or crosslinked polymers. Highly directional
	Ionic or electrostatic	0.2 – 0.3	400 – 800	Crystals. Less directional than covalent
	Metallic	0.3 – 0.5	100 - 400	Forces in welded joints
Intermolecular: secondary long range forces	Van der Waals-dispersion forces	0.4 – 0.5	0.1 – 15	Interaction between temporary dipoles. Forces fall off as the sixth power of the distance
	Van der Waals-polar forces	0.4 – 0.5	4 – 15	Interactions of permanent dipoles. Forces fall of as the third power of distance
	Hydrogen bonds	0.2	20 - 30	Sharing of protons between two atoms possessing loaned pairs of electrons

Short range molecular interactions include covalent, ionic and metallic forces. The most important forces relative to adhesion are the Van der Waals forces. These forces are

dependent on the distance between the adhesive and adherent. The bond forces fall off exponentially as this distance increases.

1.2.3 Theory of adhesion

Several theories attempt to describe the phenomenon of adhesion. However, the most common theories of adhesion are based on: adsorption and wetting; diffusion; electrostatic interactions; simple mechanical interlocking; chemical bonding and; weak boundary layer.

In the adsorption and wetting, the adhesion results from molecular contact between the two materials and the surface forces that develop. A bond develops from the adsorption of adhesive molecules on the substrate and the resulting attracting forces, usually designated as secondary or Van der Waals forces. For these forces to develop, the bonding substrate should make intimate molecular contact with the adhesive which can be established by a process of wetting. Wetting can be determined by contact angle measurements and the process of wetting largely depends on surface tension, surface area of bonding substrates. According to mechanical theory of adhesion, in order to function properly, the adhesive must penetrate the cavities on the surface, displace the trapped air at interface, and lock on mechanically to the substrate. Surface roughness generally aids in adhesive bonding by providing a mechanical interlocking effect. The benefit of mechanical interlocking is that, the rough surface will provide a crack propagation barrier. The renewal of surface by physical or chemical treatment could also produce an increase in adhesion strength. For example, the phosphating of cold-roll steel produces thin plates of iron phosphate crystals on the surface and numerous interlocking sites for enhanced adhesion.

The electrostatic theory states that driving forces for adhesion arise from the formation of electrical double layer at the adhesive-adherent interface. These forces are primarily the dispersion forces and the forces arising from the interaction of permanent dipoles. Such interactions are only operational on a very short range (less than 0.5 nm), and their effectiveness decreases with sixth power of the distance of separation. It is believed that for conventional adhesive bonds, the electrostatic contribution to the total work of

adhesion is quite small in comparison to Van der Waals forces [52] . However, the electrostatic theory is strongly evident in certain applications and well accepted for biological cell adhesion.

In diffusion theory, the adhesion arises through the inter diffusion of molecules from one material to another across the interface. This theory is primarily applicable when both adhesive and adherent are polymeric, having compatible long chains capable of movement. The adhesion by diffusion is two-stage process wherein the wetting is followed by interdiffusion of chain segments across the interface to establish an entangled network of molecules. For diffusion to occur, the adhesive and adherent must be chemically compatible in terms of miscibility. The theory is primarily applicable to the solvent or heat welding of thermoplastic substrates. However, the diffusion theory also explains the self adhesion of certain elastomers. Polyisobutylene and silicone elastomers of low molecular weight will bond to themselves under slight pressure.

In certain applications, the formation of covalent chemical bonds occurs across the interface. Chemical bond requires that there be mutually reactive chemical groups tightly bound on the substrate and the adhesive. These strong (150 to 900kJ/mol) and durable bonds are generally the result of close contact or adsorption of adhesive on the surface followed by chemical reaction. Thus, the term "chemisorption" is often used to describe this mechanism. This theory is demonstrated by one of the oldest commercial bonding applications: the rubber-brass adhesion process during vulcanization of the rubber. Polysulfur bonds appear between the copper surface atoms of the brass and the elastomers vulcanized with sulfur [53]. The grafting of reactive polymeric molecule on a substrate to improve bond strength to an adhesive is another example of chemical bonding.

Adhesive containing reactive functional groups, such as hydroxyl or carbonyl, tend to adhere more tenaciously to substrate containing similar groups. Perhaps the most widely employed example of the chemical bonding theory is with adhesion promoters or coupling agents. These multifunctional chemicals provide a molecular bridge between the substrate and the adhesive. One end of the adhesion promoter molecule has functionality that reacts with the adhesive and the other end has functionality that will react with the

substrate. Organosilanes are the most widely used adhesion promoters. They are employed as primers on glass fibers to promote adhesion between the resin matrix and the glass in fiber-glass reinforced plastics. They are also used as primers and additives to promote the adhesion of adhesives.

According to the weak boundary layer theory, first described by Bikerman[54], when bond failure seems to be at the interface, usually a rupture of a weak boundary layer occurs cohesively within the weakest component of the joint. It may happen at adhesive substrate interface, within the substrate or within the adhesive.

This theory largely suggests that true interfacial failure (i.e., adhesion failure) seldom occurs. Failure may occur so near to the interface that it is apparently at the interface, but in most cases it is ductile plastic deformation or cohesive failure of weak boundary layer. Weak boundary layer can originate from the adhesive, the adherent, the environment, or a combination of any of the three.

Weak boundary layers can occur on the adhesive or adherent if an impurity concentrates near the surface and forms a weak attachment. When failure occurs, it is the weak boundary layer that fails, although failure may seem to occur at adhesive adherent interface.

Weak boundary layers could develop during any one of these periods.

- Before and during application of adhesive
- During setting or curing of adhesive
- In the time period during which the joint is in service and exposed to stress

1.2.4 Classification of adhesives

Adhesive can be classified by many methods and schemes. Perhaps the broadest classification scheme is to categorize an adhesive as being manufactured from materials that are either synthetic or naturally occurring. Synthetic adhesives are manufactured from manmade materials such as synthetic polymers. Natural adhesives are manufactured from naturally occurring materials such as animal or agricultural by-products. Most of the

industrial adhesives are classified based on the (i) function (ii) chemical composition (iii) mode of reaction and (iv) physical form.

Based on the function, adhesives can be classified into structural and non-structural adhesives. Structural adhesives are materials of high adhesion strength and performance. In general, most structural adhesives have shear strength in excess of 1000 psi and are resistant to common operational environment. Their primary function is to hold structures together and be capable of resisting high loads without deformation. Conversely, non-structural adhesives are not required to support substantial loads, but they merely hold light weight materials in place. Non-structural adhesives creep under moderate load and are often degraded by long term environmental harsh exposures. Certain pressure sensitive adhesives (PSA), hot melt, and water emulsion adhesives are examples of non structural adhesives because they have moderate low shear strength, high creep, and poor resistance to temperature and chemicals.

The classification of adhesives by chemical composition describes adhesive in broadest sense as being thermosetting, thermoplastic, elastomeric, or blends (hybrids) of these.

Thermosetting adhesives are materials that cannot be heated and softened repeatedly after their initial cure. They form infusible and insoluble materials upon curing. The cross-linking that occurs in curing reaction is brought about by the linking of polymeric chains, resulting into a three dimensional network structure. Thermosetting adhesives may be sold as multiple or single part system. Epoxy and urethane adhesives are common examples of thermosetting adhesives.

Thermoplastic adhesives differ from thermoplastics in that they do not cure or set under heat. Thermoplastic adhesives merely soften or melt when heated. Thermoplastic adhesives have a more limited operating temperature range than thermosetting types. The thermoplastic adhesives are sold in the market as heat, solvent, or moisture activated adhesives. Wood glues (polyvinyl acetate), a common house hold item, is a thermoplastic adhesive dispersed in water as either latex or emulsion.

Elastomeric adhesives are based on synthetic or naturally occurring elastomeric polymers having great toughness and elongation. These adhesives are made from polymers that are

capable of high degree of extension and compression. Elastomeric adhesives may be either thermosetting or thermoplastic.

Hybrid adhesives are made by combining different thermosetting, thermoplastic, or elastomeric resins into a single adhesive formulation. Some of the examples of hybrid adhesives are nitrile-phenolic, epoxy-polysulfide which exhibit toughness and resilience due to the elastomeric component in the formulation.

One of the most widely used methods of classification of classification of adhesives is by the curing or hardening mechanism. These are summarized in **Table 1.3**.

Table 1.3 *Classification of Adhesives according to Cure Mechanism*

Classification terminology	Examples of base polymers	Characteristics
Single part, heat cured	Epoxy, acrylic, silicone, phenolic, polyimide	The formulation contains resin and hardener in single package and has higher adhesive strength and durability to many environments.
Single part moisture cured	Polyurethane and silicones	Once exposed to moisture, the cure mechanism becomes activated.
Two-part, room or elevated temperature cured	Epoxy, polyurethane, acrylic, polysulfide silicone	The formulation contains resin and hardener component that must be kept separate. Once mixed working life is a limitation. These are generally used as structural adhesives.
Enclosed curing	Anaerobic acrylics, cyanoacrylate	The single component adhesive cures when it is enclosed within a joint. Anaerobic systems cure due to lack of oxygen, and cyanoacrylate cure due to catalyst on substrate surface.
UV curing	Acrylates, cyanoacrylate	Adhesive cure is initiated by light in the UV range. Generally used with pressure sensitive adhesives or when adhesives are applied as thin coatings.
Solvent based	Polyvinyl acetate, acrylic, natural and synthetic elastomers	Adhesive is carried in solvent. Cure occurs when carrier is evaporated.
Pressure sensitive	Acrylic, elastomers, block co-polymer	When applied and set, adhesive is a semisolid that bonds due to its tacky surface and light application pressure.
Contact	Neoprene, styrene butadiene rubber	Similar to pressure sensitive adhesive but coating is not tacky. When two coated substrates are brought together under light pressure, the self adhesion occurs.
Hot melt	Polyolefins, ethylene vinyl acetate, polyamides, polyester, polyurethane	Thermoplastic formulations that are applied in the molten state are set when cooled to solid.

1.2.5 Epoxy resins

Epoxy adhesives were introduced commercially in 1946 and found to have applications in wide range of areas such as automobile, industrial and aerospace. Epoxies are probably the most versatile family of adhesives because they bond well to many substrates and form strong, durable joints. Epoxy resins cure with no evolution of volatile byproducts, undergo low shrinkage during cure and adhere to many different types of surfaces such as metal, wood, glass, plastics, ceramics, concrete, asphalt and rock.

The most widely used epoxy resins are based on the adduct of bisphenol A and epichlorohydrin. The resulting diglycidyl ether of bisphenol A (DGEBA) resin is a difunctional molecule with two terminal epoxide groups. Its chain length can be varied to obtain a product that ranges from moderately viscous liquid to a solid at room temperature. With an increasing demand for high performance epoxy resins, multifunctional aromatic epoxy systems which have higher epoxide content per gram of resin have been developed by Dow, Ciba-Geigy and Shell companies. Some examples of commercially available epoxy resins are shown in **Figure 1.1.**

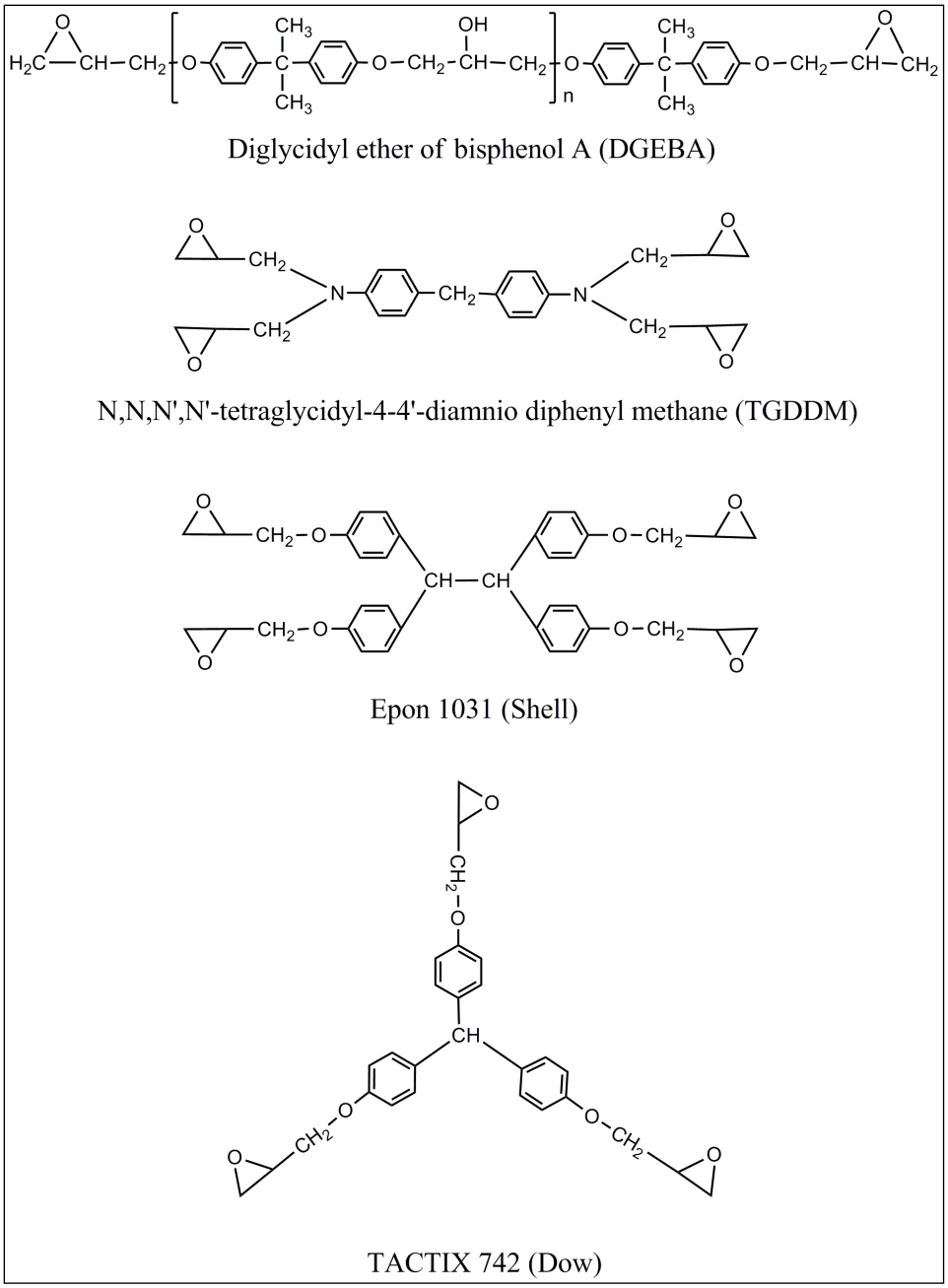

Figure 1.1 *Some commercial grades of epoxy resins*

Incorporation of aromatic and heterocyclic structures into the network structure is found to improve the thermal stability of the cured resin. Thus, these epoxy resins can be employed in high temperature applications and as matrix in composite materials.

Epoxy adhesives are commercially available as liquids, pastes, film and solids. Some of the selected epoxy adhesives and their properties are given in **Table 1.4** and **Table 1.5**.

Table 1.4 *Some of the commercially available two component epoxy adhesives*

Adhesive trade name	Adhesive supplier	Mix ratio, by weight	Curing conditions	Properties
Master Bond EP 35	Master Bond	100/70	24-48 h at RT 1-2 h at 95°C	High strength at 450-500°F
Master Bond 21 LV	Master Bond	100/100	24-48 h at RT 1-2 h at 95°C	General purpose adhesive; good chemical resistance
Araldite XB 5308/Hardener XB 5309-1	Huntsman	100/100	10 h at RT 7 min at 100°C	Thixotropic non sagging adhesive that forms resilient bonds to FRP
Bond Master 4E90 A/B	Bond master	100/35	24 h at RT 4h at 65°C	Unfilled, general purpose adhesive; transparent
Scotch-Weld 1751	3M Company	3/2	24 h at RT	Long working life; 8-12 h handling strength; rigid
Hysol EA 9300	Loctite: Henkel	100/33	5-7 days at RT 1 h at 82°C	High peel strength and excellent environmental durability
Titan Bond Plus	Bostik Findley	1/1	24 h at RT	Good adhesion to ABS and PVC bonds to wet or dry surfaces

Table 1.5 *Some of the commercially available one component epoxy adhesives*

Adhesive trade name	Adhesive supplier	Curing conditions	Properties
Supreme 10HT	Master Bond	60 min at 125°C 35-45 min at 150°C	High strength adhesive with good chemical and temperature resistance (to 200°C)
Supreme 10HT/S	Master Bond	24-48 h at RT 1-2 h at 95°C	Silver filled version of Supreme 10HT for electrical conductivity
Araldite AV 8553	Huntsman	30 min at 125°C	Tixotropic epoxy with good impact strength
Hysol 9434 NA	Loctite; Henkel	30 min at 125°C	High temperature, nonsag epoxy adhesive
Scotch-Weld 2214	3M Company	60 min at 121°C	Aluminum filled, general purpose adhesive
Magnobond 6297	Magnolia Plastics	40 min at 125°C	High temperature service; good adhesion to FRP
ESP 308	Permabond International	45 min at 150°C	Service temperature from -65 to + 350°F;3800-6000 psi shear strength
FM 94	Cytec Engineered Materials	60-90 min at 121°C	Modified epoxy; provides metal to metal and metal to honeycomb bonds

1.2.6 Characterization of uncured epoxies

Epoxies often contain isomers, oligomers, and other minor constituents. Liquid/solid epoxy resins are mainly characterized by epoxy content, viscosity, color, density, hydrolysable chloride, and volatile content [55, 56 57]. In addition, GPC, HPLC [56, 58-60], IR[61], NMR [62], etc., are performed to determine molecular weight, oligomer composition, functional groups, and impurities. The epoxy content of liquid resins is frequently expressed as *epoxide equivalent weight (EEW)* or *weight per epoxide (WPE)*, which is defined as the weight in grams that contains 1g equivalent of epoxide. A common chemical method of analysis for epoxy content is the titration of the epoxide ring by hydrochloric acid-pyridine in methanol [55, 63, 64].

The viscosity of epoxy resins is another important characteristic affecting handling, processing, and application of formulations. For example, high viscosity epoxy resins impede good mixing with curing agents, resulting in inhomogeneous mixtures, incomplete network formation, and poor performance. On the other hand, too low viscosity would affect application characteristics such as coverage and appearance.

1.2.7 Curing of epoxy resin

The selection of appropriate curing agents for epoxy resins is very important since they determine the reactivity, degree of conversion, viscosity, and gel time during curing. Different types of curing agents have been used in curing epoxy resins. The most commonly used curing agents are aliphatic, cycloaliphatic and aromatic amines. It has been reported that, primary amines react much faster than secondary amines. In general the order of reactivity follows: aliphatic amines > cycloaliphatic amines > aromatic amines [65-68]. Epoxies cured with aromatic amines give better chemical and thermal resistance than epoxies cured with aliphatic amines. Various amine curing agents are shown in **Table 1.6**.

Table 1.6 *Commercial amine functional curing agents used for epoxy curing*

Structure	Name
$NH_2CH_2CH_2NHCH_2CH_2NH_2$	Diethylenetriamine (DETA)
$NH_2CH_2CH_2NHCH_2CH_2NHCH_2CH_2NH_2$	Triethylenetetramine (TETA)
$NH_2CHCH_2(OCH_2CH)_nNH_2$ (CH$_3$ substituents)	Poly(oxypropylene diamine)
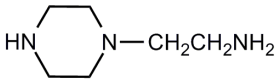	Aminoethylpiperazine (AEP)
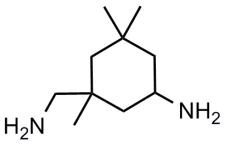	Isophorone diamine (IPDA)
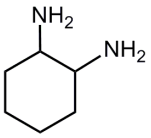	1,2-Diaminocyclohexane (DACH)
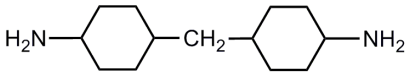	Bis(4aminocyclohexyl)methane (PACM)
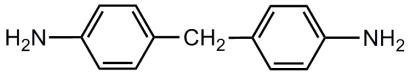	4,4'Diaminodiphenylmethane (MDA, DDM)
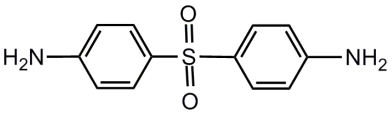	4,4'-Diaminodiphenylsulfone (DDS)
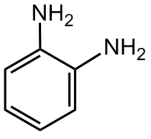	meta-Phenylenediamine (MPD)

DICY is a solid curing agent which can have a shelf-life of six months with solid or liquid epoxy resins. It is a preferred curing agent for one component epoxy adhesive.

Anhydrides are also important curing agents for heat cured epoxy resins. Epoxy-anhydride systems exhibit low viscosity and long pot life, low exothermic heat of

reaction and little shrinkage when cured at elevated temperature [69]. Anhydride cured epoxy adhesives exhibit excellent thermal, mechanical, and electrical properties. Several important anhydride curing agents are listed in **Table 1.7**.

Table 1.7 *Anhydride functional curing agents used for epoxy curing*

Structure	Name	Structure	Name
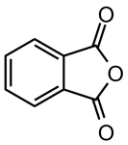	Phthalic anhydride (PA)	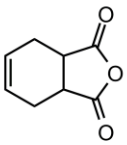	Tetrahydrophthalic anhydride (THPA)
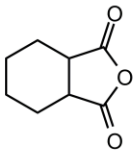	Hexahydrophthalic anhydride (HHPA)	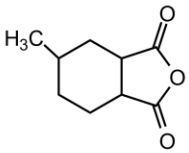	Methylhexahydro phthalic anhydride (MHHPA)
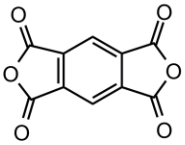	Pyromellitic dianhydride (PMDA)	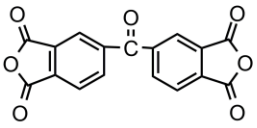	Benzophenone-3,3',4, 4'-tetracarboxylic dianhydride (BTDA)

1.2.8 Epoxy curing kinetics

Curing process is important in deciding the performance of cured epoxy adhesive. A large number of studies on curing kinetics of epoxies have been reported in the literature[67, 70-90].

In the early stages of curing prior to gelation or vitrification, the epoxy curing reactions are kinetically controlled. In the region between gelation and vitrification (rubber region) the reaction can shift from kinetic to diffusion controlled [76, 77, 80]. As curing proceeds, the viscosity of the system increases as a result of increasing molecular weight. Finally the reaction becomes diffusion-controlled and quenches as the material vitrifies [77]. The time-temperature-transformation (TTT) diagram is useful in understanding the cure kinetics, conversion, gelation, and vitrification of the curing thermoset [77, 80, 83].

1.2.9 Toughening agents for epoxy resin

Almost all the cured epoxy systems in use for high temperature structural applications are brittle. Therefore, they have been toughened using toughening agent such as thermoplastic particles, nylon and various elastomers. The most successful of these are epoxy adhesives that embody discrete nitrile rubber regions as elastomeric toughening component. Studies have been reported on enhancement of toughness of cured epoxy resins without significant reduction in thermal and mechanical properties, by the addition of low levels of reactive liquid rubbers such as carboxyl terminated butadiene acrylonitrile (CTBN), amine terminated butadiene acrylonitrile (ATBN) and epoxy terminated butadiene acrylonitrile (ETBN) copolymers. The theory is that, during initial stage of cure, the reactive liquid rubber is compatible with the epoxy-hardener mixture.

As the curing proceeds, molecular weight increases and phase separation occurs. This two phase microstructure consisting of small rubber particles dispersed and bonded to the epoxy matrix results in higher toughness because the mechanical energy is uniformly distributed by the rubber particles, thereby reducing the local stress concentration. This improvement is achieved without significant reduction in mechanical and thermal properties of cross-linked epoxy resins since the epoxy matrix contains very little or no rubber. There have been some reports on the CTBN-toughened epoxy structural adhesives [91]. Heat cured epoxy adhesives produce high joint strength at room temperature. There are scanty reports on reactive liquid polymer toughened epoxy adhesives with elevated temperature capabilities. Therefore, there is a considerable interest now in developing such type of adhesives [92]. Typical properties of ATBN and CTBN reactive liquid polymers (RLP) are shown in following **Table 1.8**.

Table 1.8 *Typical properties of ATBN and CTBN*

Properties	ATBN (1300X16)	CTBN (1300X8)
Acrylonitrile Content (%)	18	18
Amine Equivalent weight (AEW)	900	-
Carboxyl content	-	29
Brookfield viscosity (mPa.s or cP @ 27°C)	200,000	1,35,000
Specific gravity	0.95	0.948
Glass transition temperature (T_g in °C)	-51	-52

1.3 Characterization techniques used in this work

1.3.1 Dynamic mechanical analysis (DMA)

Dynamic mechanical analysis is one of the most important methods to characterize viscoelastic properties of the materials as a function of both the frequency and temperature. In dynamic mechanical analysis, a sinusoidal stress (or strain) is applied to the sample and the resulting response of strain or stress is measured as functions of both oscillatory frequency and temperature [93]. In viscoelastic studies, the applied force and resulting deformation both vary sinusoidally with time. Due to the time dependent properties of viscoelastic materials, resultant response is out of phase with applied stimulus. The strain will also be sinusoidal but will be out of phase with stress as shown in **Figure 1.2**. Viscoelastic materials exhibit phase angle, which lie between the two extremes 0° and 90°.

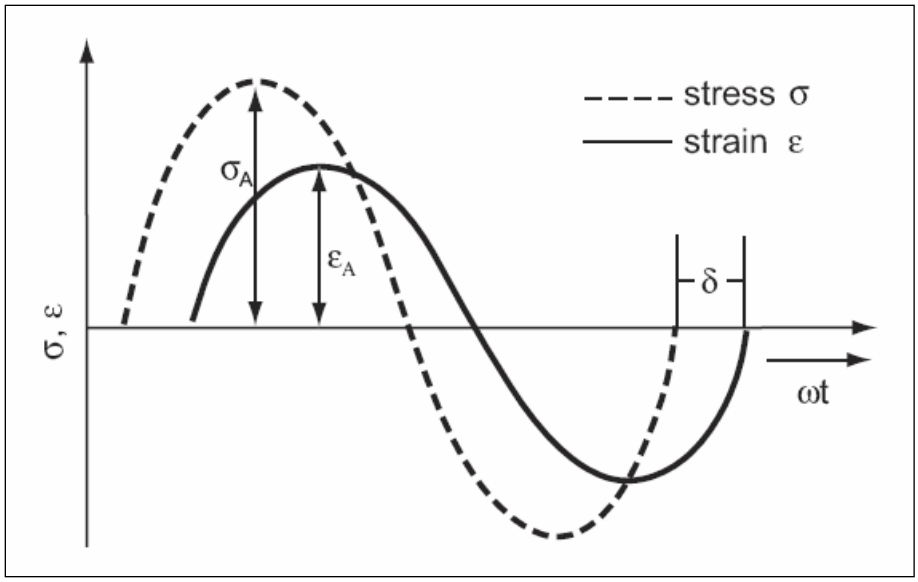

Figure 1.2 *Sinusoidal oscillation and response of a linear-viscoelastic material*

This phase lag results from the time necessary for molecular rearrangements and is associated with the relaxation phenomena. The variation of these components as a function of temperature is used to study the molecular motion in the polymers. The important information obtained from DMA are:

1. storage modulus (E′) corresponds to the elastic response to the deformation or stored energy,

2. loss modulus (E") corresponds to the plastic/viscous response to the deformation or dissipated energy,

3. tan δ corresponds to the ratio of loss modulus to storage modulus (E″/E′). Tan δ is known as loss tangent or damping factor. This is one of the important parameters and seen to increase during transitions between different deformational mechanisms. Therefore, tan δ is useful for the occurrence of molecular mobility transitions such as glass transitions of the polymers.

In a linear-viscoelastic range, the stress response has the same frequency ($\omega = 2\pi f$) as the deformation input excitation. The analytical parameters in dynamic tests are the

amplitudes of the deformation and the stress, and the time displacement δ/ω between deformation and stress, and are used to determine the specimen's characteristics.

Formulae for calculating complex modulus E^*, storage modulus E′, loss modulus E″ and loss factor tan δ are as follows:

$$\left|E^*\right| = \frac{\sigma_A}{\varepsilon_A} \quad (1)$$

$$\left|E^*\right| = \sqrt{[E'(\omega)]^2 + [E''(\omega)]^2} \quad (2)$$

$$E'(\omega) = \left|E^*\right| . \cos\delta \quad (3)$$

$$E''(\omega) = \left|E^*\right| . \sin\delta \quad (4)$$

$$\tan\delta = \frac{E''(\omega)}{E'(\omega)} \quad (5)$$

In the experiments, generally the strain is fixed suitably in the linear region by carrying out first the strain sweep test. The parameters E′, E″ and tan δ give information about the physical and mechanical properties of the polymers [94, 95].

1.3.2 Tensile properties using Instron

Understanding the relationship between composition and mechanical properties of films can provide basis for more efficient formulations. An excellent review article that discusses on stress analysis as a tool for understanding coatings performance [96] is reported in the literature. Since coating films are viscoelastic in nature, the mode of deformation can be elastic and/or viscous. In an ideal elastic deformation, a material elongates under tensile stress in direct proportion to the stress applied (according to Hooke's law). When the stress is released, the material returns to its original dimensions. On the other hand, an ideal viscous material (Newtonian fluid) elongates, flows in direct proportion to stress and undergoes permanent deformation. The modulus of elasticity is a measure of the stiffness of the material in the linear regime. **Figure 1.3** shows the schematics of stress-strain curve in which a coating film is elongated (strain) at constant rate and the resulting stress is recorded as percentage elongation.

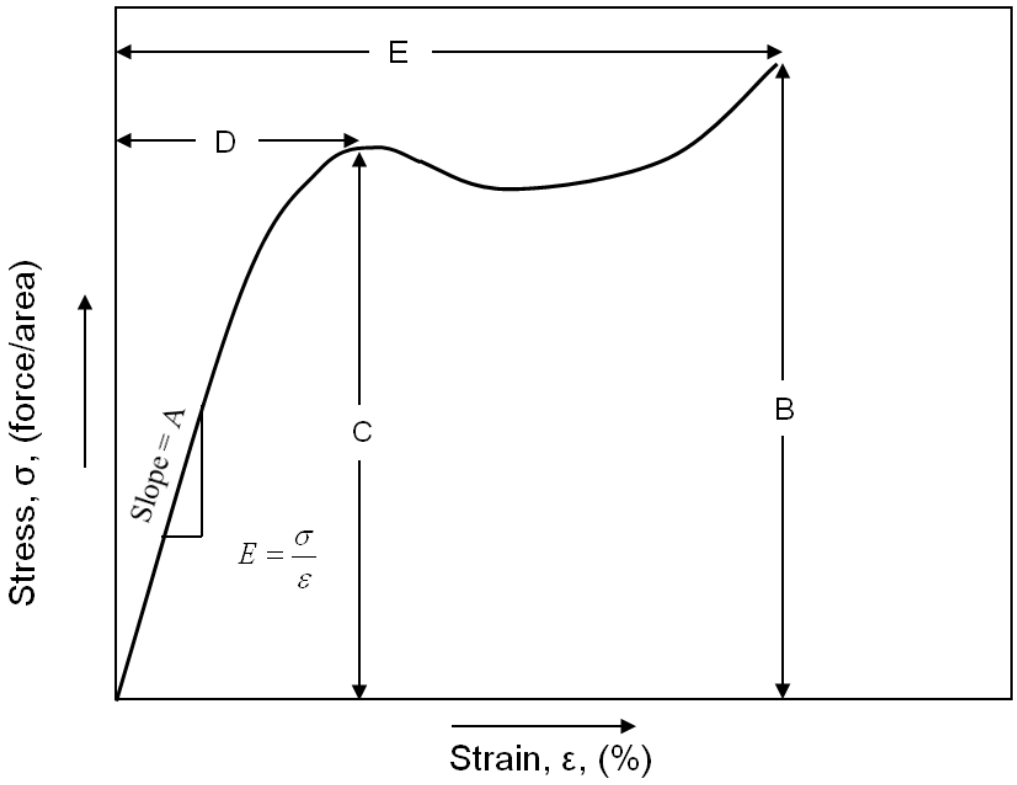

Figure 1.3 *Stress–strain plot. A is initial modulus, B is elongation-to-break, C is yield strength, D is elongation-to-break and E is tensile strength*

1.3.3 Differential Scanning Calorimetry (DSC)

Differential scanning calorimetry is an important technique to determine the thermal properties of materials. It measures the amount of energy (heat) absorbed or released by a sample when it is heated or cooled at a controlled rate or held at constant temperature.

Typically two types of DSC systems are used; one is *power compensation DSC* where the sample and reference have individual identical heaters and the temperatures of both are controlled independently. The temperature of sample and reference are made identical by varying the power input/output to the two furnaces. The energy required to establish identical temperatures is the measure of enthalpy or heat capacity change in the sample relative to the reference. Alternatively, the difference between the power output of the sample and reference cells corresponds to heat capacity of the sample at that temperature. Second is *heat flux DSC*, where the sample and reference are connected by low resistance heat flow path (a metal disc) which is assembled in a single heater. The temperature

difference between sample and reference due to enthalpy or heat capacity changes in the sample is recorded and related to the enthalpy change in the sample using calibration experiment. DSC applications include investigations of glass transition temperature, heat of melting, crystallization studies and identification of phase transformations. This method is used to study processes such as, non-isothermal melting and crystallization as a function of temperature and crystallization at constant temperature. Heat of fusion of the sample and it's comparison with the heat of fusion of fully crystalline sample which gives the crystallinity of the sample.

In the case of DSC instruments such as Perkin Elmer DSC-2 (power compensation type of DSC) and DSC-7 equipped with Thermal Analysis Data station software, the sample holder assembly contains two platinum alloy cups and has individual heater and sensor. The differential power required for maintaining identical conditions is equivalent to the rate of energy absorption or evolution of the sample. The instrument is calibrated for temperature and energy scales using indium and tin as standards. A weighed amount of sample is crimped in an aluminium sample holder with cover and is directly placed in the sample holder.

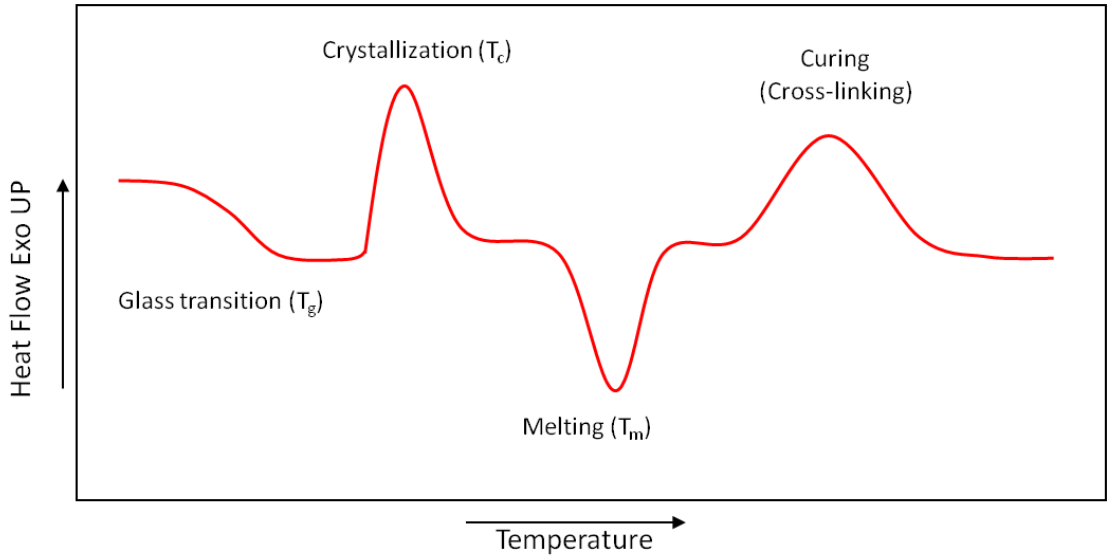

Figure 1.4 *Typical DSC thermogram for polymer*

A typical DSC thermogram for polymer is shown in **Figure 1.4**. The X-axis is the temperature and the Y-axis shows the difference in heat output at a given temperature. In the case of isothermal heating the X-axis is replaced with time instead of temperature.

The amount of heat taken up by the material to increase the temperature by a certain amount is called the heat capacity, or C_p. Heat capacity can be calculated by dividing the heat supplied as a result of the temperature increase. Polymers have a higher heat capacity above the glass transition temperature (T_g). Due to this change in heat capacity that occurs at the glass transition, DSC can be used to measure T_g of polymers. It will be seen from the **Figure 1.4** that the change doesn't occur suddenly, but takes place over a temperature range. This makes it tricky of picking one discreet T_g. However, the middle of the inclination is taken as the T_g. If the polymer is heated further, it gives off heat as it crystallizes and an exothermic transition or peak will appear in DSC curve. Usually, the temperature at the bottom of the peak is considered as crystallization temperature (T_c). Upon further heating more heat energy is added to the polymer to make it melt and an endothermic transition or peak appear. Usually, the temperature at the top of this transition is considered as melting point (T_m). Because there is a change in heat capacity, but there is no latent heat involved with the glass transition, we call the glass transition a second order transition. Transitions like melting and crystallization, which do have latent heats, are called first order transitions. Typically, during the curing of polymers like reaction of epoxy resin with amine hardener there is an exothermic transition, which can be clearly seen in DSC analysis and can be used to study the kinetics of curing.

1.3.4 Thermogravimetric Analysis (TGA)

Thermogravimetric analysis (TGA) is a thermal analysis technique used to measure the changes in the weight of samples as a function of temperature and/or time. TGA is commonly used to investigate properties such as thermal stability, oxidation or decomposition temperature, polymer degradation temperatures, residual solvent levels, absorbed moisture content and the amount of inorganic filler in polymer or composite materials. The sample is placed in a small pan attached to a sensitive microbalance and subsequently sample holder portion of the TGA balance assembly is placed into a high temperature furnace. The sample is heated at controlled manner and/or held isothermally

for a specific time. The balance assembly measures the initial sample weight at room temperature and then continuously monitors changes in sample weight (losses or gains) as heat is applied to the sample.

1.3.5 Scanning Electron Microscopy (SEM)

The SEM uses a beam of electrons to scan the surface of a sample to build a three-dimensional image of the specimen. A brief description of the instrument is given below:

An electron gun with a filament is housed on top of a column which generates a beam of electrons directing towards the sample housed in specimen chamber with vacuum. The filament in the gun is made of tungsten and is heated to generate a fine beam of electrons. To extend the life of the filament, the amount of current flowing through it is carefully regulated. As the filament current increases, there will be a point at which a maximum number of electrons are emitted from the filament. This is called filament saturation. When the electron beam hits the sample, the interaction of electrons and the atoms of the sample generate a variety of signals as shown in **Figure 1.5** (SEM schematic by Jason Kammerdiener). Depending on the sample, these can include secondary electrons (electrons from the sample itself), backscattered electrons (beam electrons from the filament that bounce off nuclei of atoms in the sample), X-rays, light, heat, and even transmitted electrons (beam electrons that pass through the sample).

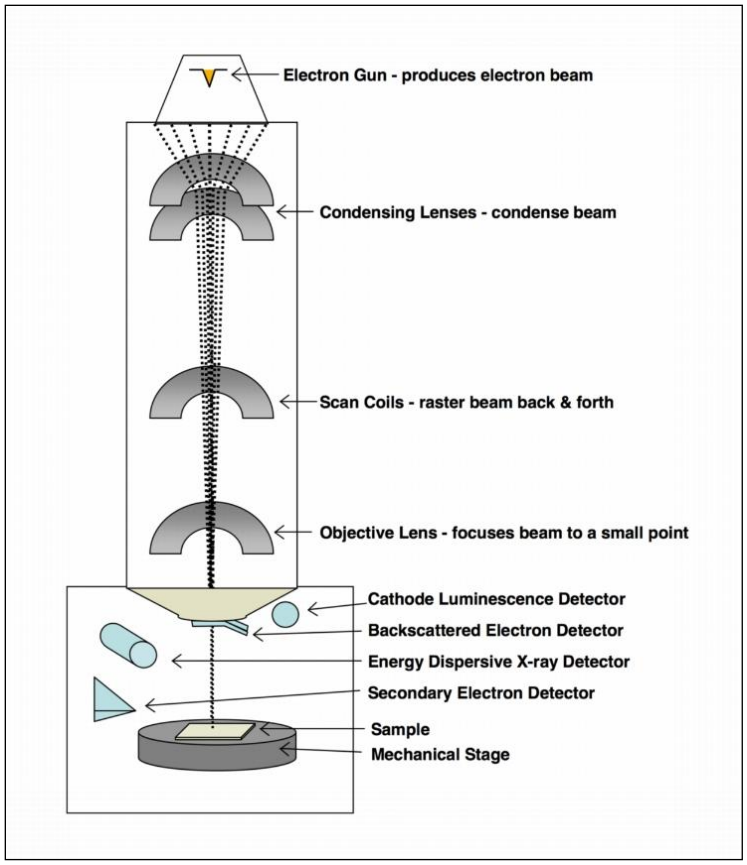

Figure 1.5 *Schematic of SEM*

SEM has several detectors to view the electron signals from the sample. Unlike the light microscope in which light forms an instant "real image" of the specimen, the electrons in an SEM don't form a real image. Instead, the SEM scans its electron beam line by line over the sample. Gradually, the image is built on a CRT monitor. The accelerating voltage is the speed of the electron in the electron beam that stream towards the specimen. It is measured in kilovolts (KV). A high accelerating voltage allows the electrons to penetrate deeply into the sample, and a low accelerating voltage provides information from the very surface of the sample. The SEM has a much greater resolution capability than the light microscope because the wavelength of the electrons is about 100,000 times smaller than the wavelength of light. Resolution is the ability to distinguish between two closely-spaced points. The resolution of scanning electron microscope is 3 to 6 nm which is almost 100 times higher than the light microscope. This is why we can see so much more detail with electron microscopes than light microscopes.

SEM has been effectively used for analyzing fractured surfaces of toughened epoxy adhesives to investigate the morphology of toughening agents in the epoxy matrix which will help in structure property relationship.

1.3.6 Transmission Electron Microscope (TEM)

The path of the electron beam in the transmission electron microscope (TEM) differs from that of the SEM as shown in **Figure 1.6**. In SEM the information is obtained from backscattered electron beam where as in TEM the transmitted electron beam gives the information.

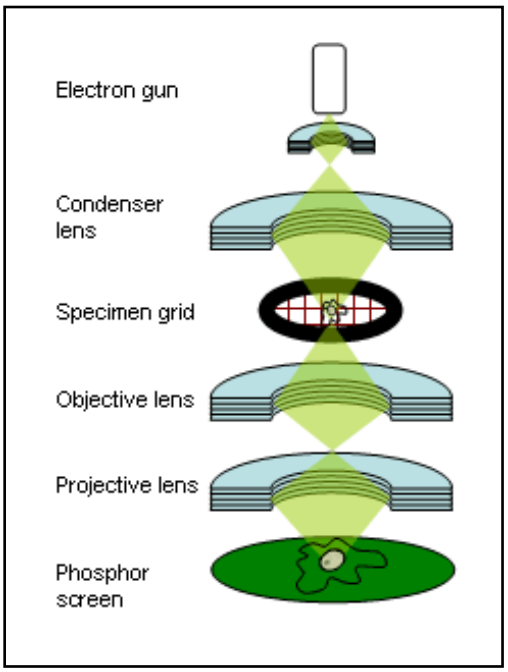

Figure 1.6 *Schematic of TEM*

Condenser focuses the ray of electrons through the object, where it is partially deflected. The degree of deflection depends on the electron density in the object. The greater the mass of the atoms, the greater is the degree of deflection. Therefore, objects with low atomic numbers (C, H, N, O) have weak contrasts. Consequently, it is necessary to treat the preparations with special contrast enhancing chemicals (heavy metals) to get at least some contrast. Additionally samples are not thicker than 100 nm, since the temperature can increase due to electron absorption which can lead to destruction of the sample. After passing the object the scattered electrons are collected by an objective where an image is

formed and subsequently enlarged by an additional lens-system called projective lens with electron microscope. The image thus formed is made visible on a fluorescent screen or it is documented on photographic material. Photos taken with electron microscopes are always black and white and the degree of darkness corresponds to the electron density (equals differences in atom masses) of the candled preparation.

1.3.7 Scratch resistance test

Scratch resistance test was carried out using Sheen made automatic scratch tester (REF 705/1). The test was conducted by increasing the load to determine the minimum load at which the coating was penetrated (ASTM D5178).

1.3.8 Abrasion resistance test

An abrasion resistance of coatings was measured by a method of rotating wheels using Taber Abraser apparatus. This apparatus/instrument is widely used for evaluating the wear abrasion resistance of organic coatings. A procedure for its use is given in ASTM test method for abrasion resistance of organic coatings by Taber Abraser (ASTM D 4060)[97]. The method utilizes a specimen in the form of a 4-inch (10.2 cm) diameter disk or a square mounted on a turntable that is rotated at a fixed speed under a weighted abrading wheel. The "calibrase" resilient abrading wheels are designated as CS-10 and CS-17 with the latter being the most abrasive. Before each test and after 500 cycles (revolutions), the abrading wheel is resurfaced with an abrasive disk. A vacuum pickup is produced to remove any loose particles generated during actual test. Wear abrasion resistance is expressed in terms of (a) wear index, which is the weight loss per specified number of revolutions (usually 1000) under specified load (500g or 1000g), and/or (b) wear cycles per mil, which is the number of cycles required to wear through a 1-mil thickness of coatings and is reported as the number of revolutions per mil.

1.3.9 Specular gloss

Standard gloss measurements were executed on Sheen made Tri-microgloss meter which complies with the ASTM Standard Method D523. This method designates three angles (20°, 60° and 85°) for measurement, depending on the gloss of the surface. Theoretically,

measurements are made relative to a highly polished black glass standard with a refractive index of 1.567. The gloss of the standard is assigned a value of 100 specular gloss units (SGU) for each geometry. The % gloss was measured at 60° angle.

References

1. H. Burrell, Off. Dig. Fed. Soc. Paint Technol. **34**(445), 131-161 (1962).
2. F. Lin and D. J. Meier, Progress in Organic Coatings **29**(1-4), 139-146 (1996).
3. E. S. Daniels and A. Klein, Progress in Organic Coatings **19**(4), 359-378 (1991).
4. D. Kotnarowska, M. Przerwa, and M. Wojtyniak, Journal of Vibroengineering **13**(4), 870-875 (2011).
5. C. W. Peng, C. H. Hsu, K. H. Lin, P. L. Li, M. F. Hsieh, Y. Wei, J. M. Yeh, and Y. H. Yu, Electrochimica Acta **58**, 614-620 (2011).
6. Q. C. Zhang, J. K. Hu, and S. L. Gong, Journal of Applied Polymer Science **122**(5), 3064-3070 (2011).
7. H. J. Naghash and B. Abili, Progress in Organic Coatings **69**(4), 486-494 (2010).
8. F. X. Qiu, J. L. Zhang, D. M. Wu, and D. Y. Yang, Plastics Rubber and Composites **39**(10), 454-459 (2010).
9. X. Wang, Y. A. Hu, L. Song, W. Y. Xing, H. D. Lu, P. Lv, and G. X. Jie, Surface & Coatings Technology **205**(7), 1864-1869 (2010).
10. D. Dieterich, Progress in Organic Coatings **9**, 281 (1981).
11. J. W. Rosthauser and K. Nachtkamp, Advances in Urethane Sci. and Tech. **10**, 121 (1987).
12. Ganss and Helmut, (2004).
13. M. G. Lu, J. Y. Lee, M. J. Shim, and S. W. Kim, Journal of Applied Polymer Science **86**(14), 3461-3465 (2002).
14. L. S. Ramanathan, K. G. Raut, S. R. Srinivasan, and S. Sivaram, U. S. 6239213 B1 (2001).
15. S. Zhou, L. Wu, J. Sun, and W. Shen, Progress in Organic Coatings **45**(1), 33-42 (2002).
16. E. Barna, B. Bommer, J. Kursteiner, A. Vital, O. von Trzebiatowski, W. Koch, B. Schmid, and T. Graule, Composites Part a-Applied Science and Manufacturing **36**(4), 473-480 (2005).
17. E. P. Giannelis, Advanced Materials **8**(1), 29-35 (1996).

18. P. B. Messersmith and E. P. Giannelis, Chemistry of Materials **6**(10), 1719-1725 (1994).
19. P. B. Messersmith and E. P. Giannelis, Journal of Polymer Science Part A-Polymer Chemistry **33**(7), 1047-1057 (1995).
20. J. W. Gilman, T. Kashiwagi, J. E. T. Brown, S. Lomakin, E. P. Giannelis, and E. Manias, "Flammability studies of polymer layered silicate nanocomposites," in *43rd International Sampe Symposium and Exhibition on Materials and Process Affordability - Keys to the Future, Vol 43* (1998), pp. 1053-1066.
21. C. X. Xiong and D. J. Wen, Transactions of Nonferrous Metals Society of China **9**(2), 312-317 (1999).
22. J. Gilberts, A. H. A. Tinnemans, M. P. Hogerheide, and T. P. M. Koster, Journal of Sol-Gel Science and Technology **11**(2), 153-159 (1998).
23. C. M. Chan, G. Z. Cao, H. Fong, M. Sarikaya, T. Robinson, and L. Nelson, "Organic/inorganic hybrid sol-gel derived hard coatings on plastics," in *Organic/Inorganic Hybrid Materials Ii* (1999), pp. 319-324.
24. J. I. Chen, R. Chareonsak, V. Puengpipat, and S. Marturunkakul, Journal of Applied Polymer Science **74**(6), 1341-1346 (1999).
25. S. E. Yoon, H. G. Woo, and D. P. Kim, Polymer-Korea **24**(3), 389-398 (2000).
26. Y. X. Pan, Z. Z. Yu, Y. C. Ou, and G. H. Hu, Journal of Polymer Science Part B-Polymer Physics **38**(12), 1626-1633 (2000).
27. Y. Kurokawa, H. Yasuda, and A. Oya, Journal of Materials Science Letters **15**(17), 1481-1483 (1996).
28. C. P. Wong and R. S. Bollampally, Journal of Applied Polymer Science **74**(14), 3396-3403 (1999).
29. R.E. Van Doren, D.N. Nash, and A. Smith, J Protective Coatings Linings **6**, 47-52. (1989).
30. B. Abramoff and J. Covino, Journal of Applied Polymer Science **46**(10), 1785-1791 (1992).
31. S. Fellahi, S. Boukobbal, and F. Boudjenana, Journal of Vinyl Technology **15**(1), 17-21 (1993).

32. H. Cochrane and C. S. Lin, Rubber Chemistry and Technology **66**(1), 48-60 (1993).
33. M. I. Aranguren, E. Mora, C. W. Macosko, and J. Saam, Rubber Chemistry and Technology **67**(5), 820-833 (1994).
34. M. I. Aranguren, E. Mora, and C. W. Macosko, Journal of Colloid and Interface Science **195**(2), 329-337 (1997).
35. M. J. Wang, Rubber Chemistry and Technology **71**(3), 520-589 (1998).
36. C. Zilg, R. Thomann, R. Mulhaupt, and J. Finter, Advanced Materials **11**(1), 49-52 (1999).
37. Z. Wang and T. J. Pinnavaia, Chemistry of Materials **10**(12), 3769-3771 (1998).
38. H. J. Glasel, F. Bauer, H. Ernst, M. Findeisen, E. Hartmann, H. Langguth, R. Mehnert, and R. Schubert, Macromolecular Chemistry and Physics **201**(18), 2765-2770 (2000).
39. F. Bauer, H. Ernst, U. Decker, M. Findeisen, H. J. Glasel, H. Langguth, E. Hartmann, R. Mehnert, and C. Peuker, Macromolecular Chemistry and Physics **201**(18), 2654-2659 (2000).
40. F. Bauer, H.Ernst, D. Hirsch, M. Pelzing, V. Sauerland, and R. Mehnert, Eurpean Coating Journal **6**, 707 (2003).
41. F. Bauer, H. J. Glasel, U. Decker, H. Ernst, A. Freyer, E. Hartmann, V. Sauerland, and R. Mehnert, Progress in Organic Coatings **47**(2), 147-153 (2003).
42. F. Bauer, H. Ernst, D. Hirsch, S. Naumov, M. Pelzing, V. Sauerland, and R. Mehnert, Macromolecular Chemistry and Physics **205**(12), 1587-1593 (2004).
43. B. K. G. Theng, *Formation and properties of clay-polymer complexes* (Amsterdam: Elsevier, 1979).
44. A. Okada, M. Kawasumi, A. Usuki, Y. Kojima, T. Kurauchi, and O. Kamigaito, "NYLON 6-CLAY HYBRID," in *Polymer Based Molecular Composites* (1990), pp. 45-50.
45. P. C. LeBaron, Z. Wang, and T. J. Pinnavaia, Applied Clay Science **15**(1-2), 11-29 (1999).
46. T. D. Ngo, M. T. Ton-That, S. V. Hoa, and K. C. Cole, Polymer Engineering and Science **47**(5), 649-661 (2007).

47. R. A. Vaia, H. Ishii, and E. P. Giannelis, Chemistry of Materials **5**(12), 1694-1696 (1993).
48. M. Kawasumi, N. Hasegawa, A. Usuki, and A. Okada, Materials Science & Engineering C-Biomimetic and Supramolecular Systems **6**(2-3), 135-143 (1998).
49. D. C. Lee and L. W. Jang, Journal of Applied Polymer Science **68**(12), 1997-2005 (1998).
50. T. Lan, P. D. Kaviratna, and T. J. Pinnavaia, Chemistry of Materials **7**(11), 2144-2150 (1995).
51. X. Kornmann, H. Lindberg, and L. A. Berglund, Polymer **42**(4), 1303-1310 (2001).
52. W. Possart, International Journal of Adhesion and Adhesives **8**(2), 77-83 (1988).
53. S. Buchan and W. D. Rae, Trans Inst Rub Ind **20**, 205 (1946).
54. N. G. Gaylord and H. Dannenberg, Journal of Polymer Science **62**(173), S21-S21 (1962).
55. H. Lee and K. Neville, *Handbook of Epoxy Resin* (McGraw-Hill, Inc., New York, 1967).
56. C. May and Y. Tanaka, eds., *Epoxy Resins: Chemistry and Technology*, 2nd ed. (Marcel Dekker, Inc, New York., 1988).
57. Annu. Book ASTM Stand. Section 8 (Plastics). Web site: http://www.astm.org.
58. D. P. Sheih and D. E. Benton, "HPLC ANALYSIS FOR EPOXY COATINGS RESINS," in *Analysis of Paints and Related Materials : Current Techniques for Solving Coatings Problems* (1992), pp. 41-56.
59. H. Pasch, R. Unvericht, and M. Resch, Angewandte Makromolekulare Chemie **212**, 191-200 (1993).
60. J. Adrian, D. Braun, and H. Pasch, Angewandte Makromolekulare Chemie **267**, 82-88 (1999).
61. D. Crozier, G. Morse, and Y. Tajima, Sampe Journal **18**(5), 17-22 (1982).
62. U. Fuchslueger, H. Stephan, H. J. Grether, and M. Grasserbauer, Polymer **40**(3), 661-673 (1999).
63. R. R. Jay, Analytical Chemistry **36**(3), 667-668 (1964).

64. B. Dobinson, W. Hofmann, and B. Stark, *The Determination of Epoxide Groups* (Pergamon Press, Elmsford, New York., 1969).
65. W. Lwowski, "Comprehensive Heterocyclic Chemistry," A. R. Katritsky and C. W. Rees, eds. (Pergamon Press, Oxford, 1984), p. 1.
66. R. E. Parker and N. S. Isaacs, Chemical Reviews **59**(4), 737-799 (1959).
67. K. Horie, H. Hiura, M. Sawada, I. Mita, and H. Kambe, Journal of Polymer Science Part A-1-Polymer Chemistry **8**(6), 1357-1372 (1970).
68. A. Bosch, "Epoxy Resins," in *Polymeric Materials Encyclopedia,* J. C. Salamone, ed. (CRC Press Boca Raton, 1996), p. 2246.
69. L. Shechter, J. Wynstra, and R. P. Kurkjy, Industrial and Engineering Chemistry **48**(1), 94-97 (1956).
70. B. Ellis, ed., *Chemistry and Technology of Epoxy Resins,* 1 ed. (Blackie Academic, 1993).
71. I. T. Smith, Polymer **2**(1), 95-108 (1961).
72. M. Gordon and W. Simpson, Polymer **2**(4), 383-391 (1961).
73. M. A. Acitelli, R. B. Prime, and E. Sacher, Polymer **12**(5), 335-343 (1971).
74. M. R. Kamal, Polymer Engineering and Science **14**(3), 231-239 (1974).
75. S. Lunak, J. Vladyka, and K. Dusek, Polymer **19**(8), 931-933 (1978).
76. A. Dutta and M. E. Ryan, Journal of Applied Polymer Science **24**(3), 635-649 (1979).
77. J. B. Enns and J. K. Gillham, Journal of Applied Polymer Science **28**(8), 2567-2591 (1983).
78. J. M. Barton, Advances in Polymer Science **72**, 111-154 (1985).
79. I. C. Choy and D. J. Plazek, Journal of Polymer Science Part B-Polymer Physics **24**(6), 1303-1320 (1986).
80. K. P. Pang and J. K. Gillham, Journal of Applied Polymer Science **37**(7), 1969-1991 (1989).
81. K. P. Pang and J. K. Gillham, Journal of Applied Polymer Science **39**(4), 909-933 (1990).
82. G. Wisanrakkit and J. K. Gillham, Journal of Applied Polymer Science **41**(11-12), 2885-2929 (1990).

83. R. A. Venditti and J. K. Gillham, Journal of Applied Polymer Science **56**(13), 1687-1705 (1995).
84. B. G. Min, Z. H. Stachurski, and J. H. Hodgkin, Polymer **34**(21), 4488-4495 (1993).
85. B. G. Min, Z. H. Stachurski, and J. H. Hodgkin, Polymer **34**(23), 4908-4912 (1993).
86. S. Vyazovkin and N. Sbirrazzuoli, Macromolecules **29**(6), 1867-1873 (1996).
87. S. Pichaud, X. Duteurtre, A. Fit, F. Stephan, A. Maazouz, and J. P. Pascault, Polymer International **48**(12), 1205-1218 (1999).
88. F. X. Perrin, T. M. H. Nguyen, and J. L. Vernet, Macromolecular Chemistry and Physics **208**(7), 718-729 (2007).
89. Z. Dai, Y. F. Li, S. G. Yang, N. Zhao, X. L. Zhang, and J. Xu, European Polymer Journal **45**(7), 1941-1948 (2009).
90. M. J. Marks and R. V. Snelgrove, Acs Applied Materials & Interfaces **1**(4), 921-926 (2009).
91. R. S. Drake and A. R. Siebert, *Adhesive Chemistry Developments and Trends*, 1 ed., Polymer Science and Technology Sereis (Springer, 1985), Vol. 29, p. 871.
92. H. Dodiuk, S. Kenig, and I. Liran, Journal of Adhesion **22**(3), 227-251 (1987).
93. D. S. Jones, International Journal of Pharmaceutics **179**(2), 167-178 (1999).
94. E. E. Shafee and H. F. Naguib, Polymer **44**(5), 1647-1653 (2003).
95. J. Duncan, "Mechanical Properties and Testing of Polymers," G. M. Swallowe, ed. (Kluwer Academic, 1999), p. 43.
96. L. W. Hill, Progress in Organic Coatings **5**(3), 277-294 (1978).
97. J. V. Koleske, ed., *Paint and Coating Testing Manual*, 14 ed. (American Society for Testing and Materials, 1995), p. 925.

Polyurethane based coatings

Polyurethanes (PUs) are a unique class of polymers and exhibit both hard and soft segments within the same polymer chain. This combination results in PU coatings with high surface hardness, very good chemical resistance and toughness along with excellent flexibility, particularly at low temperatures where other polymers may become brittle [1, 2]. Furthermore, PUs displays excellent durability and abrasion resistance and offer excellent choice for coating applications.

Solvent-based polyurethane-acrylates have been extensively used in industrial coatings, especially automotive top-coat and refinishes due to their excellent chemical and abrasion resistance, durability and flexibility cum toughness properties. However, owing to increasing environmental awareness, stringent environmental controls on air emission have been imposed and the amount of organic solvents emitted from coating systems has been restricted. Consequently, extensive R&D efforts have been focused on the development of cost effective and low VOC waterborne coatings with high solids.

At the same time, organic–inorganic hybrid coatings have become increasingly important since they combine the advantages of both organic polymers (flexibility, ductility, dielectric strength, etc.) as well as inorganic materials (rigidity, high thermal stability, UV-shielding property, and high refractive index, etc.) [3-6]. The properties of organic–inorganic hybrid coatings strongly depend on the method of preparation, dispersion of inorganic filler into organic matrix and the interaction between organic and inorganic phases. It is reported that nano-silica could increase the hardness and scratch resistance of a coating without affecting the transparency of coatings [7, 8].

Although there are extensive studies on the PUDs and polyurethane nano composites, these are only a few reports on the water-borne organic-inorganic hybrid coatings based on polyurethane matrix and silane modified silica nano particles. Therefore, the first part of the thesis work is focused on preparation and characterization of coatings from the blends of PUDs and acrylic emulsion. A new approach for the preparation of coatings

from dispersions obtained by reacting mixtures of polyols (polyester polyol and acrylic polyol) with diisocyanate is discussed. Finally, organic-inorganic hybrid coatings were prepared using PUDs and silica nano particles and characterized/evaluated in terms of coating properties.

Epoxy resin based adhesives

The second part of the thesis is dealt with epoxy resin based adhesives modified with reactive liquid polymers (RLPs).

Epoxy resins were introduced commercially in 1947 and their consumption increased by about 20% per year over the first four decades [9]. Epoxies are the most studied thermoset materials and have a very wide range of industrial applications which include adhesives, molding powders, potting and encapsulating materials, tooling compounds, etc. The attractive features are the ease of processing, adhesion to a variety of substrates, outstanding corrosion resistance and low shrinkage upon cure. Despite several merits the major drawback of epoxies is brittleness or lack of crack growth resistance. Therefore, toughening of epoxies has become extremely important to ensure the feasibility of these materials for practical applications. Several studies have been reported on the enhancement of toughness of epoxy resin using reactive liquid polymers such as carboxyl-terminated butadiene acrylonitrile (CTBN), amino-terminated butadiene acrylonitrile (ATBN), etc [10, 11]. However, only scanty reports are available on the high temperature applications of these adhesives. In view of this, the work was undertaken to modify the epoxy adhesive by incorporating RLPs namely, CTBN and ATBN and the thermo mechanical properties, adhesion strength at high temperature (150°C) and morphology were studied by using DMA, UTM and SEM.

The main objectives of the present research work are as follows;

- To prepare silane modified silica nano particles using functional silane coupling agents
- To develop high performance Organic-Inorganic hybrid polymeric coatings with improved scratch and abrasion resistance
- To understand and correlate the structural attributes, which are responsible for exhibiting the scratch and abrasion resistant properties to the coatings
- To prepare epoxy adhesives using reactive liquid polymers (RLPs) such as carboxyl terminated acrylonitrile butadiene rubber (CTBN) and amine terminated acrylonitrile butadiene rubber (ATBN)
- To study the curing kinetics of toughened epoxy adhesives
- To study structure property relationship in toughened epoxy resin

References

1. J. W. Rosthauser and Nachtkamp, "Waterborne Polyurethanes, Advances in Urethane Science and Technology," Klaus, ed. (1987), pp. 121 - 162.
2. R. E. Tirpak and P. H. Markusch, Journal of Coatings Technology **58**(738), 49-54 (1986).
3. X. Y. Shang, Z. K. Zhu, J. Yin, and X. D. Ma, Chemistry of Materials **14**(1), 71-77 (2002).
4. Y. Y. Yu, C. Y. Chen, and W. C. Chen, Polymer **44**(3), 593-601 (2003).
5. Y. Y. Yu and W. C. Chen, Materials Chemistry and Physics **82**(2), 388-395 (2003).
6. S. X. Zhou, L. M. Wu, J. Sun, and W. D. Shen, Progress in Organic Coatings **45**(1), 33-42 (2002).
7. M. L. Bock, DE), Engbert, Theodor (Koln, DE), Groth, Stefan (Leverkusen, DE), Klinksiek, Bernd (Bergisch Gladbach, DE), Yeske, Philip (Koln, DE), Jonschker, Gerhard (Spiesen-Elversberg, DE), Dellwo, Ulrike (Saarbrucken, DE), (2000).
8. B. M. Novak, Advanced Materials **5**(6), 422-433 (1993).
9. C. A. May, *Introduction to Epoxy Resins, Epoxy Resins, Chemistry, and Technology* (Marcel Dekker: New York, 1988).
10. A. C. Garg and Y. W. Mai, Composites Science and Technology **31**(3), 179-223 (1988).
11. R. Bagheri, B. T. Marouf, and R. A. Pearson, Polymer Reviews **49**(3), 201-225 (2009).

3.1 Aqueous polyurethane dispersions

3.1.1 Introduction

Waterborne coatings based on aqueous polyurethane dispersions are attracting increasing attention recently, because of their non-toxic, non-flammable and environmentally friendly nature [1].

Polyurethanes owe their versatility of application to the wide range of properties possible. This is due to their morphology in which the soft segment is usually formed by a polyol and the hard segment by the diisocyanate. Phase separation results in the hard segment aggregating into domains in the soft segment matrix. Polyurethane dispersions (PUDs) share this morphology with conventional solvent based and moisture curing PU and so a wide range of properties are possible. A further advantage of this type of morphology is the excellent film forming properties due to the soft, i.e. low, glass transition temperature (T_g) segment. In addition, the exceptional performance properties, for example, toughness, abrasion resistance, hardness, low temperature flexibility, chemical resistance and adhesion, make PUDs suitable for a wide range of coating applications.

Although the chemistry and technology of PUDs has been established for more than 20 years, it is only in the last 10 to 15 years that they have achieved real commercial significance. Evidence for this is shown in the rise of patent applications for PUDs in recent years. The majority of recent patents focus on tailoring PUDs for specific end applications.

Polyurethane dispersions are binary colloidal systems having polyurethane (PU) particles (size 0.01 to 1 μm) dispersed in continuous aqueous phase. In order to enhance the dispersibility in aqueous media, ionic groups are introduced along the polymer chains by using hydrophilic monomers or hydrophilic internal emulsifiers. The dispersions obtained using internal emulsifier, such as dimethylol propionic acid (DMPA) have fine particle size, better stability and give films with good water resistance. Most of the work on aqueous PUDs has been replaced from industrial laboratories and is patented. These patents have been well revised and documented by Dieterich [2], Rosthauser and Nachtkamp [3]. The dispersions can be formulated into coatings and adhesives containing

little or no solvent and can be applied on to plastics or other substrates, which are sensitive to solvent attack. The viscosity of dispersion is independent of molecular weight of the polyurethane but dependent on average particle size, particle size distribution and solids content. Therefore, PUDs can be prepared at high molecular weight with low viscosity and can be easily coated on to substrates. The coating properties of PUDs such as gloss, water resistance are comparable to those of conventional solvent borne polyurethane lacquers and two component polyurethanes coatings [4-7]. The basic building blocks used for the preparation of aqueous PUDs are the same as those used for conventional solvent borne polyurethanes. However, cycloaliphatic diisocyanates are preferred over aromatic ones due to their higher light stability and lower reactivity with water.

This chapter is divided in two parts: in the first part (A), synthesis and characterization of water-borne PUDs with the blends of acrylic emulsion (AE) is discussed. In the second part (B), a new approach for making PUDs using two polyols (polyester polyol and acrylic polyol) simultaneously is reported.

3.2 Part A: Aqueous polyurethane dispersion (PUD) based on blends of PUDs and acrylic emulsion

3.2.1 Introduction

Polymer blends have become important for both scientific investigation and commercial product development, because polymer blends can be tailored to meet the requirements of specific applications. They can be developed much more quickly than new polymers and require less capital investment. Polymer blends provide an efficient way to satisfy new requirements for material properties, in which improved process ability and properties are achieved by combining the individual properties of pure components [8]. Polymer blends are produced by mechanical mixing of two or more molten polymers or polymer solutions. However, the incompatibility of most polymers is generally a major problem for the homogeneous blending of polymers. The properties of the blends are largely dependent upon the degree of miscibility between the blend components. Polyurethane ionomer blends have been prepared by mixing two polyurethane ionomers in equimolar amounts of two oppositely charged groups in their respective polyurethane structures.

The greater mixing of soft and hard segments in the presence of charged groups has been demonstrated [9].

Acrylic polymer latex or acrylic emulsion and polyurethane dispersions have their own characteristic advantages and disadvantages. Acrylic polymer latex films posses excellent weatherability, hardness, water and alkali resistance due to the main polymer backbone i.e. carbon-carbon bonds, and have been widely used for coatings, paper and textile finishes, cement additives and other applications. The elasticity and abrasion resistance of acrylate polymers are inferior to those of polyurethanes. On the other hand polyurethanes show performance properties such as excellent mar resistance, toughness, adhesion and superior low temperature impact. PUDs have been used in various coatings, but suffer from poor hardness, water and alkali resistance.

The properties of polyurethane dispersions can be modified by varying the composition of their building blocks, such as polyols and polyisocyanates or by using the chain extension chemistry [1].

In addition, PU coatings are solvent and chemical resistant offering good weather stability. It is possible to formulate both clear coats and pigmented topcoats with a high gloss finish. The films have very good mechanical properties and provide the ideal balance of hardness and flexibility, even at low temperatures. Good scratch resistance is also a feature of polyurethane coatings. This high level of quality results from the primary and secondary structures of the polyurethane chains. PU coatings allow high or variation of the property profile and can be fitted for a specific application by changing, for example, the chemical structure of the soft segments (polyether, polyester or polycarbonate), the distribution and length of the hard segments or the molecular weight and degree of branching of the chains. The hard segments are related to the hardness, strength and toughness of the paint film and the soft segments determine the flexibility and the glass transition temperature (T_g) [10].

Blending of PUDs and AEs can offer cost/performance advantages over common 1K coating materials such as polyurethane dispersions and acrylic emulsions. Further, the use of undesired solvent such as, NMP can be avoided in blend systems. Although some

solvent free PUDs have been reported [11] they are relatively expensive, and formulators have sought to reduce the cost by blending with other PUDs [12].

Blending is a simple and useful technique in coatings technology, and is very important in water-borne paints [13-21]. Acrylic emulsions (AEs) and polyurethane dispersions (PUDs) have their own characteristic advantages and disadvantages. AE films posses excellent weatherability, hardness, water and alkali resistance. However, adhesion, toughness, mar resistance, elasticity and abrasion resistance of AEs are inferior to those of PUDs. Therefore, in this work we have made an effort to develop environmentally friendly water borne coatings that combine the properties of both polymers in a synergistic way by blending PUD with AE. The influence of blending ratios on mechanical and coating properties of the films have been studied.

3.3 Experimental

3.3.1 Materials

Polyester polyol used in the preparation of polyurethane dispersions (PUD) was prepared from adipic acid, neopentyl glycol and trimethylol propane. Dimethylolopropoinic acid (DMPA) was supplied by M/s. Perstorp Chemicals, Sweden; Isophorone diisocyanate (IPDI) was procured from M/s. Hulls Corporation, Germany; N-methyl-2-pyrrolidone (NMP) was received from M/s. SD Fine Chem., India; and tri-ethylamine (TEA, M/s. Ranbaxy Laboratories, India) were of extra pure grade and were used as received. Acrylic monomers, *n*-butyl acrylate (*n*-BuA), methyl methacrylate (MMA), methacrylic acid (MAA) used for making acrylic emulsion were of commercial grade and were obtained from Acros Organics, India. Surfactants used were sodium dodecyl sulfate (SDS) from SD Fine Chem., India and Triton X 405 as nonionic surfactant form Aldrich Chemicals USA.

3.3.2 Preparation of polyester polyol (PEP)

In this work, branched polyester polyol was prepared by using neopentyl glycol (NPG), adipic acid (AA) and 1,2,6-hexane triol (HT) in the presence of a catalyst, dibutyltin oxide (DBTO) [6]. The HT was used to increase the average number of hydroxyl groups per molecule, which in turn increased the crosslink density of the film. The reaction scheme for the preparation of polyester polyol is shown in **Figure 3.1**. The procedure for the preparation PEP is described in the following: into a 2 L four neck round bottom flask equipped with a mechanical stirrer, a thermowell, a nitrogen gas inlet and a Dean Stark apparatus, predetermined quantities of neopentyl glycol (NPG) (423 g), adipic acid (AA) (594 g), hexane triol (HT) (140 g) and dibutyltin oxide (DBTO) (0.5 g) were charged. The flask was heated from room temperature to 210°C in a span of 8 h. The water of condensation was removed with the help of Dean Stark apparatus. The reaction was further continued for 3 h under nitrogen atmosphere. Upon collecting the required amount of water, the heating was stopped and the product was cooled to room temperature and analyzed for hydroxyl and acid values. The hydroxyl and acid values were found to be 200 mg KOH/gm and 2.06 mg KOH/gm respectively.

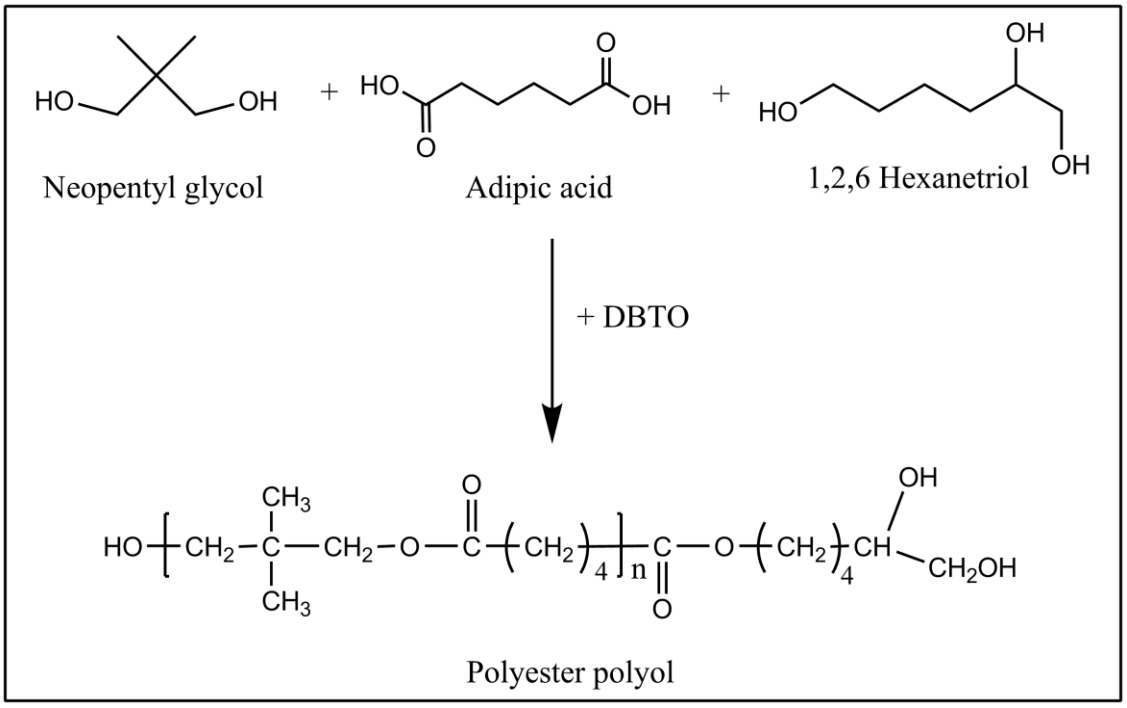

Figure 3.1 *Reaction scheme for the preparation of polyester polyol*

3.3.3 Preparation of polyurethane dispersion (PUD)

Urethane forming reaction was carried out in 500 ml four neck round bottom flask equipped with mechanical stirrer, thermowell, nitrogen gas inlet, condenser and dropping funnel, mounted in a constant temperature oil bath. Initially polyester polyol, DMPA and NMP were charged in the flask and the flask was heated to 70°C with continuous stirring in the flow of nitrogen gas. The contents were stirred for one hour at 70°C so that homogeneous polyol composition was obtained. Then from the dropping funnel, in a continuous stream of dry nitrogen gas, the required amount of IPDI was added drop wise, care being taken not to allow the temperature of flask to rise above 70°C for two hours. Progress of the reaction was determined by the percentage of isocyanate left unreacted in the flask. When the desired isocyanate content was reached, the flask was cooled below 50°C and the NCO terminated prepolymer was dispersed into the distilled de-ionized (DDI) water in the presence of neutralizing agent triethyl amine with the help of overhead stirrer. The composition and the reaction pathway for the preparation of polyurethane dispersion is shown in **Table 3.1** and **Figure 3.2** respectively**.**

Table 3.1 *Composition for Polyurethane Dispersion*

Raw Materials	Charge (g)
Polyester polyol	44.95
DMPA	5.15
NMP	37.25
IPDI	38.23
TEA	4.42
Water	120
Total	**250**

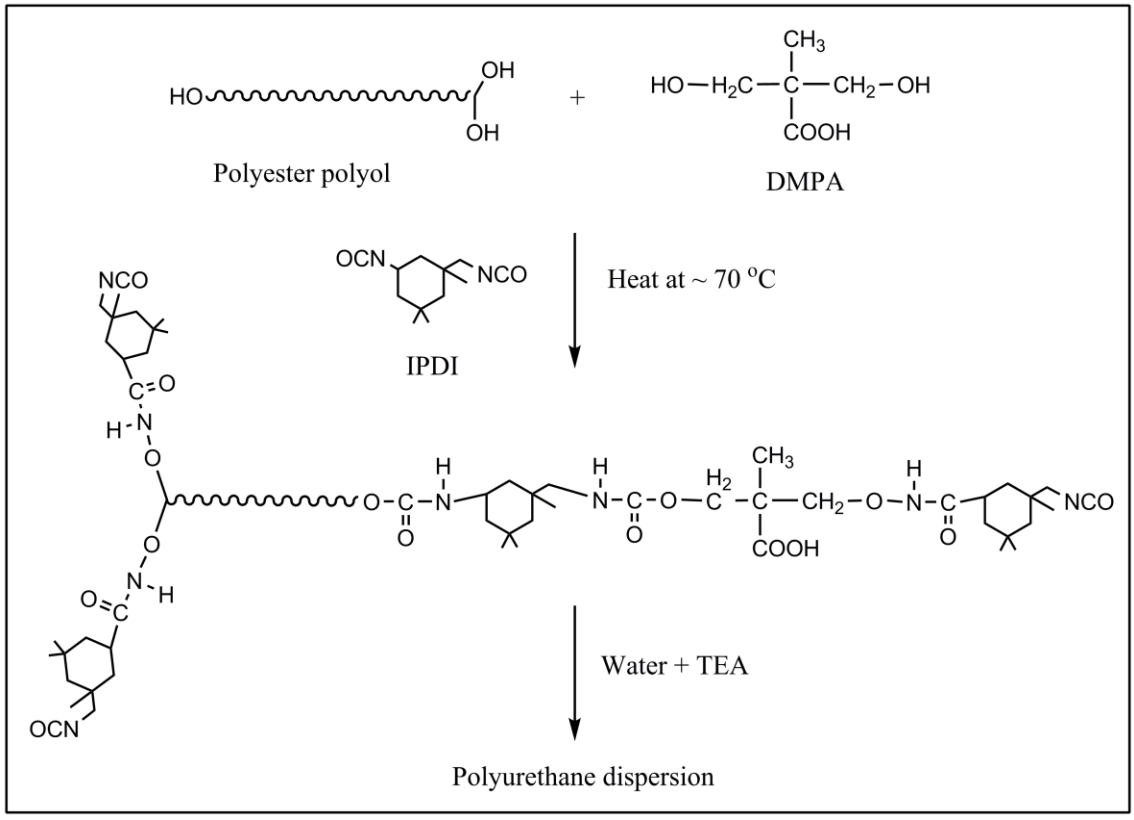

Figure 3.2 *Reaction scheme for the preparation polyurethane dispersion*

3.3.4 Preparation of acrylic emulsion

The recipe for the preparation of acrylic emulsion is given in **Table 3.2.** In a 500 ml four neck round bottom flask equipped with mechanical stirrer, gas bubbler, dropping funnel, condenser and thermowell, initially water and 1.8 g of emulsifier (mixture of Triton X405 and SDS in ratio 70:30 by weight) were charged. Monomer pre-emulsion was prepared by adding monomer mixture into DDI water with help of 4 g of emulsifier. Initiator solution was prepared by dissolving 0.54 g of ammonium persulphate in 3 gm of DDI water. The flask was heated to 80°C and the monomer pre-emulsion and initiator solution were added slowly to the flask over a period of about 3 hours by using peristaltic metering pump. The initiator addition lasted for about 2 hours. After completing the addition of monomers, the flask was maintained at 80°C for further ten minutes and then cooled to 55°C. At 55°C the contents of the flask were neutralized by adding ammonia solution and the emulsion was allowed to cool. The emulsion was then filtered and stored in a closed container. A typical laboratory setup for the preparation of acrylic emulsion is shown in **Figure 3.3.**

Table 3.2 *Recipe for the preparation of acrylic emulsion*

Raw Materials	**Charge (g)**
MMA	48
BA	46
EHA	2
MAA	1.6
Initiator	0.54
Emulsifier	5.8
Ammonia sol	2.06
DI Water	144
Total	**250**

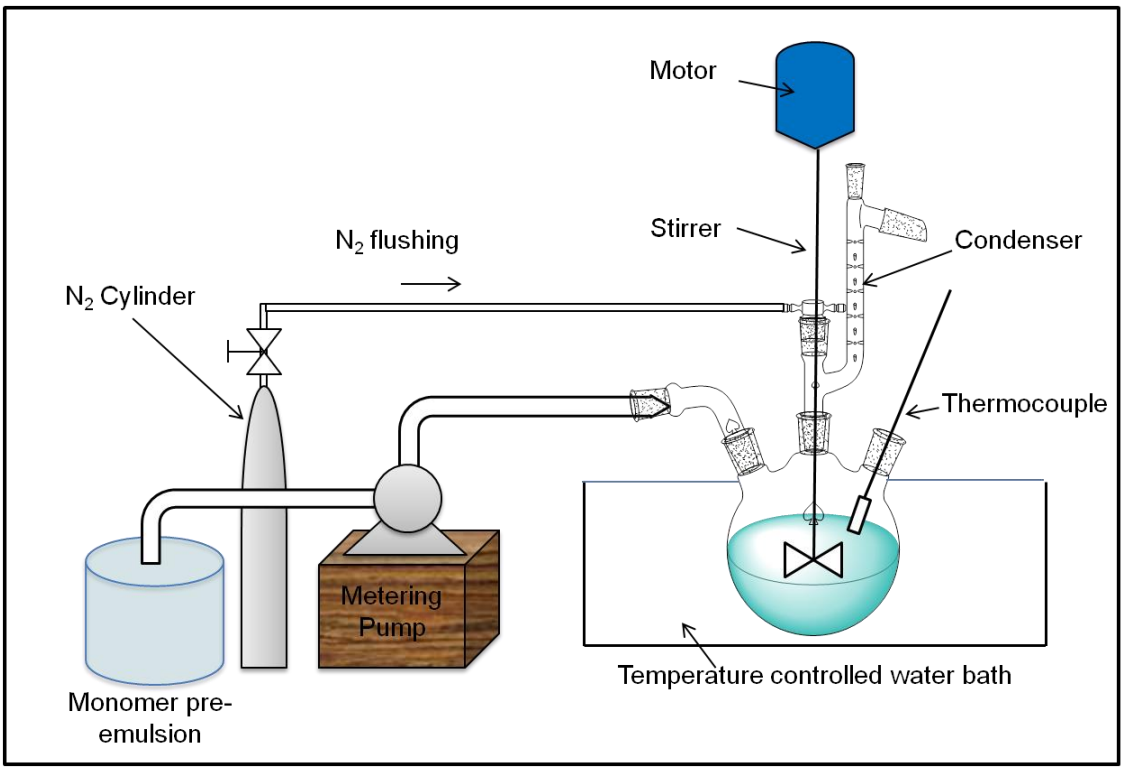

Figure 3.3 *A typical laboratory setup for the preparation of acrylic emulsion*

3.3.5 Preparation of blends from polyurethane dispersion (PUD) and acrylic emulsion (AE)

Polyurethane dispersion and acrylic emulsion prepared were mixed together with varying ratios (PUD/AE as 100/0, 75/25, 50/50 25/75 and 0/100) in wt% to form the blends. These blends were then coated on substrates for the evaluation of their coating properties.

3.4 Measurements and characterization

3.4.1 Characterization of dispersion

All the blends, PUD and AE were characterized for appearance, pH, and % solids. Viscosity was measured using Brookfield viscometer at room temperature and values were reported in centipoises (cps). The freeze–thaw stability test was performed in a glass vials filled with 15 ml dispersion. According to ASTM D2243, the samples were subjected to repeated cycles of 16 hours at -26°C followed by defrosting and storing at 23°C for 8 h. After each cycle, the blends were inspected for any visual change, like

phase separation or coagulation. Particle size was determined by dynamic light scattering (DLS) using Malvern II C instrument.

3.4.2 Film casting from dispersions

Films were cast by pouring the blends in Teflon mold and drying it at room temperature (27-30°C) for a week. The obtained films were having thickness around 1mm and were dried over night at 60°C in an oven at the reduced pressure of 20 mm Hg before testing.

3.4.3. FTIR-ATR analysis of films prepared from blends

Infrared spectra of blends were recorded on a Perkin Elmer GX, Fourier transform infrared spectrophotometer (FTIR) coupled with attenuated total reflectance (ATR). Spectra were taken with a resolution of 2 cm^{-1} and were averaged over 60 scans. The dispersion blends were cast on clean PTFE mold and dried at room temperature for a week, then dried at 60°C in vacuum oven for a day to prepare the films around 60µm thickness for FTIR-ATR analysis.

3.4.4 Mechanical properties of cast films

Tensile properties were measured using a universal tensile testing machine (Instron) according to ASTM D412 at a cross head speed of 50mm/min. Tests were performed at room temperature with dumb-bell type specimens. At least five runs were performed for each data point and an average was taken.

Dynamic mechanical properties were determined with a dynamic mechanical analyzer (Rheometry Scientific DMTA), using a rectangular tension compression geometry mode at a heating rate of 5°C/min and at the frequency of 10 rad/s.

3.4.5 Properties of coatings

Water based dispersions were coated on previously degreased aluminum substrates with the help of bar coater and allowed to dry for seven days before evaluating the coating properties of films. The dry film thickness of coating was around 80µm.

3.4.5.1 Scratch resistance

Scratch resistance test was carried out using Sheen made automatic scratch tester. The test was conducted by increasing the load to determine the minimum load, at which the coating was penetrated.

3.4.5.2 Abrasion resistance

Abrasion resistance of coatings was determined by using Teledyne Taber make Taber Abraser. In this test the coated test specimen was spun against two rotating abrasive wheels (CS-10) under 1 Kg load. The results of the test were expressed as weight loss of the coated test specimens in milligrams after 1000 cycles.

3.4.5.3 Gloss measurement

The % gloss was measured by using Sheen made Tri-microgloss instrument at 60° angle according to ASTM D523 method.

3.4.5.4 Water resistance

Water resistance test was performed by dipping the coated panel in water for a period of seven days and examining the haziness or blister formation on the film.

3.4.5.5 Solvent scrub resistance

Solvent scrub resistance test was performed manually using methyl ethyl ketone (MEK) as a solvent. The number of MEK double scrubs at which the coated film got removed from the substrate was reported as a solvent double scrub value.

3.5 Results and Discussion

The blends of PUD and AE were prepared by simple physical mixing of varying ratios of PUD/AE in wt % and analyzed for their dispersion and coating properties.

3.5.1 Dispersion properties

Table 3.3 shows dispersion properties of the systems used in this work. In general, the emulsion polymerization technique results in lower particle size of latexes as compared to the PUDs. The lower particle size of acrylic emulsion gives an indication of very fine dispersion of acrylate particles in the water with slightly higher viscosities as compared to PUD. The blends have similar particle sizes of PUD. There is no profound effect on the viscosities of the blends upon variation of the blend ratio. The particle size values were obtained in the range of 110 nm to 130 nm. The coating properties were not much influenced by particle size and viscosities. All the systems showed better dispersion stability as observed from zeta potential and Freeze-Thaw results.

Table 3.3 *Dispersion properties*

Properties	PUD	PUD:AE 75:25	PUD:AE 50:50	PUD:AE 25:75	AE
Appearance*	B	B	B	B	A
pH	8.77	8.74	8.83	8.16	9.11
Viscosity, cps, 30^0 C	17.5	13.1	9.72	8.1	37.4
% solid	40	40	40	40	40
Freeze-Thaw stability [a]	Passes	Passes	Passes	Passes	Passes
Particle size (nm)	126	130	113	130	80
Zeta potential (mV)	-46.26	-50.07	-56.51	-43.84	-70.60

* A = Milky white with blue tint, B = Milky white

a = -80^{o}C for 16h followed by 8h at room temperature.

3.5.2 FTIR analysis

Figure 3.4 shows the FTIR spectra of dried films of the blends and individual systems. The N-H and C=O stretching regions are shown in **Figure 3.5** and **Figure 3.6** respectively. It can be clearly seen from **Figure 3.4** that there is decrease in the peak intensity in the N-H stretching region with increase in AE content of the blends. And there is a decrease in the peak intensity of –CONH stretching at 1550 cm^{-1} with the increase in AE amount. The decrease in the –CONH intensity arises due to decrease in the overall PUD content in the blends.

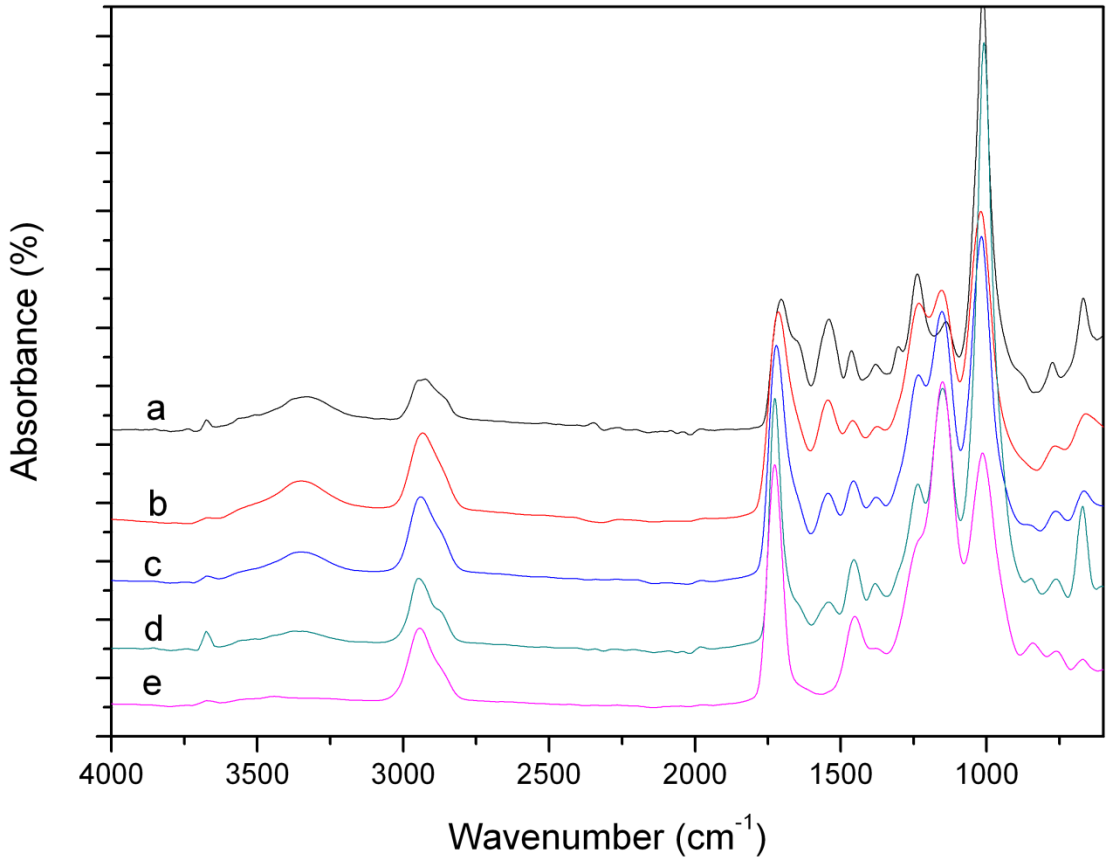

Figure 3.4 *FTIR spectra of the blends with different ratios of PUD/AE a) 100/0, b) 75/25, c) 50/50, d) 25/75 and e) 0/100.*

Figure 3.4

FTIR spectra have clearly demonstrated H-bonding interactions in polyurethanes [22]. The N-H group in PU can form H-bonding with the carbonyls of urethane/urea group and hard-soft segments of polyester. In general, the strength of hard-hard segment H-bonding is stronger than the hard-soft segment hydrogen bonding [23]. **Figure 3.5** indicates that the H-bonded N-H and free N-H absorption band at 3320 and 3340 cm^{-1} gradually decreased with the increase of AE content. The FTIR spectra in **Figure 3.6** also shows the decrease in H-bonded carbonyl peaks at about 1640 cm^{-1} and 1710 cm^{-1} and increase in the free carbonyl peak intensity with the increase of AE. Thus, the FTIR study of the films clearly revealed that there is a decrease in hydrogen bonding with increase of AE in PUD. It also goes in line with the absence of H-bonding interactions in neat acrylic emulsion films.

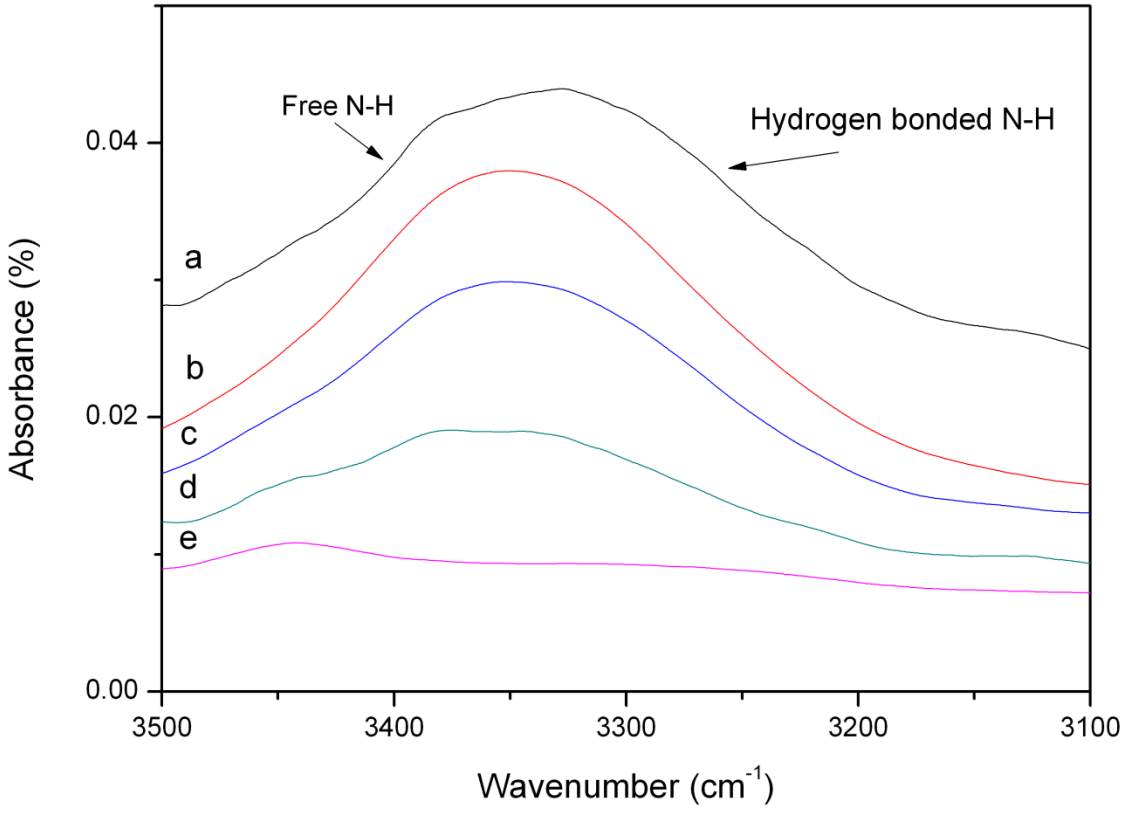

Figure 3.5 *FTIR spectra of the blends with different ratios of PUD/AE a) 100/0, b) 75/25,c) 50/50, d) 25/75 and e) 0/100 in NH stretching region*

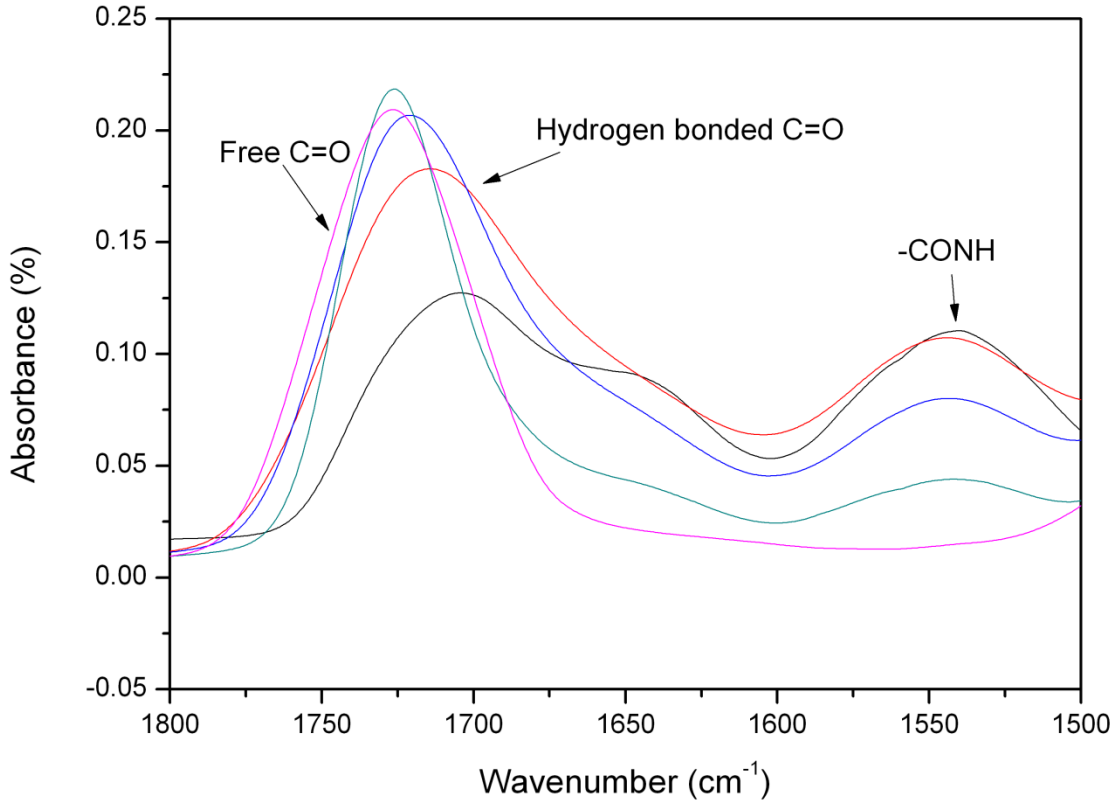

Figure 3.6 *FTIR spectra of the blends with different ratios of PUD/AE a) 100/0, b) 75/25, c) 50/50, d) 25/75 and e) 0/100 in C=O stretching region*

3.5.3 Dynamic mechanical analysis

Figure 3.7 presents DMA data, where the storage modulus (*E'*) versus temperature plot is shown in **(a)** and the tan δ versus temperature plot is shown in **(b)**. All samples showed a typical behavior of cross linked material with a glassy plateau region below -30 ^{o}C. The modulus of samples decreased with increasing AE content in the blend as shown in **Figure 3.7 (a)**. This behavior must be associated with the decrease in hydrogen bond interactions between the –NH groups of PUD and –COO groups of AE as a result of the decreasing amount of PUD content. The storage modulus of samples decreased continuously with increase of temperature. The tan δ variation with temperature is shown in **Figure 3.7 (b)**. However, there are no two or more distinct peaks in tan δ verses temperature curve indicating better mixing of the blends at all ratios. The shift in the peak, for α transition from 31°C for the blend with ratio of PUD/AE as 25/75 to 35°C for AE had shown that there is increase in T_g with the increase of AE content. However,

there is no clear peak for the blends containing the other ratios of PUD/AE. This may be attributed to the soft/hard segment interface association [25] which restricts the mobility of the chains of individual polymers.

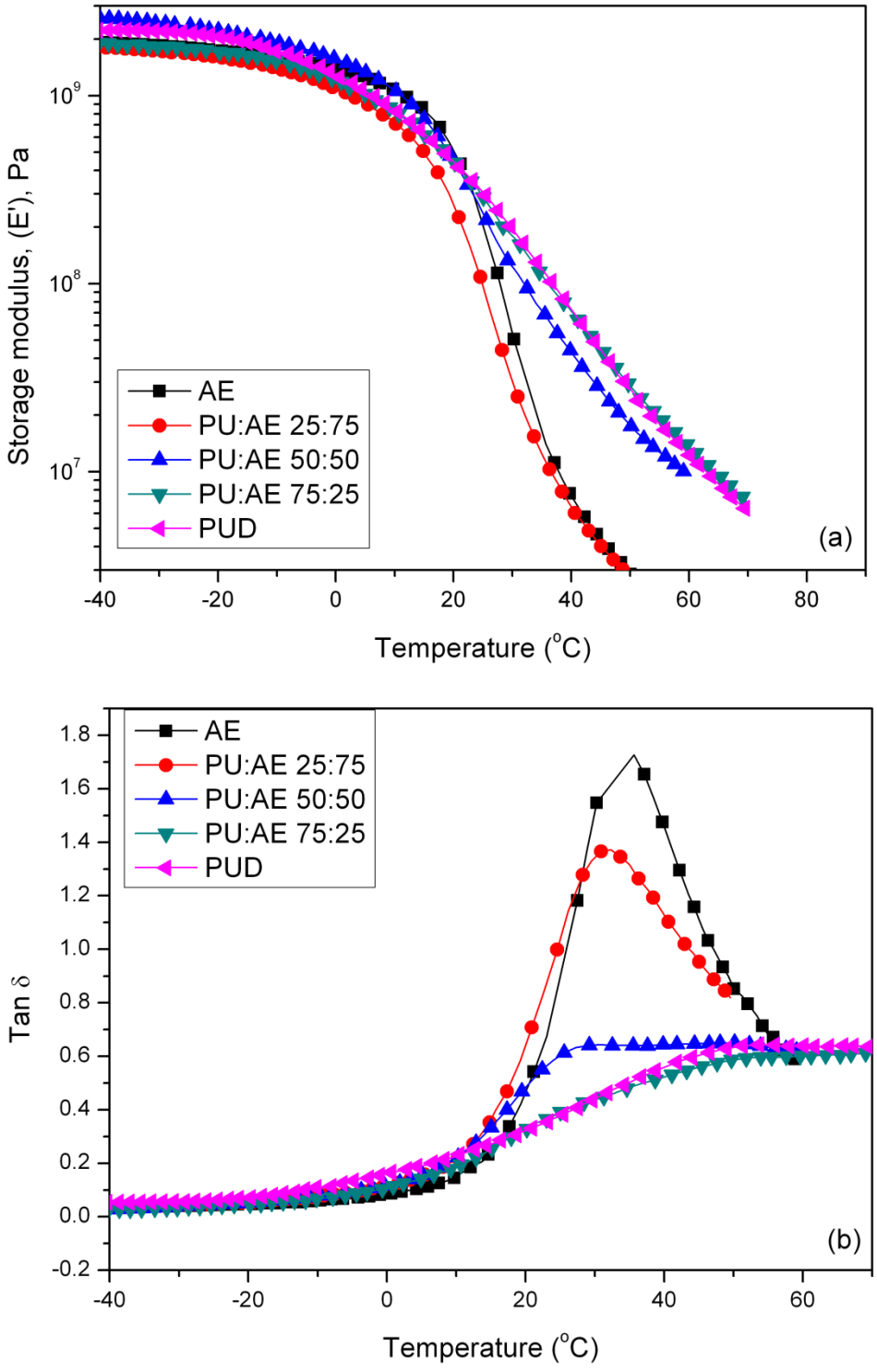

Figure 3.7 *Dynamic mechanical analysis plots of blends and individual polymers a) storage modulus vs temperature b) Tan δ vs temperature*

3.5.4 Mechanical properties of the films

The results of % elongation and tensile strength verses PUD/AE ratio for the films cast from all the samples are shown in **Figure 3.8.** There is no significant difference in % elongation of the films prepared from individual polymers (two points with circles joined by dotted lines in **Figure 3.8**). Whereas, the films prepared from the blends showed increase in % elongation. This could be attributed to the fact that in blends there can be better mixing and segmental interaction of flexible polyurethane chains with acrylate chains inducing the elongation property. Particularly, the film with ~50-60% PUD exhibited the highest % elongation (~60%). It can also be seen from the figure that the film cast from only PUDs showed the highest tensile strength. However, upon addition of acrylic emulsion, the tensile strength gradually decreased and almost reached the tensile strength of AE cast films. The decrease in tensile strength could be due to the dominance of rigid nature of the acrylic polymer as well as the absence of H-bonding interactions between the constituent components.

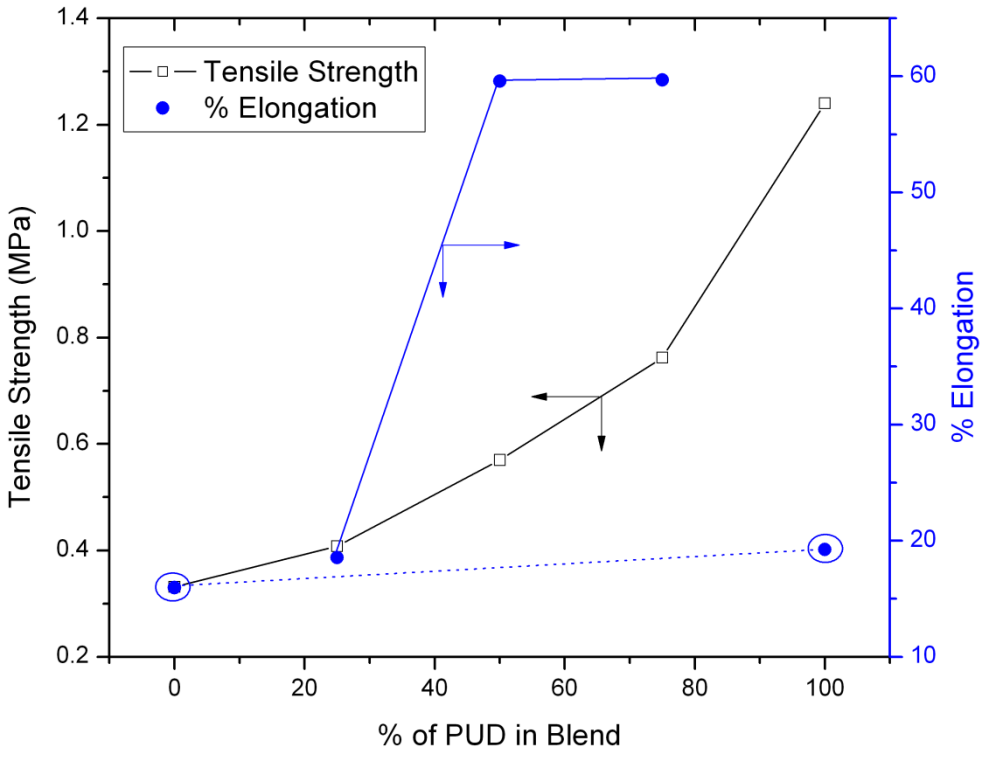

Figure 3.8 *Effect of PUD content on the mechanical properties of blends*

3.5.5 Properties of coatings

PUD, AE and their blends with varying ratios of PUD/AE were coated on metal panel and evaluated for coating properties such as scratch resistance, abrasion resistance, gloss level and solvent scrub resistance. The results obtained are shown in **Table 3.4**. It can be seen that, the scratch resistance of the films was maximum for coatings prepared from PUDs but decreases with the incorporation. It could be due to the fact that, the PUD containing polyester polyol, having functionality more than two, gives more cross linked coatings/films with high modulus as compared to the coatings prepared only from AE.

Table 3.4 *Properties of coatings*

Properties	PUD	PUD:AE 75:25	PUD:AE 50:50	PUD:AE 25:75	AE
Scratch hardness, gm	2500	2500	2400	2200	2100
Abrasion resistance[#]	35	43	48	54	60
Gloss @60°	+90	+90	+90	+85	+80
Water resistance	Good	Good	Good	Good	Good
Solvent resistance*	Poor	Poor	Poor	Poor	Poor

= mg loss @ 1 kg load using CS-l0 wheels & at 1000 revolutions; * = MEK double rubs.

Figure 3.9 shows the decrease in abrasion resistance (i.e. increase in weight loss) of coated films with increase in AE content. It is well known that, the abrasion resistance of PU films strongly depends upon the H-bonding interactions within the polymer matrix. The greater the H-bonding, higher is the resistance to abrade the film. Therefore, the decrease in H-bonding with increase of AE in blends manifests in the decrease of abrasion resistance of films. It can also be seen from **Table 3.4** that the blending of PUD and AE did not show improvement in solvent scrub resistance of the coatings. However, water resistance was found to be good with no sign of blistering, haziness or delamination of coating after water immersion test. It is also important to note that, gloss is perhaps the most important property required for most of the coatings, specifically when it is used as top coat. Normally, a decrease in gloss is observed with the presence of acrylics [10]. However, it is observed that the coatings prepared from the blends of all ratios

of PUD/AE showed glossy finish. This implied the smooth and better film forming characteristics of the dispersions.

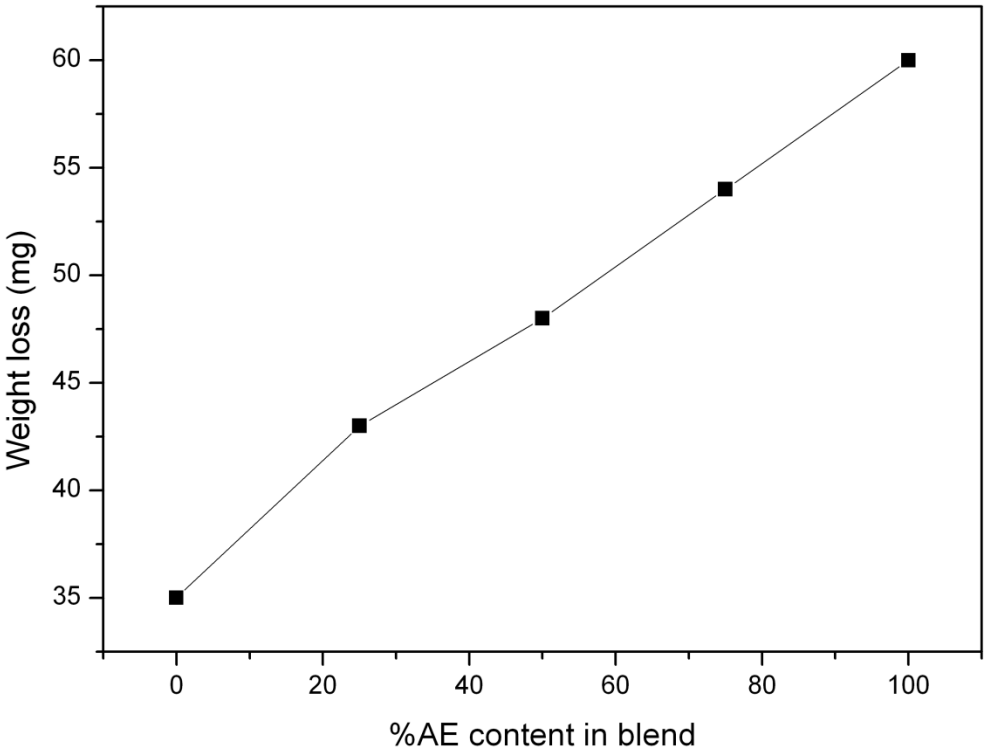

Figure 3.9 *Effect of AE content on abrasion resistance of coatings*

3.6 Conclusion of Part A

Stable dispersions of blends were successfully prepared by simple mixing of PUD and AE in different ratios. The dispersion properties such as particle size and viscosities of all the samples have more or less similar values and their effect on coating properties are negligible. From the FTIR study, the blends showed decrease in H-bonding interactions with increases of AE content in the system. The decrease in H-bonding interactions is responsible for the decrease in the mechanical properties, such as tensile strength and storage modulus of the films which was also confirmed by UTM and DMA studies. The simple technique of mixing of PUD and AE did not exhibit synergistic effect in scratch and abrasion resistance of coatings but all the blend systems showed smooth glossy finish.

3.7 Part B: Hybrid aqueous polyurethane dispersions based on polyester polyol and acrylic polyol

3.7.1 Introduction

Recently, urethane-acrylate hybrids have become important [26-40] because of their high performance properties and environmental advantages. These hybrid emulsions are expected to give synergistic properties of both acrylics and PUs.

Different combinations of PU with acrylic dispersions have been reported in the literature where PU is used as a co-binder of acrylic emulsions [41], dispersions [42], physical mixtures and composites [29, 32, 43, 44]. In some of the novel urethane-acrylate hybrids [45-48], a chemical coupling has been established between the urethane and acrylic component. For example, hydroxyalkyl acrylate terminated PU pre-polymers were synthesized and dissolved in acrylate monomers, followed by self-emulsification with water. The acrylate monomers were subsequently polymerized via radical initiation to synthesize solvent free PU acrylate hybrid dispersions. Furthermore, chemical coupling was also used to prepare UV-curable polyurethane-acrylate composites [49-51] and emulsions [52].

Polyurethane-acrylates have their own advantages and disadvantages. Acrylic polymers generally exhibit excellent weather properties and water/alkali resistance. However, elasticity and abrasion resistance of acrylic polymers are inferior to those of urethane polymers. PUs on the other hand, exhibit excellent elasticity and abrasion resistance but suffer from poor water and alkali resistance. Therefore, combining these two polymer systems will be a suitable approach to get beneficial attributes of both the polymers.

The so-called “hybrid” systems include both the urethane and the acrylic polymers into the same dispersion. As outlined in the process flow diagram (**Figure 3.10**), there are generally two methods for preparing the hybrids (Type 1 and Type 2). For Type 1 hybrids, a PUD is first prepared and then acrylic monomer is polymerized in the presence of the PUD. This gives semi-IPN kind of morphology to the structure. In the case of Type 2 hybrids, PU prepolymer and acrylic monomers are dispersed in water, and then acrylic polymerization and chain extension of PU is performed concurrently. One would expect a

IPN morphology for the Type 2 hybrids. Both the approaches involve the additional steps for the incorporation of acrylic component in the hybrid.

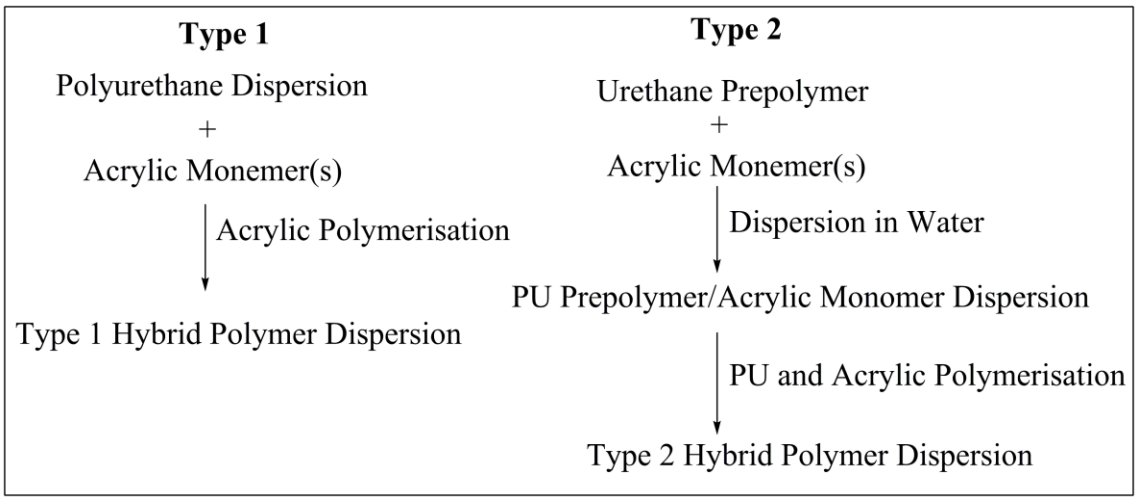

Figure 3.10 *Process flow diagrams for preparation of Type 1 and Type 2 hybrids*

Despite several studies on PUDs, it was observed that, there are not many reports on the combination of polyester polyol (PEP) and acrylic polyol (ACP) for the preparation of hybrid PUDs. The present work considers a new approach for the preparation of aqueous PUDs by reacting polyester polyol (based on adipic acid, neopentyl glycol and 1, 2, 6-hexane triol), acrylic polyol and di-isocyanate and dimethylol propionic acid as one pot synthesis. We also propose to make hybrid PUDs with varying equivalent ratios of PEP/ACP and study the performance of coatings prepared from them.

3.8 Experimental

3.8.1 Materials

Acrylic polyol (ACP) used in this work (MW=1000 g/mol and functionality=2) was procured from M/s. Krosslink Polymers Pvt. Ltd., Pune, India. Dimethylol propionic acid (DMPA) was procured from M/s. Perstorp Chemicals, Sweden. Isophorone diisocyanate (IPDI) was obtained from M/s. Hulls Corporation, Germany. N-Methyl pyrrolidone (NMP) and triethylamine (TEA) were procured from M/s. S.D. Fine Chemicals, India and M/s. Ranbaxy Laboratories, India respectively. All the chemicals were of extra pure grade and were used as received. Polyester polyol (PEP) was prepared as per the procedure described in section **3.2.2.**

3.8.2 Preparation of hybrid polyurethane dispersion

In to a 500 mL four-neck round bottom flask equipped with a mechanical stirrer, a thermowell, a nitrogen gas inlet and an addition funnel, the stoichiometric quantities of PEP, ACP, DMPA and NMP were charged. The flask was heated to 70°C with continuous stirring and homogenized for approximately 1h, followed by controlled addition of IPDI using addition funnel. The reaction was allowed to continue at this temperature until the isocyanate content decreased to around 3%. The isocyanate content was determined by standard dibutylamine back-titration method (ASTM D1638). The flask was cooled to 40°C and further stirred for 10 minutes after the addition of neutralizing agent, TEA. Into another flask equipped with mechanical stirrer, a required amount of water (to adjust the % solids to about 40) was added. Then the isocyanate terminated prepolymer was dispersed slowly into the water to control excessive foaming. The reaction scheme for the preparation of polyurethane dispersion is shown in **Figure 3.11**. Following the same procedure, six different compositions of PUDs were prepared by varying the equivalent ratios of PEP/ACP and by keeping NCO/OH ratio around 1.4 (see **Table 3.5**).

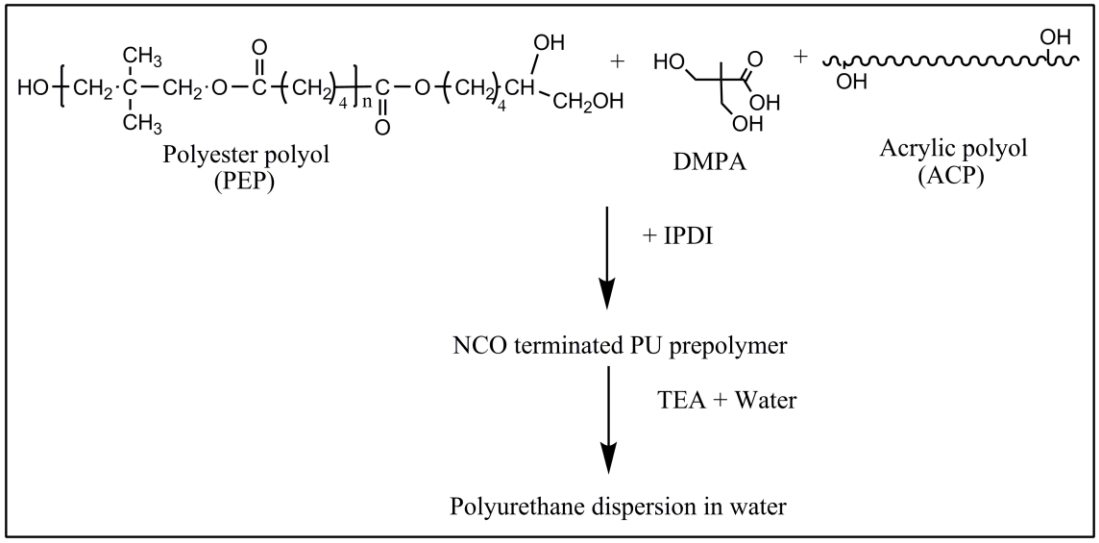

Figure 3.11 *Reaction scheme for the preparation of polyurethane hybrid dispersion*

Table 3.5 *Polyurethane dispersion (PUD) compositions (grams)*

Raw materials	**Sample 1**	**Sample 2**	**Sample 3**	**Sample 4**	**Sample 5**	**Sample 6**
Polyester polyol	63.64	43.3	30.3	24	18.5	-
Acrylic polyol	-	19.32	35.86	43.16	49.66	71.8
DMPA	6	6	6	6	6	6
IPDI	49.18	44.5	41.5	40.5	39.5	36
TEA	4.53	4.53	4.53	4.53	4.53	4.53
NMP	45	45	45	45	45	45
Water	137	137	137	137	137	137

3.9 Results and discussion

3.9.1 Properties of dispersions

Table 3.6 shows the properties of PUDs with respect to increasing content of acrylic polyol (Sample 2 to 5). The composition (Sample 1) without the acrylic polyol showed the particle size of 116 nm. Upon increasing the acrylic polyol content, the particle size showed an increasing trend with small dip in the initial composition of 80/20 (PEP/ACP). The increase in particle size can be attributed to the hydrophobic nature of acrylic polyol, which enhances the growth of the particles due to hydrophobic interactions. The PUD with 100% acrylic polyol showed the highest particle size (750 nm), which is almost 5 times more than the particle size of PUD, based only on PEP under the same conditions of pH (8 to 9) and % solids (40%). It is also important to note that the particle size strongly depends on the ionic character of the PUD, which in turn influences the hydrophilic/hydrophobic balance of the dispersion. However, in the present study we have kept the amount of DMPA constant in all the compositions so that the particle size is predominantly affected by the hydrophobic nature of acrylic polyol. In the viscosity study, it was observed that there is no significant change in the viscosity of PUDs that are prepared by mixture of polyols. However, there is a large difference in the viscosities of PUDs with 100% PEP (high viscosity, Sample 1) and 100% ACP (low viscosity, sample 6), which is due to the larger swelling of dispersed particles with 100% PEP in aqueous medium resulting into higher viscosity. The lower swelling of dispersed particles with 100% ACP is attributed to the more hydrophobic nature of the polymer resulting into significant reduction in the viscosity. Therefore, the viscosity is majorly governed by the hydrophilic and hydrophobic characters of PUDs rather than the particle size. It was also observed that there was no phase separation or agglomeration in all the PUDs even after five cycles of Freezing-Thawing. This observation clearly indicated the good stability of dispersions, of all the compositions. Since the dispersion prepared from 100% ACP showed phase separation, further evaluations of this sample were not performed.

***Table 3.6** Dispersion Properties of PUDs*

Properties	**Sample 1**	**Sample 2**	**Sample 3**	**Sample 4**	**Sample 5**	**Sample 6**
Appearance*	A	B	B	B	B	C
Particle size (nm)	116	92.6	120.6	151.4	156.1	757.3
pH	8.4	8.6	8.35	8.7	8.6	8.5
Viscosity (cps) @ 25°C	225	28	22	21	20	11
% solids	40	40	40	40	40	40
Freeze-Thaw stability [a]	No phase separation	No phase separation	No phase separation	No phase separation	No phase separation	-

* A = Milky white with pink tint, B = Milky white with blue tint, C = Milky white.
a = -26 ^{o}C for 16 h followed by 8 h at room temperature.

3.9.2 FTIR analysis

Figure 3.12 shows the FTIR spectra of dried films of dispersions with different ratios of PEP/ACP. For clarifying and ensuring changes, the N-H and C=O stretching regions are separately showed in **Figure 3.13** and **Figure 3.14** respectively.

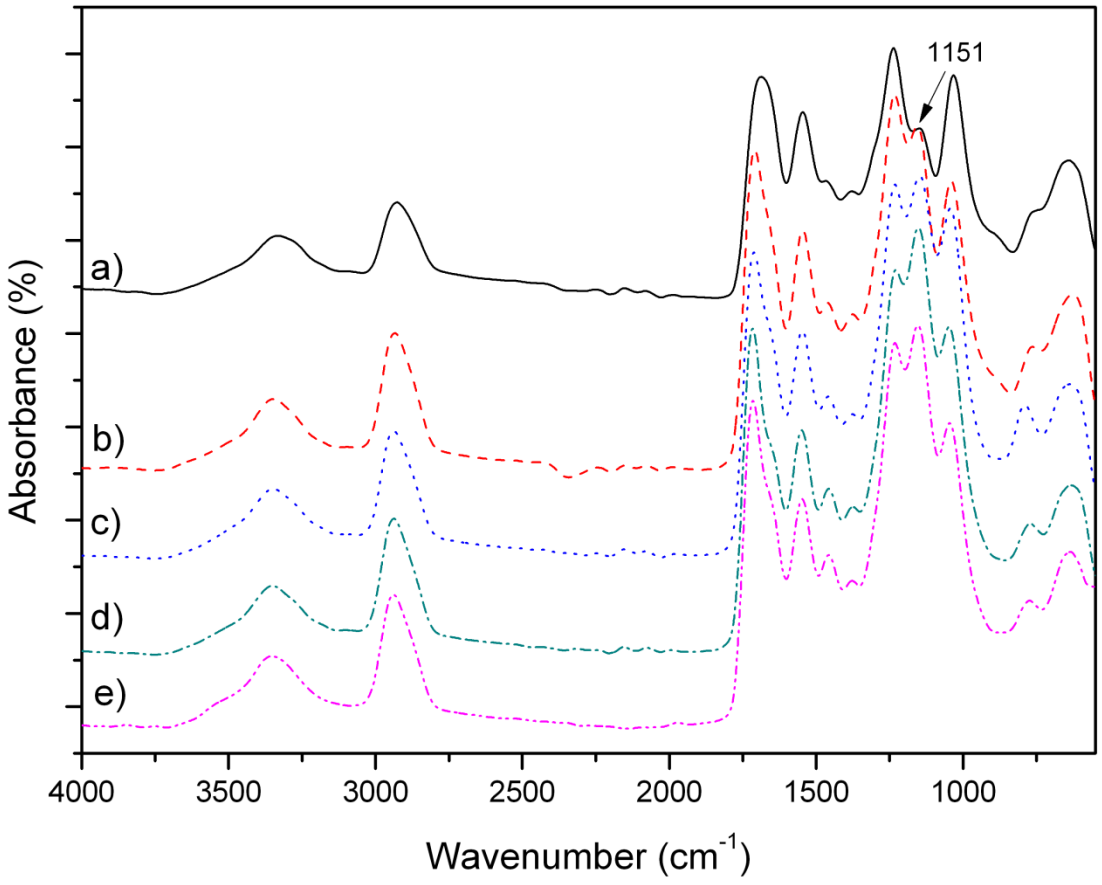

Figure 3.12 *Typical FTIR spectra of the films from the dispersions with different ratios of PEP/ACP a) 100/0, b) 80/20, c) 60/40, d) 50/50 and e) 40/60*

It can be clearly seen from **Figure 3.13** that the peak intensity in the N-H stretching region (from 3100-3600 cm^{-1}) and –CONH stretching region (~1550 cm^{-1}) are almost same for all compositions. This is because in all the compositions the NCO/OH ratio was kept constant. In addition, the intensity of a peak due to acrylic ester function at 1151cm^{-1} increases with increasing ACP content which confirms the efficient incorporation of ACP into hybrid dispersions.

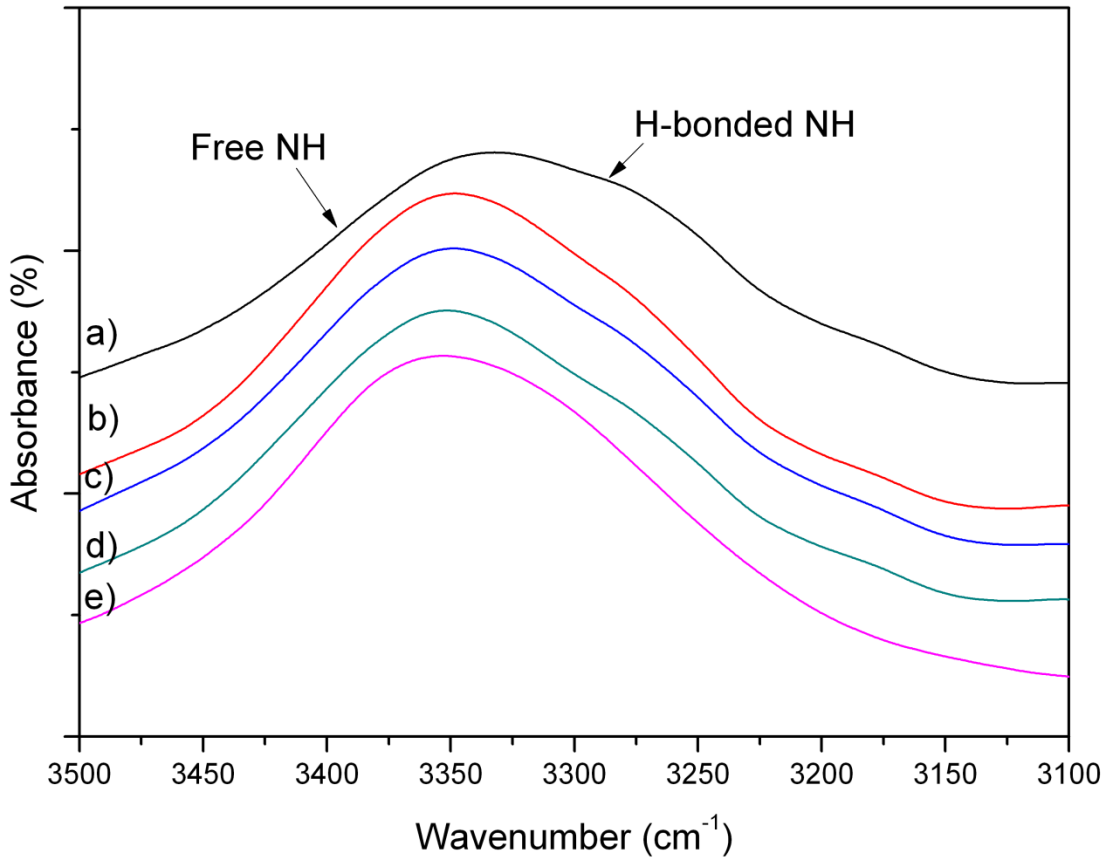

Figure 3.13 *Typical FTIR spectra of the films from the dispersions with different ratios of PEP/ACP a) 100/0, b) 80/20, c) 60/40, d) 50/50 and e) 40/60 in NH stretching region*

The N-H group could form hard-hard segment H-bonding with the carbonyl of urethane or urea group and hard-soft segment bonding with carbonyl of PEP or ACP. In general the strength of hard-hard segment H-bonding is stronger than the hard-soft segment hydrogen bonding [23]. **Figure 3.13** indicates the H-bonded N-H and free N-H absorption bands at 3320 and 3340 cm^{-1}. There is no increase or decrease in these stretching with the variation in the ratio of PEP/ACP in all compositions. The FTIR spectra in **Figure 3.14** also shows that there is no increase or decrease in the intensity of H-bonded carbonyl peaks, but there is an increase in the intensity of free C=O peaks at about 1720 cm^{-1} with the increase of ACP content. Thus, FTIR study of the films clearly reveled that there is no effect on hydrogen bonding in the system with the variation in PEP/ACP ratio as the NCO/OH was maintained constant. Further, an increase in free carbonyl peaks with the increase of ACP content indicates the probability of phase separation in the system.

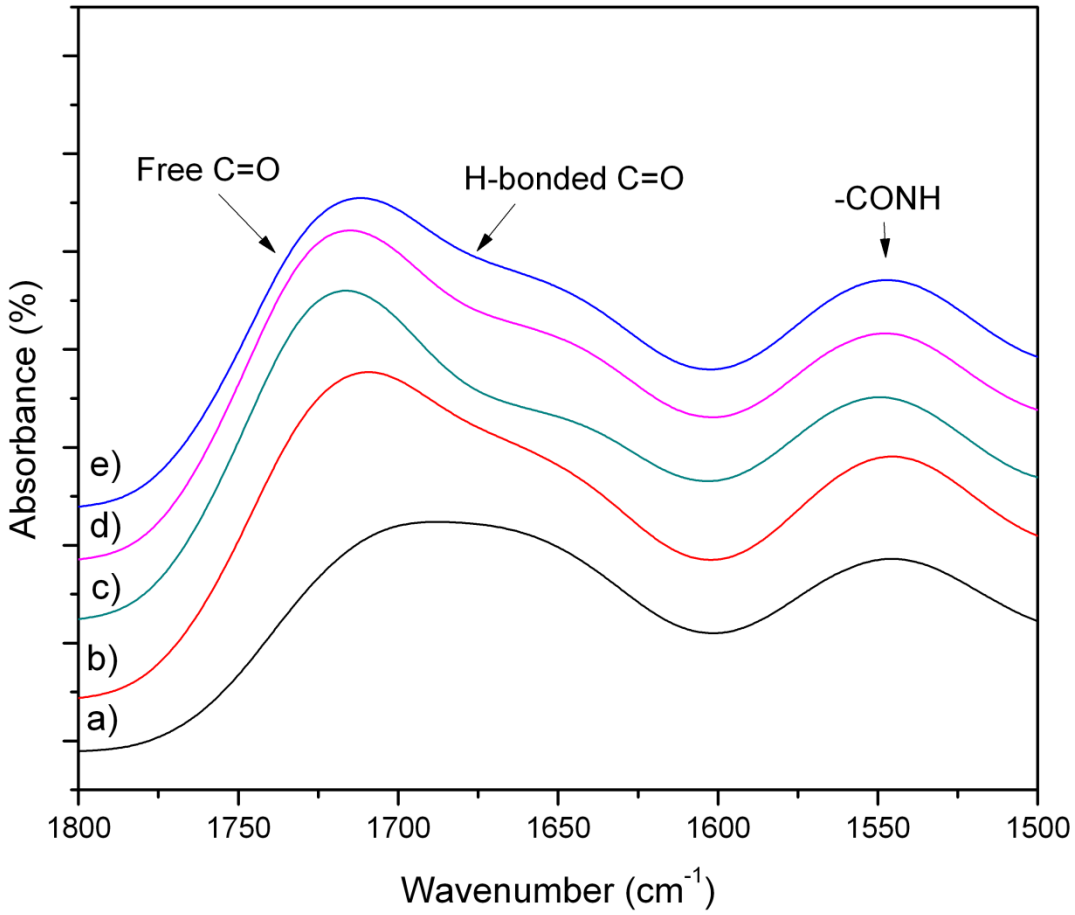

Figure 3.14 *Typical FTIR spectra of the films from the dispersions with different ratios of PEP/ACP a) 100/0, b) 80/20, c) 60/40, d) 50/50 and e) 40/60 in C=O stretching region*

3.9.3 Thermal properties

The results of differential scanning calorimetric study are shown in **Figure 3.15**. It can be clearly seen that there is an increase in glass transition temperature (T_g) with an increase of ACP content in the film composition. This could be attributed to the formation of more and more branched structures which can decrease the segmental mobility of chains.

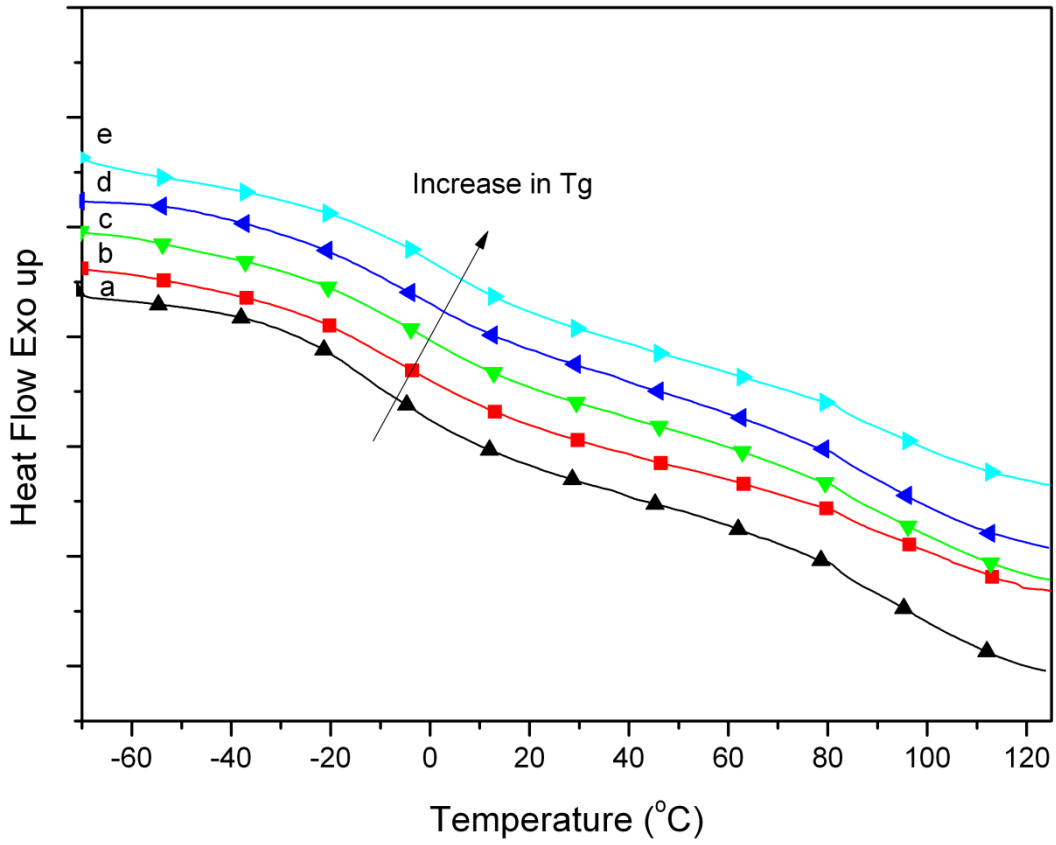

Figure 3.15 *DSC curve overlay of the films from the dispersions with different ratios of PEP/ACP a) 100/0, b) 80/20, c) 60/40, d) 50/50 and e) 40/60*

3.9.4 Mechanical properties

Tensile behavior of the cast films is shown in **Figure 3.16**. The initial modulus increased and elongation at break decreased with an increase in ACP content. It is worth to note that the composition with PEP/ACP ratio 40/60 had shown highest value of tensile stress which is three times higher than the sample with 100% PEP. It is known that the extensibility of the polymer decreases with the increment in of crosslinking [53]. Therefore, with an increase in ACP content, there is a decrease in elongation at break. The loss of

extensibility can also be attributed to the formation semi-interpenetrating polymer network (Semi-IPN) in between polyester-polyurethane and acrylate-polyurethane. This is in line with the earlier observations reported in the literature [34, 35].

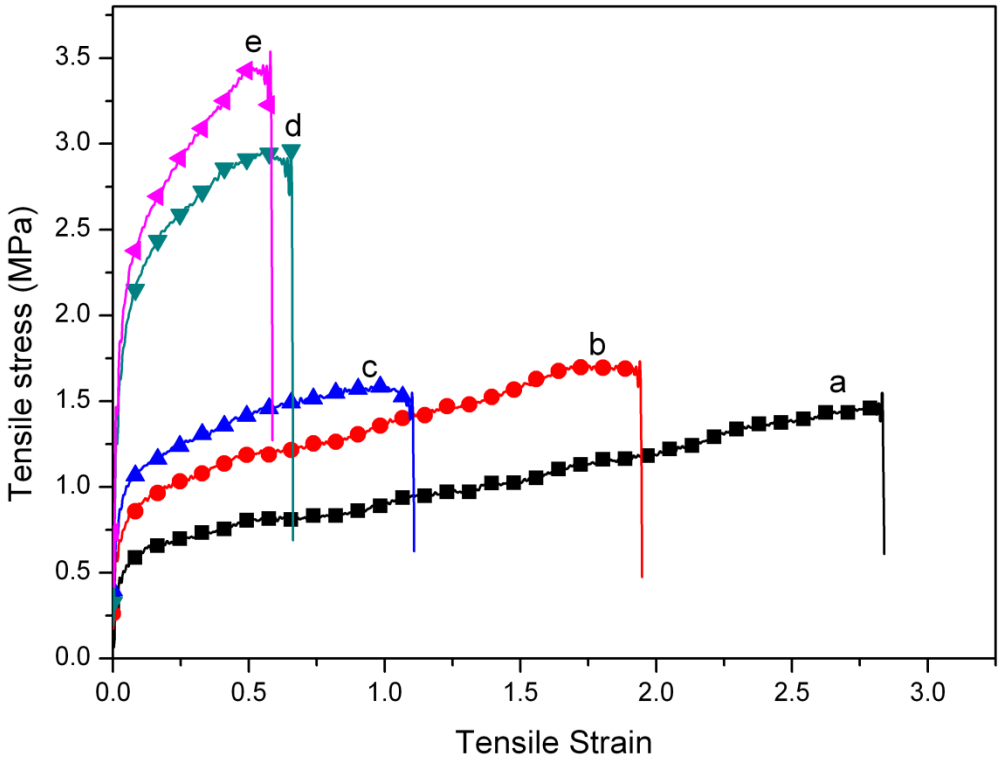

Figure 3.16 *Tensile stress vs tensile strain curve of the films from the dispersions with different ratios of PEP/ACP a) 100/0, b) 80/20, c) 60/40, d) 50/50 and e) 40/60*

It is also observed that the films with 100% PEP and 40/60 PEP/ACP showed maximum and minimum elongations respectively.

3.9.5 Properties of coatings

Table 3.7 shows the properties of PUD coatings obtained from the compositions containing different ratios of PEP/ACP. It can be seen that, there is an increase in scratch resistance with the increase of ACP content. The scratch resistance of the films was maximum at 40/60 ratios of PEP/ACP. It could be due to the fact that with the increase of ACP content, there is a formation of more and more rigid structure as a result of the increased entanglement of ACP and PEP components into PUD network. This increase in

rigidity results in increase in modulus of the film (as confirmed by tensile study) which in turn attributes to higher scratch resistance.

Table 3.7 *Effect of acrylic polyol incorporation on the ensuing properties of coatings*

Properties	**Sample 1**	**Sample 2**	**Sample 3**	**Sample 4**	**Sample 5**
Scratch resistance (g)	2500	2400	2500	3200	3400
Abrasion resistance[#]	34	52	62	65	72
Gloss @ 60^{o}	+90	+90	+90	+90	+90
Water resistance	←	———	No haziness	———	→
Solvent resistance*	40	>200	>200	>200	>200

= mg loss, 1kg load, CS-10 wheels, 1000 revolutions; * = MEK double rubs.

It can also be seen from **Table 3.7** that, the solvent double rub values for the coatings containing PEP and ACP were more than 200. Whereas, the coatings prepared from 100% PEP showed very low value of 40. The higher solvent resistance of the coatings containing PEP and ACP is due to the increase in rigidity which is evidenced by the increased scratch resistance as well. In water immersion, the films did not develop blisters or haziness and no delamination of the films from the substrate was observed. It shows that the water resistance property of dispersion coatings is quite good.

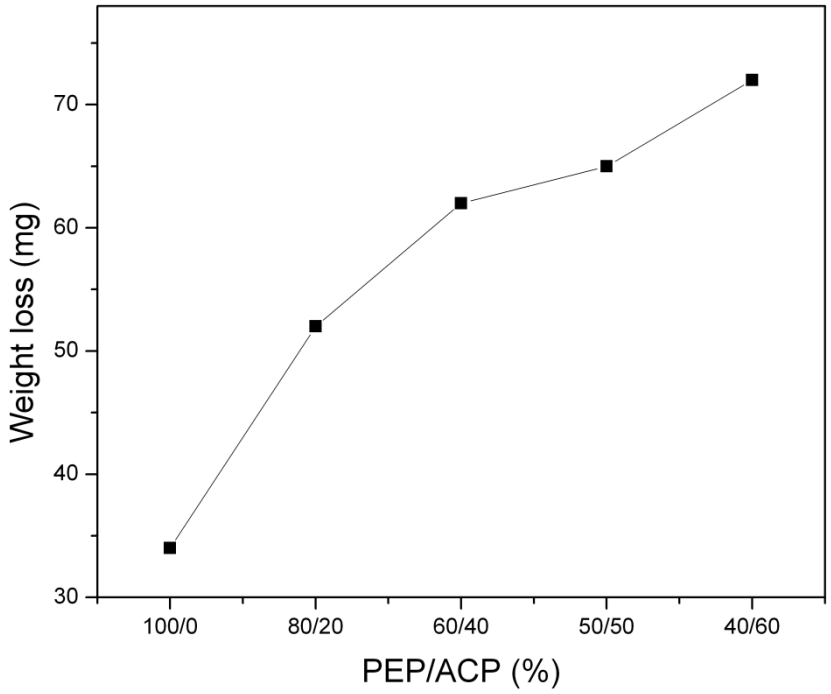

Figure 3.17 *Abrasion resistance as a function of PEP/ACP ratio*

Figure 3.17 shows the decrease in abrasion resistance of coated films with an increase of ACP content. This may be explained by FTIR studies which showed that, with the increase in ACP content, there is an increase in C=O groups which leads to decrease in the compatibility of soft segments i.e. PEP and ACP.

3.9.6 Conclusions

PUDs were prepared by reacting mixtures of polyols (PEP and ACP) with diisocyanate. With the increase of ACP content, there was increase in tensile strength and modulus which leads to the increase in scratch resistance. There was a decrease in viscosity of dispersions and abrasion resistance of the coatings upon increase in ACP content due to increased incompatibility between PEP and ACP. It was also observed that the films were unaffected by water which was evidenced by the absence of blisters, haziness and resistance to delamination in water immersion test. The study clearly indicates that one can take the advantage of reacting PEP and ACP to obtain PUDs with improved scratch resistance.

References

1. B. Vogt-Birnbrich, Progress in Organic Coatings **29**(1-4), 31-38 (1996).
2. D. Dieterich, Prog. Org. Coat. **9**, 281 (1981).
3. J. W. Rosthauser and K. Nachtkamp, Advances in Urethane Sci. and Tech. **10**, 121 (1987).
4. Ganss and Helmut, WO/2004/003045 (2004).
5. M. G. Lu, J. Y. Lee, M. J. Shim, and S. W. Kim, Journal of Applied Polymer Science **86**(14), 3461-3465 (2002).
6. L. S. Ramanathan, K. G. Raut, S. R. Srinivasan, and S. Sivaram, U. S. 6239213 B1 (2001).
7. S. Zhou, L. Wu, J. Sun, and W. Shen, Progress in Organic Coatings **45**(1), 33-42 (2002).
8. Y. T. Sung, M. S. Han, J. C. Hyun, W. N. Kim, and H. S. Lee, Polymer **44**(5), 1681-1687 (2003).
9. K. Hsieh, J. Pan, L. Chen, and K. Frisch, Adv. Urethane Sci. Technol., **10** 77 (1987).
10. A. C. Aznar, O. R. Pardini, and J. I. Amalvy, Progress in Organic Coatings **55**(1), 43-49 (2006).
11. E. C. Galgoci, C. R. Hegedus, F. H. Walker, D. J. Tempel, F. R. Pepe, K. A. Yoxheimer, and A. S. Boyce, JCT CoatingsTech **2**(13), 28-36 (2005).
12. L. I. M. Tae Jun, Galgori, C. Emest, Walker, H. Frederick, Yoxheimer, and A. Kenneth, *Hybrid vigour : Waterborne urethane-acrylics combine high performance with low voc content* (Vincentz, Hannover, ALLEMAGNE, 2005), p. 7.
13. T. Nabuurs, R. A. Baijards, and A. L. German, Progress in Organic Coatings **27**(1-4), 163-172 (1996).
14. S. T. Wang, F. J. Schork, G. W. Poehlein, and J. W. Gooch, Journal of Applied Polymer Science **60**(12), 2069-2076 (1996).
15. X. Q. Wu, F. J. Schork, and J. W. Gooch, Journal of Polymer Science Part a-Polymer Chemistry **37**(22), 4159-4168 (1999).

16. D. de Wet-Roos, J. H. Knoetze, B. Cooray, and R. D. Sanderson, Journal of Applied Polymer Science **71**(8), 1347-1360 (1999).
17. H. Kawahara, T. Goto, K. Ohnishi, H. Ogura, H. Kage, and Y. Matsuno, Journal of Applied Polymer Science **81**(1), 128-133 (2001).
18. J. F. Stumbe, F. Calderara, and G. Riess, Polymer Bulletin **47**(3-4), 277-282 (2001).
19. L. M. Wu, B. You, and D. Li, Journal of Applied Polymer Science **84**(8), 1620-1628 (2002).
20. G. R. Pan, L. M. Wu, Z. Q. Zhang, and D. Li, Journal of Applied Polymer Science **83**(8), 1736-1743 (2002).
21. C. Wang, F. Chu, C. Graillat, and A. Guyot, Polymer Reaction Engineering **11**(3), 541-562 (2003).
22. J. D. Vanheumen and J. R. Stevens, Macromolecules **28**(12), 4268-4277 (1995).
23. H. S. Xu and C. Z. Yang, Journal of Polymer Science Part B-Polymer Physics **33**(5), 745-751 (1995).
24. L. Zha, M. Wu, and J. Yang, Journal of Applied Polymer Science **73**(14), 2895-2902 (1999).
25. R. Adhikari, P. A. Gunatillake, S. J. McCarthy, and G. F. Meijs, J. of App. Poly. Sci. **78**(5), 1071-1082 (2000).
26. S. Chen and L. Chen, Colloid Polym Sci **282**, 14-20 (2003).
27. A. Dong, A. Yingli, F. Shiyou, and S. Duoxian, J Colloid Interface Sci **214**, 118-122 (1999).
28. C. R. Hegedus and K. A. Kloiber, presented at the Proceedings of the Waterborne High-Solids and Powder Coatings Symposium, New Orleans LA, 21st Feb 9-11, 1994.
29. C. R. Hegedus and K. A. Kloiber, J Coat Techno **68**, 39 (1996).
30. M. Hirose, F. Kadowaki, and J. Zhou, Prog Org Coat **31**, 157-169 (1997).
31. M. Hirose, J. Zhou, and N. Katsutoshi, Prog Org Coat **38**, 27-34 (2000).
32. Y. H. Jan, Y. T. Hwang, C. Y. Shih, and H. C. Li., presented at the Waterborne High-Solids and Powder Coating Symposium New Orleans USA, 1995.

33. I. H. Kim, J. S. Shin, I. W. Choeng, J. I. Kim, and J. H. Kim, Colloids Surf A **207**, 169-176 (2002).
34. D. Kukanja, J. Golob, and M. Krajnc, J Appl Polym Sci **84**, 2639-2649 (2002).
35. D. Kukanja, J. Golob, A. Zupancˇicˇ-Valant, and M. Krajnc, J Appl Polym Sci **78**, 67-80 (2000).
36. U. Sˇebenik, J. Golob, and M. Krajnc, Polym Int **52**, 740-748 (2003).
37. U. Sˇebenik and M. Krajnc, Colloids Surf A **233**, 51-62 (2004).
38. U. Sˇebenik and M. Krajnc, J Polym Sci Part A: Polym Chem **43**, 844-858 (2005).
39. L. Wu, B. You, and D. Li, J Appl Polym Sci **84**, 1620-1628 (2002).
40. L. Wu, H. Yu, J. Yan, and B. You, Polym Int **50**, 1288-1293 (2001).
41. F. Bakker, Polym. Paint Col. J. **182**, 376 (1992).
42. Y. S. Huang, S. L. Ding, K. H. Yang, C. P. Chwang, and D. Y. Chao, J. Coating Technol. **69**, 69 (1997).
43. I. Bechara and T. Brown, American Paint Coat J. **October**, 59 (1994).
44. R. Tennebroek, J. Geurts, A. Overbeek, and A. Harmsen, Eur. Coat J. **11**, 1016 (1997).
45. A. Benlefki and A. Feghouli, Eur. Coat J. **12**, 926 (1996).
46. B. K. Kim and J. C. Lee, J. Appl. Polym. Sci **58**, 1117 (1995).
47. J. Y. Kim and K. D. Suh, Coll. Polym. Sci. **274**, 920 (1996).
48. H. P. Klein and M. Schawb, Polym. Paint Col. J. **184**, 444 (1994).
49. B. K. Kim, K. H. Lee, and N. J. Jo, J. Polym. Sci.: Part A: Polym. Chem. **34** 2095 (1996).
50. B. K. Kim, K. H. Lee, and H. D. Kim, J. Appl. Polym. Sci. **60**, 799 (1996).
51. H. D. Kim and T. W. Kim, J. Appl. Polym. Sci. **67**, 2153 (1998).
52. M. E. Song, J. Y. Kim, and K. D. Suh, J. Appl. Polym. Sci. **62**, 62 (1996).
53. G. R. Hamed and N. Rattanasom, Rubber Chemistry and Technology **75**(2), 323-332 (2002).

4.1 Organic-inorganic hybrid coatings

4.1.1 Introduction

Organic-inorganic hybrids combine the advantage of both organic polymers (flexibility, ductility, film forming property, etc.) and those of inorganic materials (rigidity, high thermal stability, UV-shielding property and high refractive index etc.) The properties of organic-inorganic hybrids strongly depend on the method of preparation, homogeneous dispersion of inorganic material in organic matrix and the interaction between the organic and inorganic phases. Many researchers have studied organic/inorganic nano composite systems and tried to understand the mechanism by which the improvement over traditional organic materials takes place. The organic matrices studied included epoxy resin, polystyrene, polypropylene, polyacrylates, nylon etc. and the inorganic phases were usually clay, layered silicates and nano particles such as SiO_2, TiO_2, ZnO, $CaCO_3$ etc [1-5]. Nano silica particles have been widely incorporated into polymers to improve the heat resistance, radiation resistance, mechanical and electrical properties of polymer materials[6-9]. For example, Zhou et al.[10] found that nanosilica particles could effectively improve the hardness, abrasion resistance, and scratch resistance of acrylic-based polyurethane coatings. Wu et al.[11] indicated that nanosilica particles could simultaneously provide PP with stiffening, strengthening, and toughening effects at lower filler content (typically 0.5% by volume). Manna et al.[12] found that the storage modulus and T_g of epoxidized natural rubber increased due to addition of silica. Properties of polyurethane such as rigidity, toughness, heat resistance improved by SiO_2 addition, because silanol groups on the nano silica could react with the urethane groups and other groups of polyurethane [13].

In addition, the use of sol-gel process to prepare highly intermingled organic–inorganic hybrid polymer networks is of current scientific interest since it offers the possibility of tailoring the properties of materials by variation of relative compositions of inorganic and organic phases [14-17]. Depending on the desired application, polymers with different mechanical properties could be obtained by varying the formulations. Because of the hybrid character, these product exhibited superior thermal and weather resistance, and more excellent abrasion resistance than traditional polymers.[18-21]

Lately, polyurethanes (PUs) have attracted great attention for the preparation of hybrid sol-gel materials and functional materials. For example, PU-SiO_2 hybrid materials have been prepared by suspension[22] and an acid-catalyzed sol-gel processes [23]. Ho Tak Jeon [24] has reported water borne polyurethane-silica composites using both hydrophilic and hydrophobic silica. Jui-Ming Yeh [25] has prepared amino-terminated anionic water borne polyurethane-silica hybrid materials through a sol-gel process in the absence of an external catalyst. Tzong-Liu Wang[26] synthesized a series of polyurethane/polyaniline/silica, organic/inorganic hybrids via the conventional polyurethane prepolymer technique. Nano silica particles were also used to improve and optimize properties of 2-pack polyurethane clear coats based on acrylic polyol [27].
Many researchers have used silanes to improve the surface morphology of substrates on which adhesives/coating has been applied. The silanes are found to increase the interaction between mineral substrates and the organic polymers [28].

It is reported that nano-silica could increase the hardness and scratch resistance of a coating without affecting the transparency of the coating[29, 30]. Nanosilica could also enhance the tensile strength and elongation of polyurethane elastomer, though the modulus and hardness were lower than the corresponding micro size filled polyurethane[31].

Although there are reports on the study of organic-inorganic hybrids, only a few reports are available on waterborne polyurethane-silica hybrid coatings prepared by using PUD and surface modified silica nano particles. The aim of this work is to prepare waterborne polyurethane-silica (organic-inorganic) hybrid coatings with improved scratch and abrasion resistance. In this work, polyurethane dispersions (PUD) based on polyesterpolyol, isophorone diisocyanate and dimethylol propionic acid were prepared and the effect of silica content and its modifications on mechanical and coating properties were studied.

4.2 Experimental

4.2.1 Materials

Dimethylol propionic acid (DMPA) was supplied by M/s. Perstorp Chemicals, Sweden; isophorone diisocyanate (IPDI) was procured from M/s. Hulls Corporation, Germany; N-methyl-2-pyrrolidone (NMP) and tri-ethylamine (TEA) were purchased from M/s. SD Fine Chem., India and M/s. Ranbaxy Laboratories, India respectively; Colloidal silica (containing 30 % SiO_2), having particle size around 20 nm was received from Clariant India and aminopropyl triethoxy silane (APTES) was purchased from Aldrich Chemicals. All the chemicals were of extra pure grade and were used as such.

4.2.2 Preparation of polyester polyol

Polyester polyol used in the preparation of polyurethane dispersions (PUDs) was prepared from adipic acid (AA), neopentyl glycol (NPG) and hexane triol (HT) and was having an acid value 2.06 mg KOH/gm and hydroxyl value 200 mg KOH/gm. The detail procedure for the preparation of polyester polyol is given in Section 3.3 of Chapter III.

4.2.3 Preparation of –NCO terminated PU prepolymer

The reaction pathway for the preparation of polyurethane dispersion is shown in **Figure 4.1**. A typical procedure for the preparation of PUD is given as follows: Into a 500 ml four neck round bottom flask equipped with mechanical stirrer, thermo well, nitrogen gas inlet, condenser and dropping funnel, polyester polyol (52.5g), DMPA (5.3g) and NMP (37.5g) were charged and the flask was heated to 70°C in oil bath with continuous stirring under nitrogen atmosphere. The contents were stirred for one hour at 70°C so that homogeneous polyol composition was obtained. Then from the dropping funnel, a required amount of IPDI (42.5g) was added drop wise, care being taken not to allow the temperature of the flask to rise above 70°C. The reaction was continued for two hours and the progress of the reaction was monitored by NCO content using back titration method. When the desired isocyanate content was reached, the reaction was stopped and the flask was cooled to room temperature.

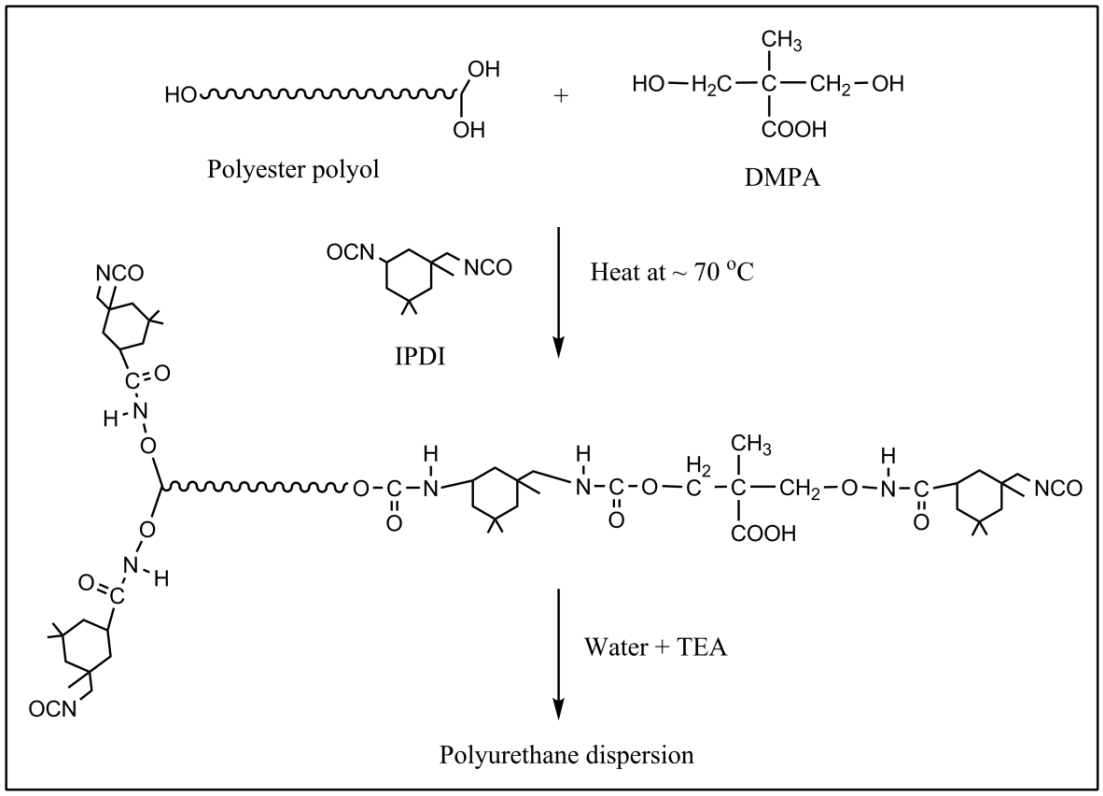

Figure 4.1 *Preparation of PUD*

4.2.4 Preparation of coatings from PU silica nanocomposite

Isocyanate terminated PU prepolymer (as described in section 4.2.3) was neutralized with TEA and dispersed in DI water. To this, varying quantities of silica sol (3, 6, 9 and 12 weight %) were added to form PU silica nano composite dispersions. For casting films, the dispersion was poured into the PTFE mould and dried in air circulated oven at 60°C. The coated test panels were prepared by brush application method. The films and coatings were aged for seven days before evaluating the properties.

4.2.5 Preparation of modified silica nano particles (G-silica)

In to another 500 ml round bottom flask equipped with mechanical stirrer, silica nano particles in the form of silica sol were dispersed in the de-ionized water. To this mixture APTES was added and stirred for 1h. The modified silica nano particles as shown in Figure 4.2 were termed as G-silica.

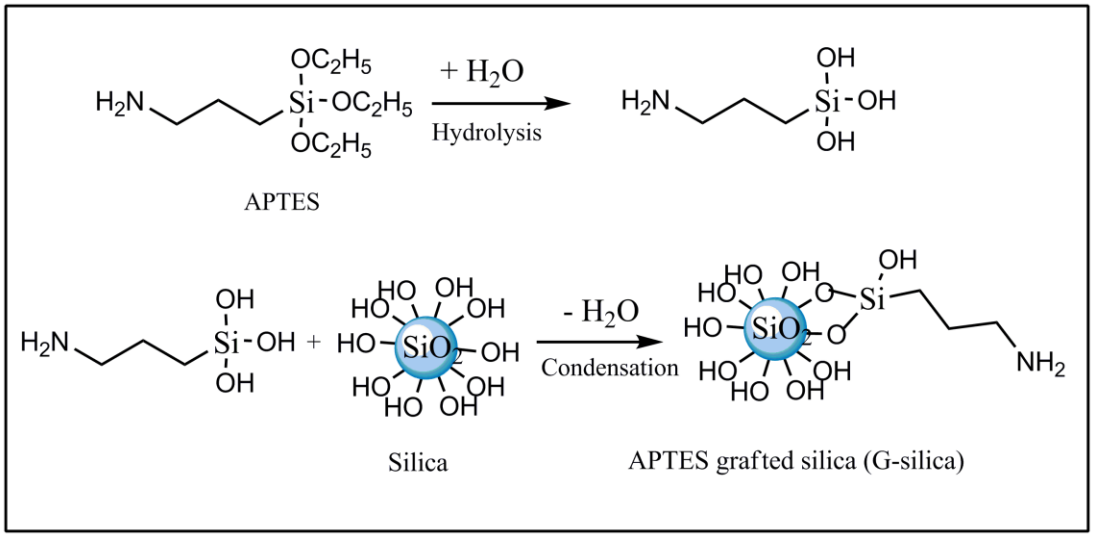

Figure 4.2 *Preparation of modified silica nano particles*

4.2.6 Preparation of polyurethane nanosilica hybrid dispersion

NCO terminated polyurethane pre-polymer prepared as discussed earlier in **section 4.2.3** was dispersed into deionized water containing APTES modified silica nanoparticles (i.e. G-silica) and allowed to mix and react for 2 hrs at room temperature to give polyurethane nano silica hybrid dispersion as shown in **Figure 4.3**.

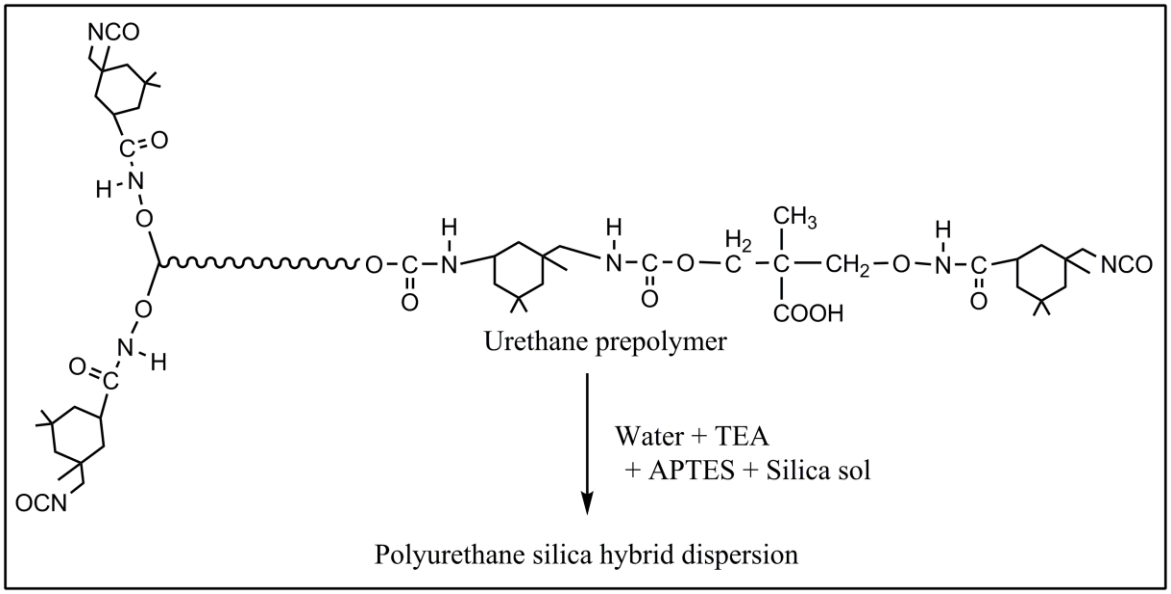

Figure 4.3 *Preparation of polyurethane silica hybrid dispersion*

4.2.7 Preparation of films and coatings from PU-silica hybrid system

Films of PUD, PUD-silica and PUD-G-Silica dispersion were cast in PTFE mould. In a typical procedure around 40g of dispersion with 40% solid content was poured in PTFE mould and dried at 60°C in air circulated oven. The films were having thickness of 1mm and were aged for seven days at room temperature. For testing the tensile properties, the dumbbell shaped specimens as per the ASTM D 632 were cut from the dried films. DMA test specimens with dimensions of 10mm X 25mm were cut from the cast films. On the other hand, to obtain coatings, the dispersions were coated on surface of the panel by brush and allowed to dry at room temperature for seven days before testing.

4.3 Characterization and evaluation

4.3.1 NMR spectroscopy

The solid-state ^{29}Si CP-MAS NMR spectra were recorded using a Bruker MSL-500 spectrometer operating at ^{29}Si frequency of 33.36 MHz. The magic angle sample spinning was performed at 5 kHz and the cross polarization contact time was 1–5 ms. About ~2417 number of accumulation were made to get good spectrum.

4.3.2 Scratch resistance test

Scratch resistance test was carried out using Sheen made automatic scratch tester (made in UK). In this test, the coated panel was moved against the needle with 1 mm diameter along with the load. The test was conducted by increasing the load to determine the minimum load at which the coating was penetrated.

4.3.3 Abrasion resistance test

Abrasion resistance test was performed using a Teledyne Taber Abraser (made in USA) with CS-10 wheels, with 1 Kg load for 1000 cycles. The test sample is spun against abrasive wheels. The test results are expressed as weight loss in milligrams.

4.3.4 Specular gloss

The measurement of the gloss value is a relative measurement. Results are related to a highly polished black glass with a refractive index of 1.567. The glass has an assigned

specular gloss value of 100. Gloss is measured using a Gloss Meter which directs a light at a specific angle to the test surface and simultaneously measures the amount of reflection. It is common to report the result in % reflection of the illuminated light. The % gloss was measured by using Sheen made Tri-microgloss instrument (made in UK) at an angle of 60°.

4.3.5 Mechanical properties of the films

The mechanical properties of cast films were determined by using an Instron tensile tester. The dumbbell shape specimen with thickness of ~ 1 mm was prepared as per ASTM D638. The samples were pulled at the rate of 5 mm/min. The tensile strength and elongation at break were automatically calculated using software in a computer, which is interfaced with the Instron. Tests were carried out at room temperature and each reading taken was the average of at least five measurements.

Dynamic mechanical properties were determined with a dynamic mechanical analyzer (Rheometry Scientific DMTA), using a test specimen of the dimension 25x8x0.5 mm in tension compression mode at a heating rate of 5°C/min and at the frequency of 10 rad/s.

4.3.6 Morphological properties

The morphology of silica particles were obtained by a transmission electron microscopy (Jeol - 1200 EX TEM). All the dispersions were deposited on copper grids and vacuum dried before TEM analysis.

4.4 Results and Discussions

Polyurethane silica nano composite coatings were prepared by incorporating silica sol into PUD and evaluated for their coating properties. The films of these dispersions were also obtained by casting and were used for analyzing mechanical properties. Detail discussion is presented here.

4.4.1 Tensile properties of PU-silica nano composite

The mechanical properties of polymers significantly improve upon incorporation of nano size fillers into the polymer matrix. The nano size silica with particle diameter of 10-20

nm exhibit large active surface area and interface very well with the polymer structure. **Figure 4.4** shows the effect of unmodified silica content on the tensile strength and % elongation of polyurethane-silica hybrids. The tensile strength of PUD films increased with the increase in silica content up to 9% and then decreased with further increase in silica. On the other hand, % elongation remained almost constant till 6% silica and then decreased. This can be attributed to the fact that the polyurethane-silica hybrid system became more compact and the volume fraction of rigid silica phase increases with increase in silica. As a result, the tensile strength increased continuously with an increase in silica content. However, above 9% silica content, the tensile strength decreased which could be attributed to the aggregation of silica phase. It can be observed from TEM micrographs (as shown in **Figure 4.6)**, that the densification of silica particles is more at 9% silica content as compared to 3% and 6% silica content. Therefore, there is no significant decrease in elongation up to 6% silica content but, rapid decrease thereafter.

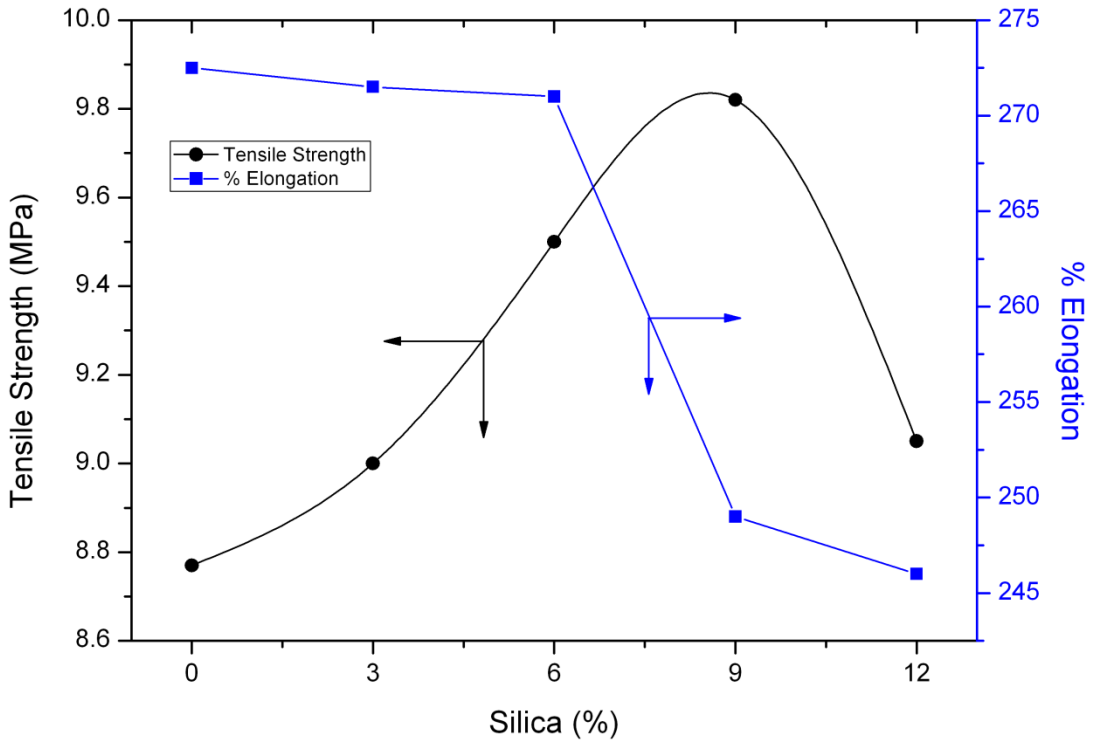

***Figure 4.4** Tensile strength and % elongation as function of silica content*

At low nano silica content, the interaction between the nano particles and polymer molecules is strong due to large surface area of nano particles. This situation is favorable

for enhancing the mechanical properties of films. However, when relatively higher silica content is used, more and more silica particles could aggregate leading to the deterioration of the mechanical properties [31]. This observation was made in our measurements also.

4.4.2 Dynamic Mechanical properties of PU-silica nano composite

Figure 4.5 shows the storage modulus against temperature of PU-silica nano composite with varying silica content. It can be clearly seen that below 60 °C, there is an increase in storage modulus with an increase in silica content. It can be attributed to the homogenous dispersion and better reinforcement of silica nano particles. Further, higher silica content can increase hydrogen bonding between PU matrix and surface silanol groups, which can enhance the storage modulus.

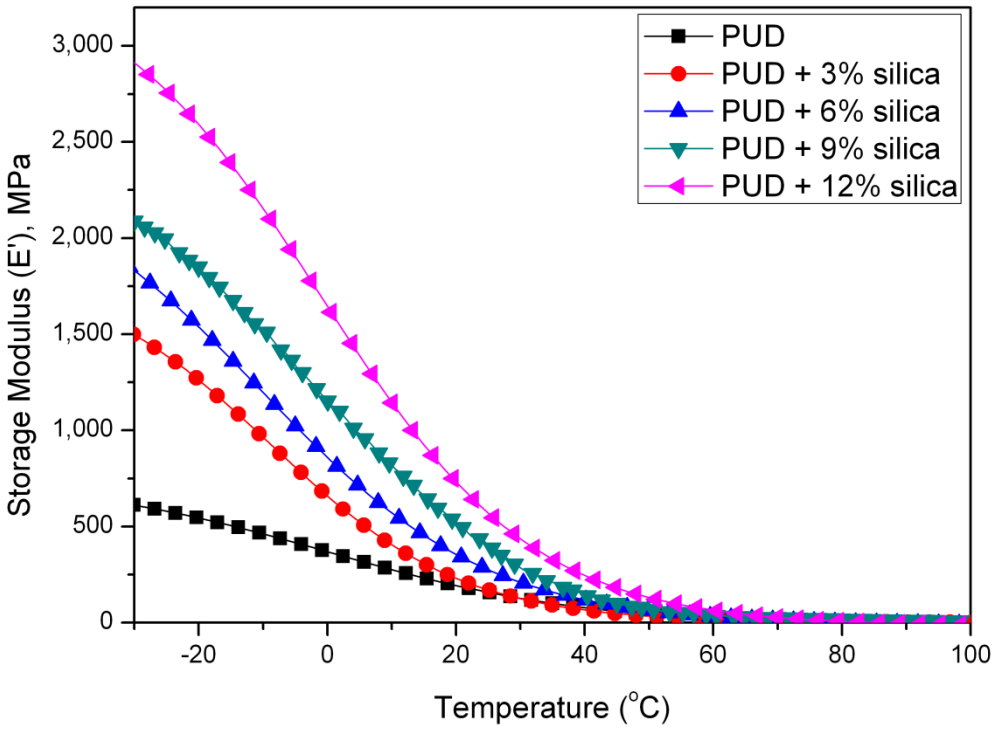

Figure 4.5 *Plot of storage modulus against temperature of PUD-silica nano composite films*

4.4.3 Coating properties of PU-silica nanocomposite

Film properties such as scratch resistance, abrasion resistance, gloss etc. of PU dispersion and the nano composite coatings prepared using nano silica are given in **Table 4.1b.** It can be observed from **Table 4.1** that, the scratch hardness of PU films increased with increase in silica content and reached maximum of 3200g with 12% silica content. Further addition of silica could give heterogeneous films and hence the silica content was restricted to 12% in our studies. It is also important to note that, upon incorporation of silica, there is no loss in the abrasion resistance and all the nano composite films exhibited abrasion resistance close to the pure PU films. On the other hand, the gloss of the coatings decreased with increase in silica content, which could be attributed to the agglomeration of silica particles leading to roughness at the surface. However, agglomeration of silica particles into clusters reduces the solvent permeability and hence improved the solvent resistance of the coatings with the increasing amount of silica, as clearly observed from **Table 4.1**. Further, in order to examine water resistance property of coatings, the coated substrates were immersed in distilled water. After seven days of immersion, the coated substrates were taken out and visually observed. It was found that, the coatings did not develop blisters or haziness and there was no delamination of the films from the substrates. This indicates good water resistance of coatings.

Table 4.1 *Properties of PU-silica nano composite coatings*

Properties	**PUD**	**PUD+ 3%Silica**	**PUD+ 6%Silica**	**PUD+ 9%Silica**	**PUD+ 12%Silica**
Scratch hardness, g	2500	2600	2700	2900	3200
Abrasion resistance[#]	20	21	21	22	21
Gloss @60°	+90	+90	+70	+60	+45
Solvent resistance*	40	50	70	80	100

= mg loss @ 1 kg load using CS-l0 wheels & at 1000 revolutions; * = MEK double rubs.

4.4.4 Morphology of PU-silica nanocomposite

The morphology of PU-silica nano composite and pure PU were studied using transmission electron microscopy (TEM). Typical transmission electron micrographs of dispersions of colloidal silica particles in polyurethane-silica nano composites are shown in **Figure 4.6.** Homogeneous dispersion of nanosilica particles appear in nano-composite containing 3% and 6% loading of silica **(Figure 4a** and **4b)**. However, upon increasing the silica content (9%-12%), some aggregation occurs in polyurethane/silica nano composite which could be seen in **Figure 4c** and **4d**. This may be due to the densification nano particles with increase in volume fraction of silica nano particles in the PU matrix.

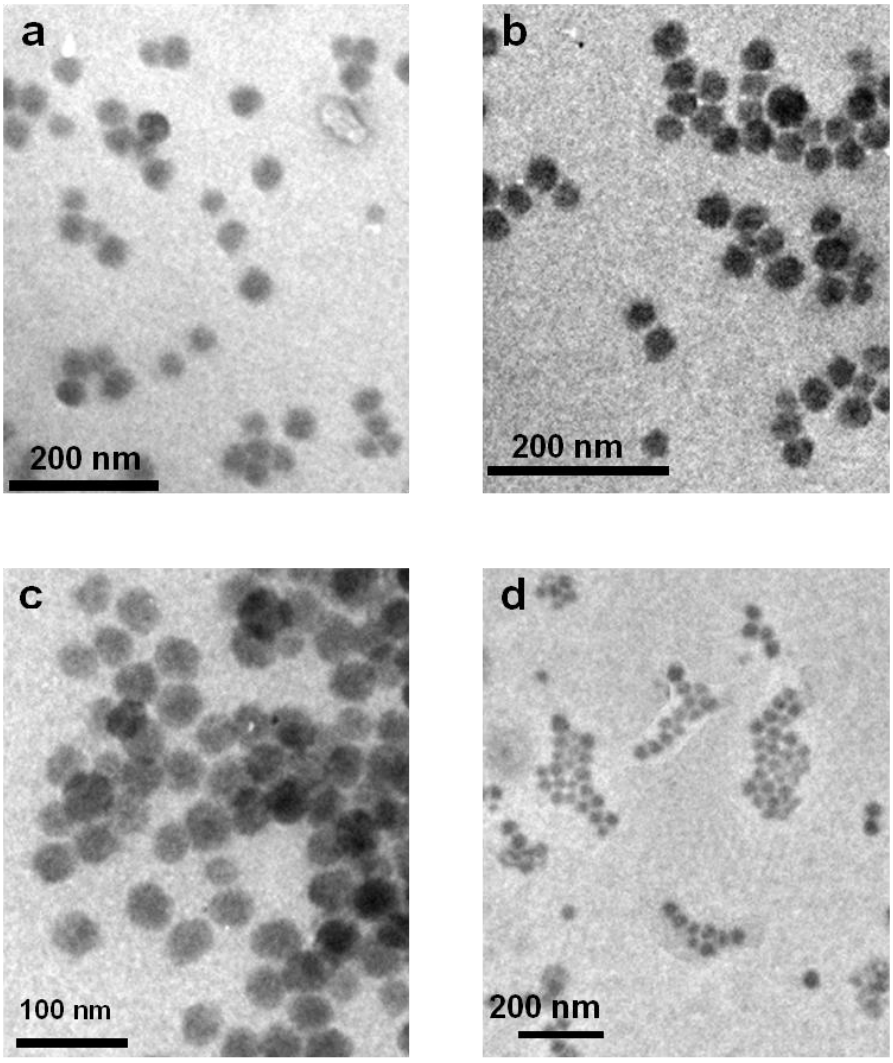

Figure 4.6 *TEM images of dispersion cast PUDs with a) 3% silica, b) 6% silica, c) 9% silica and d) 12% silica content*

4.4.5 Preparation of polyurethane-silica hybrid films and coatings with modified silica

In order to obtain stronger interaction between inorganic silica particles and the organic PU prepolymer, silica particles were modified by functionalized silane, aminopropyl triethoxy silane (APTES). **Figure 4.2** describes the modification of silica particle with APTES, where in, the APTES undergoes hydrolysis in the first step and then react with silica to form APTES grafted silica particle (G-Silica). Subsequently, with the combination of PU prepolymer and G-silica, we prepared hybrid composite films and coatings were prepared and studied the structure property relations were studied.

4.4.6 NMR spectroscopy

^{29}*Si CP MAS NMR* is a well known technique for the characterization of silicate materials. In our work, we have used ^{29}*Si CP MAS NMR* to analyze nano silica particle and its modification with APTES. We show in **Figure 4.7**, the ^{29}*Si CP MAS NMR* spectra of silica and G-silica. It could be readily seen from the figure that, the spectrum of unmodified silica showed two signals at –102.65 (*Q*3), and –112.3 (*Q*4) ppm, which arises due to free silanols and siloxane groups, respectively in the silica structure. Whereas, G-silica exhibited two additional signals at –52.92 and –69.96 ppm indicating silane condensation to give bidental and tridental grafting respectively. It was also noted that there was no signal observed in the range from 0 ppm to –50 ppm, which confirms the absence of free triethoxy linked Si atoms.

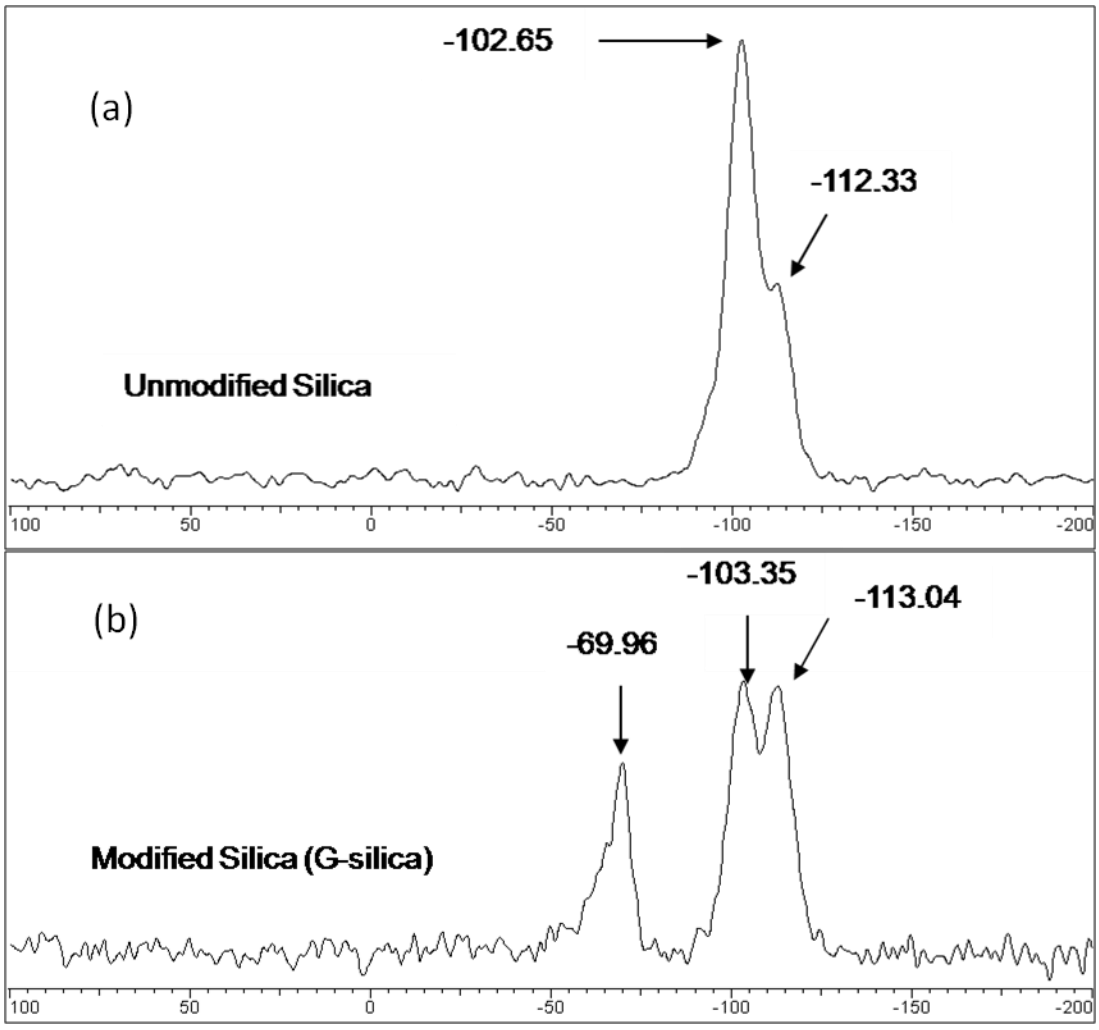

Figure 4.7 *^{29}Si CP MAS NMR spectra of (a) silica and (b) G-silica*

Thus, the signals observed in the range of –50 to –80 ppm clearly indicate the chemical modification of silica particle [32]. The chemical shifts δ_{Si} and the commonly assigned chemical structures are shown in **Table 4.2**. This study confirmed the structure of the G-silica.

Table 4.2 *δ_{Si} for different grafting structures of silane on silica*

	Structure	δ_{Si} in ppm
Siloxane (Q^4)	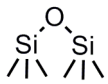	-120 to -110
Silanol (Q^3)		-100
Geminal Silanol (Q^2)	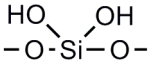	-90
Tridental grafting (T^3)	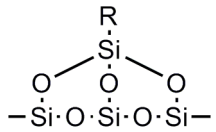	-70 to -60
Bidental grafting (T^2)	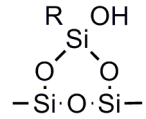	-55
Monodental grafting (T^1)	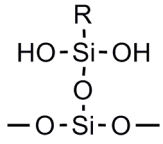	-50 to -45

4.4.7 Properties of coatings

Properties of coatings prepared from PU dispersions and its hybrid with (3 wt %) unmodified silica and G-silica are given in the **Table 4.3**. It was observed that the hybrid coatings, PUD-silica and PUD-G-silica showed higher scratch resistance compared to coatings prepared with only PUD. The enhanced scratch hardness for the hybrid coatings could be attributed to the reinforcing nature of inorganic filler in PU matrix. The scratch hardness for PUD-G-silica is more than 4000 g. In order to understand the dispersibility of both silica and G-silica into PU matrix, transmission electron microscopy (TEM) studies were carried out for both PUD-silica and PUD-G-silica.

Table 4.3 *Coating properties of PU-silica hybrid coatings*

Properties	**PUD**	**PUD + 3% Silica**	**PUD +3% G-silica**
Scratch hardness (g)	2500	3000	>4000
Abrasion resistance[#] (mg)	30	43	31
Gloss @ 60^{o}	+90	+90	+90
Solvent resistance*	40	50	250

= mg loss, 1Kg load, CS-10 wheels, 1000 cycles; * = MEK double rubs.

We show in **Figure 4.8**, the transmission electron micrographs of PUD-silica and PUD-G-silica systems recorded under same magnification. The TEM image of PUD-silica reveals the dispersion of silica nano particle into the PU matrix. Whereas, the TEM image of PUD-G-silica system showed a morphology which is similar to the crosslinked structure as a result of the reaction between the silica particle and PU prepolymer via the APTES bridges. This enhanced network density of the hybrid structure, resulted into excellent scratch resistance (>4000) of the hybrid coatings. The network density also enhanced the solvent scrub resistance of the hybrid films significantly which is evident from the results obtained in **Table 4.3**. Further, the gloss of the coatings obtained at 60^{o} were >90 which indicated no loss of gloss upon addition of modified silica particles into the matrix.

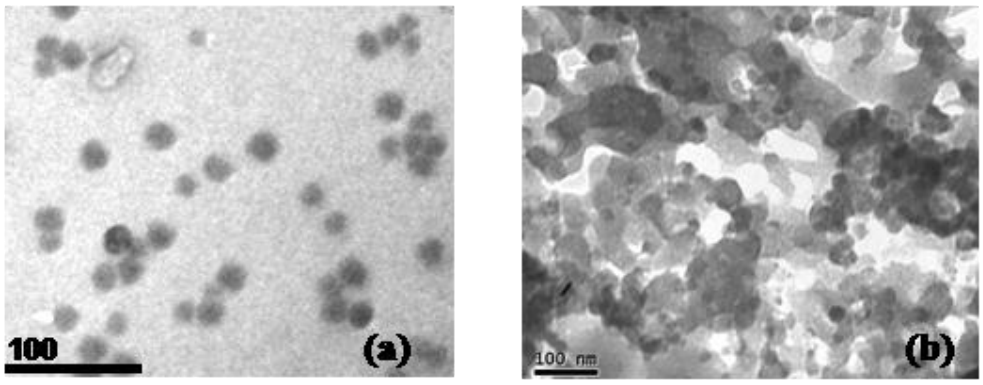

Figure 4.8 *TEM images of a) PU-silica and b) PU-G-silica hybrid system*

4.4.8 Mechanical properties of films

The best hardness and flexibility in hybrid coatings are achieved when an organic matrix is combined with inorganic nano particles. It is expected that while the organic matrix provides the flexibility, the inorganic nano particles increases the hardness by distributing applied stresses throughout the film. The flexibility can be studied quantitatively by tensile testing or by dynamic mechanical analysis on free films or coatings on substrates.

We show in **Figure 4.9**, the bar chart results of tensile strength and % elongation of the films obtained from PUDs and polyurethane-silica hybrids. It can be seen that, the tensile strength of PUD film increased from 3 MPa to 6.4 MPa upon addition of 3% nano silica which is due to the reinforcement of silica nano particle into the PU matrix. The hybrid films containing 3% modified silica (G-silica) showed further increase in tensile strength from 6.4 MPa to 7.7 MPa. This could be attributed to the enhanced chemical linkage/compatibility between silica nanoparticles and PU matrix through the silane coupling agent which increases the tensile strength of the films. However, it can be seen from **Figure 4.9** that the % elongation of the hybrid films slightly decreased due to the reinforcement of nano silica into PU matrix which reduces the flexibility of films. Nevertheless, the decrease in elongation is not very significant.

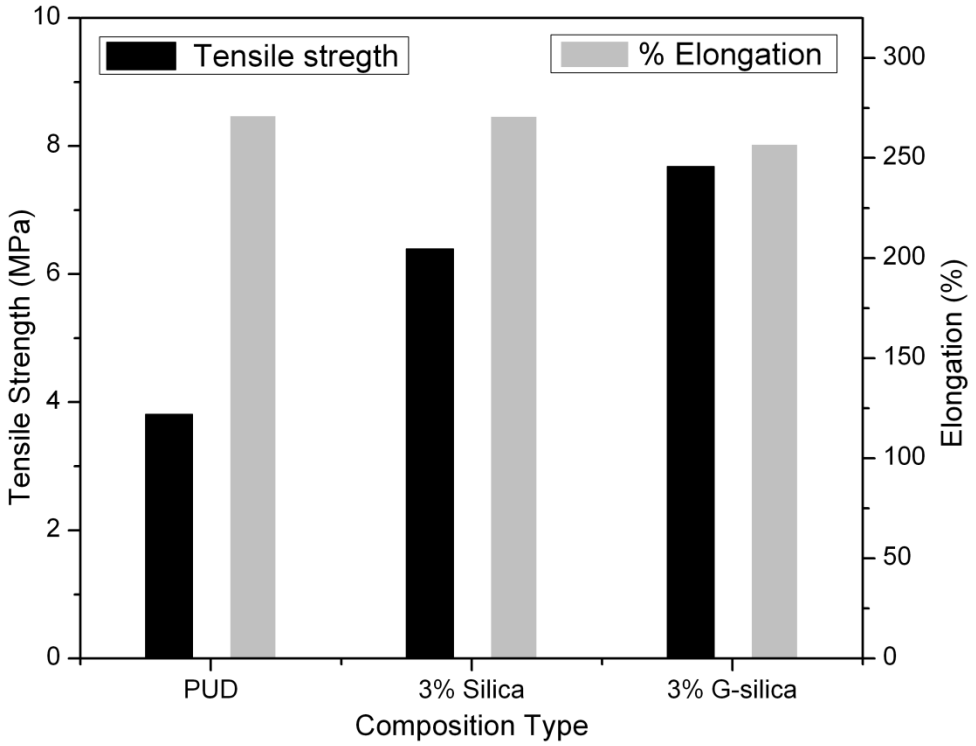

Figure 4.9 *Tensile strength and % elongation of the films*

Figure 4.10 shows the temperature dependant storage modulus (E′) of PU, PU-silica and PU-G-silica. It can be readily seen that, at subzero temperatures there is a systematic increase in storage modulus (E′) of the PUD film upon addition of 3% nano-silica and 3% G-silica. The enhanced storage modulus at low temperature could be attributed to the increased network density in the hybrid structure as a result of crosslinking between PU matrix and G-silica particles. However, with the increase in temperature the storage modulus decreases drastically and all the curves merge at 60°C. This clearly demonstrates the predominance of loss modulus (E″) over the storage modulus at high temperature.

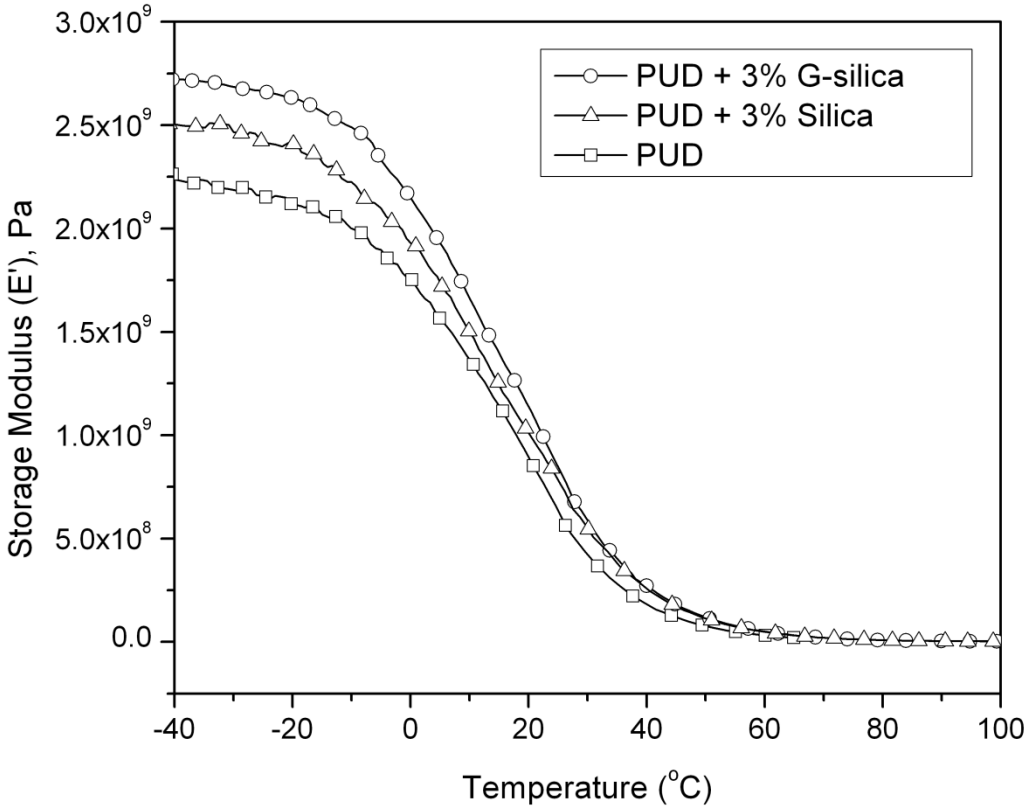

Figure 4.10 *Storage modulus verses temperature curve*

We also show in **Figure 4.11**, the plot of tan δ versus temperature of PUD, PUD-silica and PUD-G-silica films. It is observed that there is a small increase in tan δ peak (T_g) upon addition of nano-silica and G-silica into PU matrix. This is due to the restricted mobility of polymeric chains as a result of cross-linking between PU chains and silica particles.

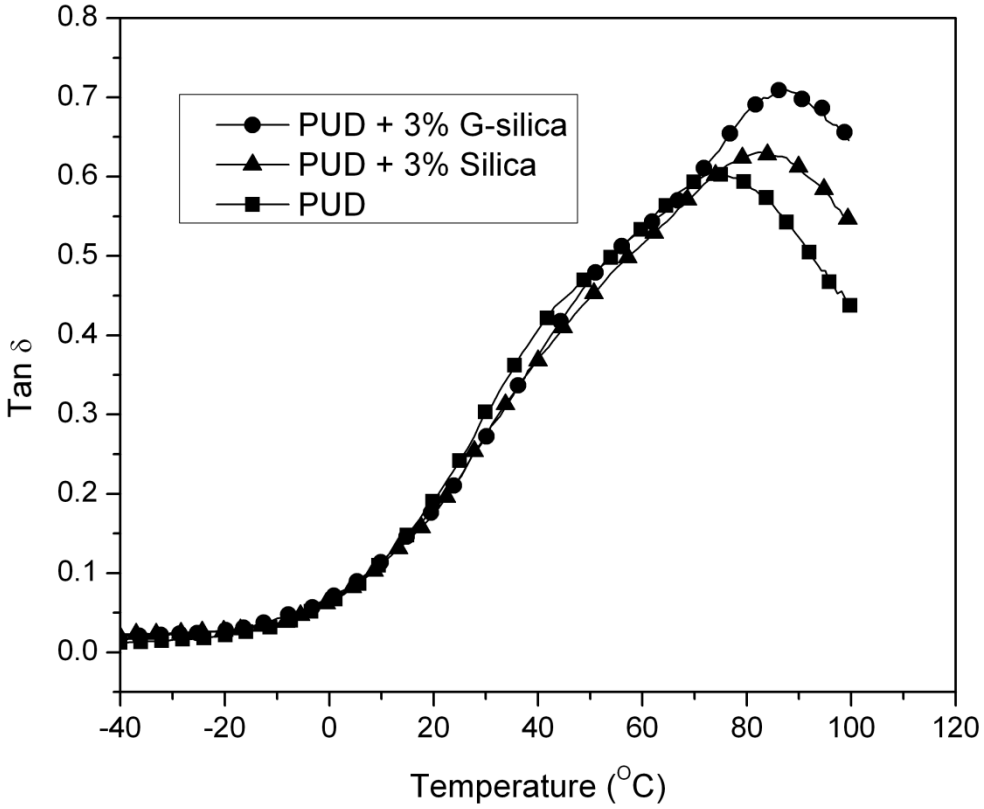

Figure 4.11 *Tan δ verses temperature curve*

4.5 Conclusion

In conclusion, the organic-inorganic hybrid coatings and films were prepared using PUDs in combination with nanosized silica and APTES modified silica. The ^{29}Si NMR studies confirmed the modification of silica nano particle. The hybrid coating exhibited improved scratch and solvent scrub resistance over PUD coating, while the gloss and abrasion resistance remained unaffected. The hybrid films also showed higher tensile strength due to the presence of nano silica and modification of nano-silica with APTES gave further improvement in the properties of films. This can be attributed to the better reinforcement of modified silica (G-silica) with PU matrix. Thus, these hybrid systems show promising applications in glossy scratch and abrasion resistant coatings.

References

1. T. C. Chang, Y. T. Wang, Y. S. Hong, and Y. S. Chiu, Journal of Polymer Science Part A: Polymer Chemistry **38**(11), 1972-1980 (2000).
2. N. Hasegawa, H. Okamoto, M. Kawasumi, and A. Usuki, **74**(14), 3359-3364 (1999).
3. Limin L, Zongneng QI, and Z. Xiaoguang, Journal of Applied Polymer Science **71**(7), 1133-1138 (1999).
4. M. Okazaki, M. Murota, Y. Kawaguchi, and N. Tsubokawa, Journal of Applied Polymer Science **80**(4), 573-579 (2001).
5. C. Zilg , R. Mülhaup, and J. Finter, Macromolecular Chemistry and Physics **200**(3), 661-670 (1999).
6. S. C. Jana and S. Jain, Polymer **42**(16), 6897-6905 (2001).
7. G. Leder, T. Ladwig, V. Valter, S. Frahn, and J. Meyer, Progress in Organic Coatings **45**(2-3), 139-144 (2002).
8. J. L. Luna-Xavier, A. Guyot, and E. Bourgeat-Lami, Journal of Colloid and Interface Science **250**(1), 82-92 (2002).
9. A. M. Torro-Palau, J. C. Fernandez-Garcia, A. C. Orgiles-Barcelo, and J. M. Martin-Martinez, International Journal of Adhesion and Adhesives **21**(1), 1-9 (2001).
10. S. X. Zhou, L. M. Wu, J. Sun, and W. D. Shen, Progress in Organic Coatings **45**(1), 33-42 (2002).
11. C. L. Wu, M. Q. Zhang, M. Z. Rong, and K. Friedrich, Composites Science and Technology **62**(10-11), 1327-1340 (2002).
12. A. K. Manna, P. P. De, and D. K. Tripathy, Journal of Applied Polymer Science **84**(12), 2171-2177 (2002).
13. Y. P. Mamunya, V. I. Shtompel, E. V. Lebedev, P. Pissis, A. Kanapitsas, and G. Boiteux, European Polymer Journal **40**(10), 2323-2331 (2004).
14. S. Frings, R. van der Linde, A. J. ten Hagen, and H. A. Meinema, Progress in Organic Coatings **34**(1-4), 248-248 (1998).
15. S. Frings, C. F. van Nostrum, R. van der Linde, H. A. Meinema, and C. H. A. Rentrop, Journal of Coatings Technology **72**(901), 83-89 (2000).

16. A. Rekondo, M. J. Fernandez-Berridi, and L. Irusta, European Polymer Journal **42**(9), 2069-2080 (2006).
17. J. H. Zou, W. F. Shi, and X. Y. Hong, Composites Part a-Applied Science and Manufacturing **36**(5), 631-637 (2005).
18. Y. Chen, S. Zhou, G. Gu, and L. Wu, Polymer **47**(5), 1640-1648 (2006).
19. H. Ni, W. J. Simonsick, A. D. Skaja, J. P. Williams, and M. D. Soucek, Progress in Organic Coatings **38**(2), 97-110 (2000).
20. H. Ni, A. D. Skaja, and M. D. Soucek, Progress in Organic Coatings **40**(1-4), 175-184 (2000).
21. J. W. Xu, W. F. Shi, and W. M. Pang, Polymer **47**(1), 457-465 (2006).
22. S. Chen, J. J. Sui, L. Chen, and J. A. Pojman, Journal of Polymer Science Part a-Polymer Chemistry **43**(8), 1670-1680 (2005).
23. S. M. Lai, C. K. Wang, and H. F. Shen, Journal of Applied Polymer Science **97**(3), 1316-1325 (2005).
24. H. T. Jeon, M. K. Jang, B. K. Kim, and K. H. Kim, Colloids and Surfaces a-Physicochemical and Engineering Aspects **302**(1-3), 559-567 (2007).
25. J.-M. Yeh, C.-T. Yao, C.-F. Hsieh, H.-C. Yang, and C.-P. Wu, European Polymer Journal **44**(9), 2777-2783 (2008).
26. T.-L. Wang, C.-H. Yang, Y.-T. Shieh, and A.-C. Yeh, European Polymer Journal **45**(2), 387-397 (2009).
27. M. M. Jalili and S. Moradian, Progress in Organic Coatings **66**(4), 359-366 (2009).
28. E. P. Plueddemann, *Silane Coupling Agents* (Plenum Press, New York, 1982).
29. Bock M, T. Engbert, S. Groth, B. Klinksiek, P. Yeske, G. Jonschker, and U. Dellwo, (US Patent 6020419, 2000).
30. B. M. Novak, Advance Materials **5**(6), 422-433 (1993).
31. Z. S. Petrović, I. Javni, A. Waddon, and G. Bánhegyi, Journal of Applied Polymer Science **76**(2), 133-151 (2000).
32. F. Bauer, V. Sauerland, H. Ernst, H. J. Gläsel, S. Naumov, and R. Mehnert, Macromolecular Chemistry and Physics **204**(3), 375-383 (2003).

5.1 Introduction

Glassy and highly crosslinked thermoset epoxy resins have been used for formulating structural adhesives because of their properties such as good wetting, formation of strong bonds with many polar high-energy substrates, low cure shrinkage without evolution of low molecular weight substances, superior mechanical properties, and environmental stability. For structural adhesives with good elevated temperature capability, high glass transition temperature is an essential requirement to retain the adhesive strength at high temperature. All unmodified cured epoxy resins with relatively high T_g have a major drawback, i.e., their brittleness or lack of crack growth resistance, which can produce catastrophic failure of the adhesive joint. Therefore, toughening of epoxies has become very important to ensure the feasibility of these materials for practical applications.

The addition of a second phase, either rigid or soft can be a solution to this problem [1]. Rigid particles used to improve the fracture toughness of epoxies comprises of either inorganic or organic particles. When inorganic particles are employed, the modified epoxy polymer is named "particulate-filled epoxy". Whereas, the soft particles used for this purpose are basically rubbery particles with glass transition temperatures much lower than that of service conditions. The technique of incorporation of the rubbery phase is known as "rubber-toughening" or "rubber modification" of epoxide. Sultan et al. [2] were the first one to show that the fracture toughness of epoxies can be improved by the introduction of a dispersed rubber phase.

Butadiene-acrylonitrile copolymers with reactive functional end groups (CTBN, ETBN and ATBN) are widely used as toughening agents. The rubber is initially miscible with the epoxy but during the curing the rubber particles phase separate due to slight immiscibility with the matrix. At the appropriate concentration of rubber, the dispersed rubber phase can improve the toughness without a significant decrease in the other properties of epoxies [3, 4]. The improved toughness of rubber-toughened epoxies has been proposed through three mechanisms; crazing, shear banding and elastic deformation of rubber partials. These mechanisms can either act alone, or in combination, to produce toughening effect.

McGarry and co-workers [5] investigated the behavior of rubber toughened epoxy and suggested the toughening mechanism involving generation of crazes and shear banding in the vicinity of rubber particles.

Acrylic terpolymer with pendant epoxy groups were effectively used to reduce the brittleness of bisphenol-A diglycidyl ether epoxy resin. And it was found that, the toughening effect is hypothesized to be due to cavitation, which relieves the triaxial tension at the crack tip, and shear band formation, which creates a large plastic zone. The addition of 20 wt% of the terpolymer resulted in an 80% increase in the fracture toughness (KIC) of the cured resin at a slight expense of its mechanical properties [6, 7].

A series of blends were prepared by adding a polyetherimide, in varying proportions, to a trifunctional epoxy resin, triglycidylparaminophenol, cured with 4,4′-diaminodiphenylsulphone. All the materials showed two-phase morphology when characterized by dynamic mechanical thermal analysis and scanning electron microscopy. Addition of the thermoplastic resulted in improved fracture properties (KIC and GIC), as measured by three-point bending experiments, although no obvious correlation with blend morphology was observed [8]. Chen and Hourston studied the miscibility and fracture behavior of an EP-bisphenol-A polycarbonate blend [9] cured with diethylenetriamine.

Polyphenylene oxide (PPO) has been studied as a novel toughening agent for epoxy systems[10, 11]. Upon curing, two-phase solids were formed, which contained discrete PPO particles. However, the two-phase particulate morphology was not uniform and numerous large, occluded PPO particles were observed. In order to improve the uniformity, several styrene-maleic anhydride copolymers were evaluated as potential surfactants for PPO-DGEBA blends [4].

Barcia et al. [12] employed HTPB as a surface modifier in carbon fiber (CF) reinforced, epoxy matrix composites. The surfaces of carbon fibers (CFs) were grafted with HTPB, and this formed a flexible interface between CF and epoxy matrix, which ultimately improved the mechanical behavior of the system. In an interesting study, the DGEBA based epoxy resin was modified with block copolymers from isocyanate terminated

polybutadiene [13]. Ozturk et al. [14] employed modified HTPB rubbers to improve thermal and mechanical properties and ultimately to toughen an epoxy thermoset matrix.

Epoxy-cyclic anhydride-HTPB system was studied to develop structure property relationship to propose the mechanism of failure based acoustic emission and morphological studies [15]. A wide range of deformation mechanisms have been prepared in the literature to explain the observed improvements in toughness [16-30]. Structures of some of the toughening materials are given in **Figure 5.1**.

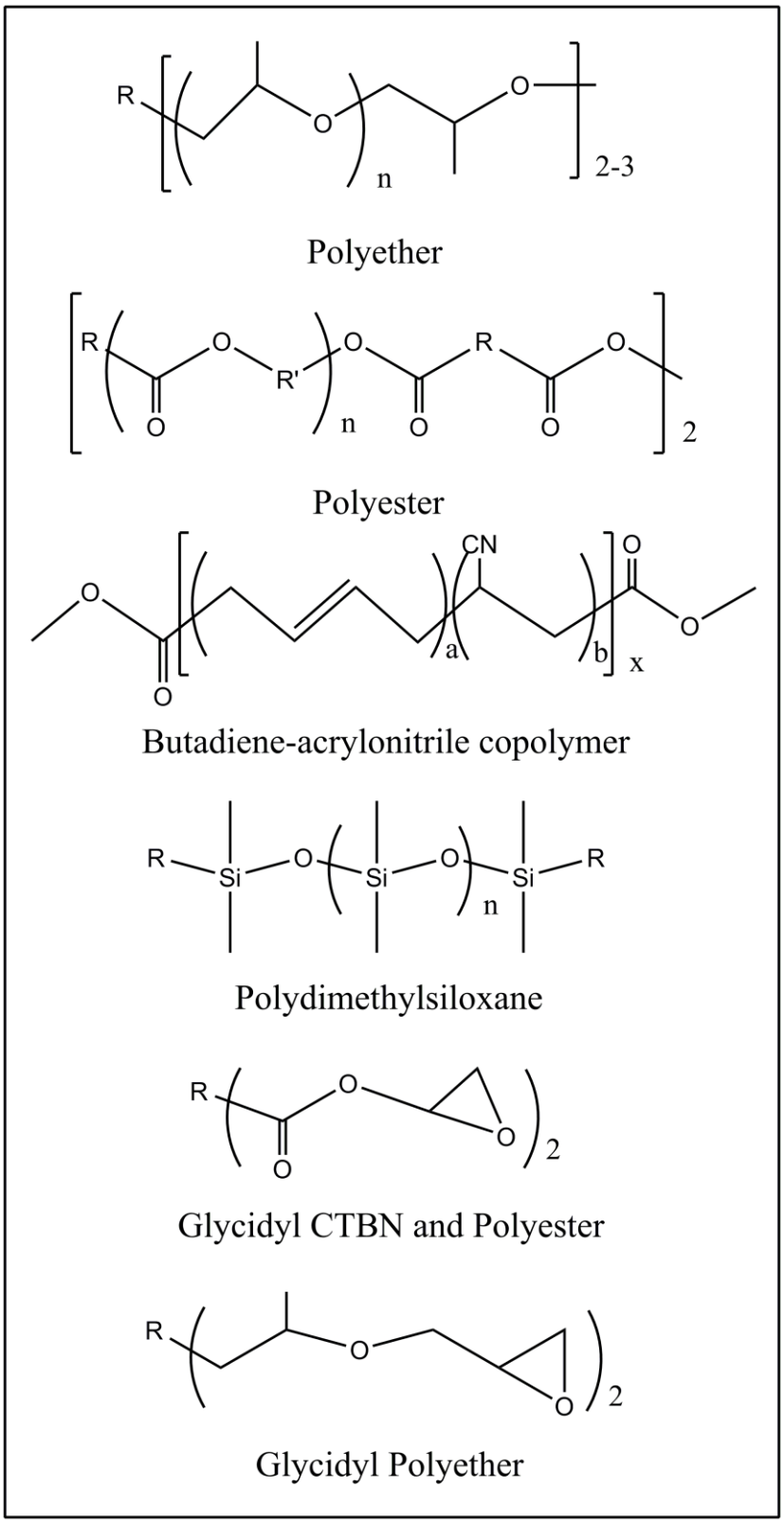

Figure 5.1 *Chemical structures of some toughening agents used in epoxy resins*

Despite several studies on the enhancement of toughness of the cured epoxy resin using reactive liquid polymers such as CTBN and ATBN, only scanty reports are available on the high temperature applications of these adhesives. Therefore, in the present work the influence of CTBN and ATBN incorporation on the elevated temperature adhesion strength and mechanical properties of epoxy adhesive were studied.

5.2 Experimental

5.2.1 Materials

The epoxy resin, liquid diglycidyl ether of bisphenol A (DGEBA) with an epoxy equivalent value of 5.7 eq/Kg and a hardener namely, 3,3´-dimethyl-4,4´-diaminodicyclohexyl methane were obtained from HAL, Bangalore, India. The reactive liquid polymers (RLPs), carboxyl terminated acrylonitrile butadiene copolymer (CTBN) under the trade name Hypro CTBN 1300X8 and amino terminated acrylonitrile butadiene copolymer (ATBN) under the trade name Hypro ATBN 1300X16, were obtained from Emerald Performance Material, UK and used as received. Chemical structures of epoxy resin, CTBN and hardener are shown in **Figure 5.2** and the characteristics of CTBN and ATBN are given in **Table 5.1**.

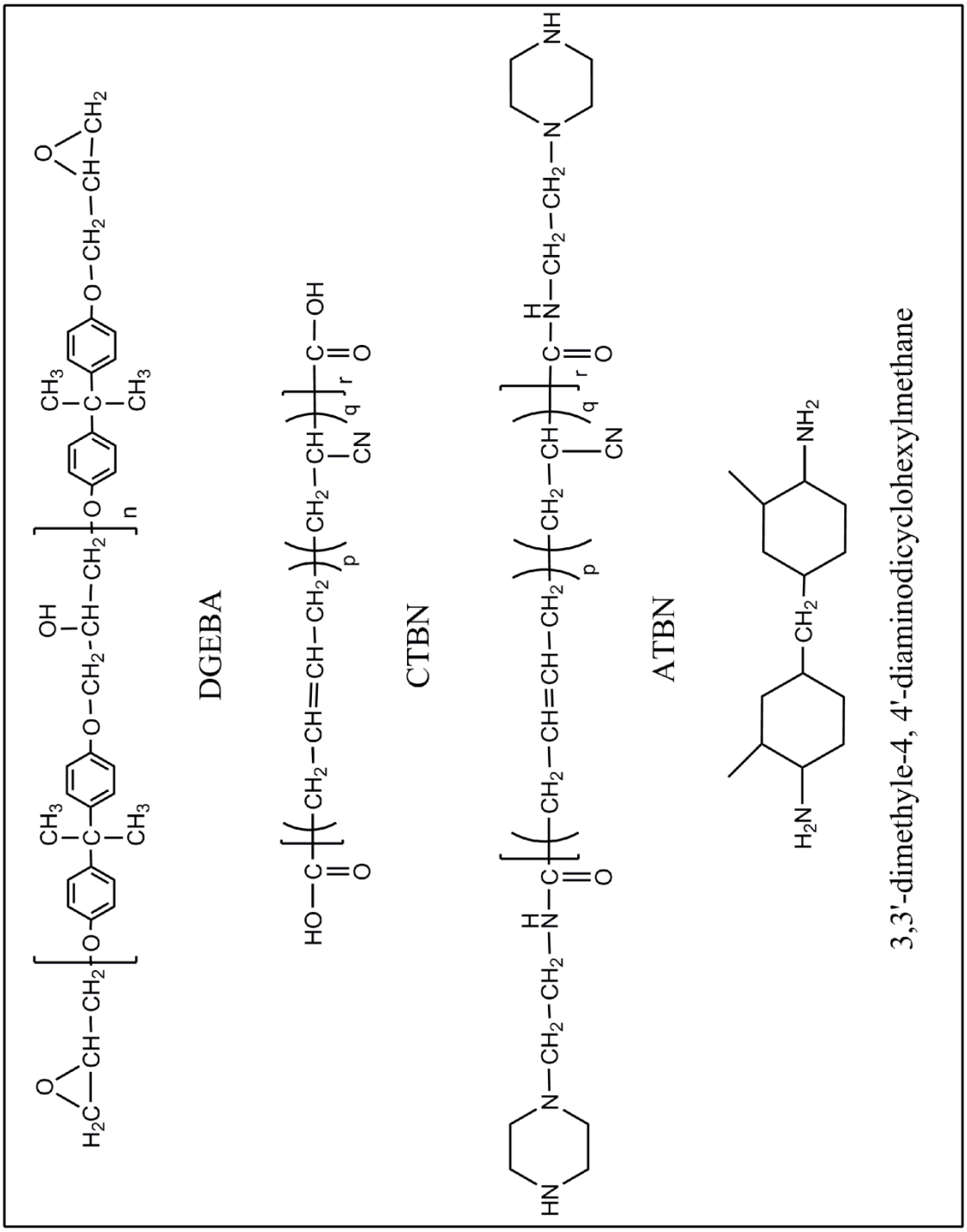

Figure 5.2 *Chemical structure of epoxy resin (DGEBA), CTBN, ATBN and hardener*

Table 5.1 *Characteristics of CTBN and ATBN*

Characteristics	**CTBN**	**ATBN**
Acrylonitrile content (%)	18	18
Carboxyl content (Acid Number)	29	-
Amine Value	-	62
Brookfield viscosity (cP) @ 27°C	1,35,000	2,00,000
Specific gravity	0.948	0.95
Glass transition temperature (T_g) (°C)	-52	-51

5.2.2 Preparation of epoxy-CTBN adduct

Epoxy terminated CTBN adduct was prepared as per the scheme shown in **Figure 5.3**. In a typical procedure 100 parts by weight of CTBN was added to 100 parts by weight epoxy resin containing 0.25 parts by weight triphenylphosphine (TPP) and mixed with a mechanical stirrer and reacted under inert atmosphere at 100 °C until carboxyl groups were completely utilized. The conversion of carboxyl group was determined by titrating against 0.1N alcoholic potassium hydroxide solution.

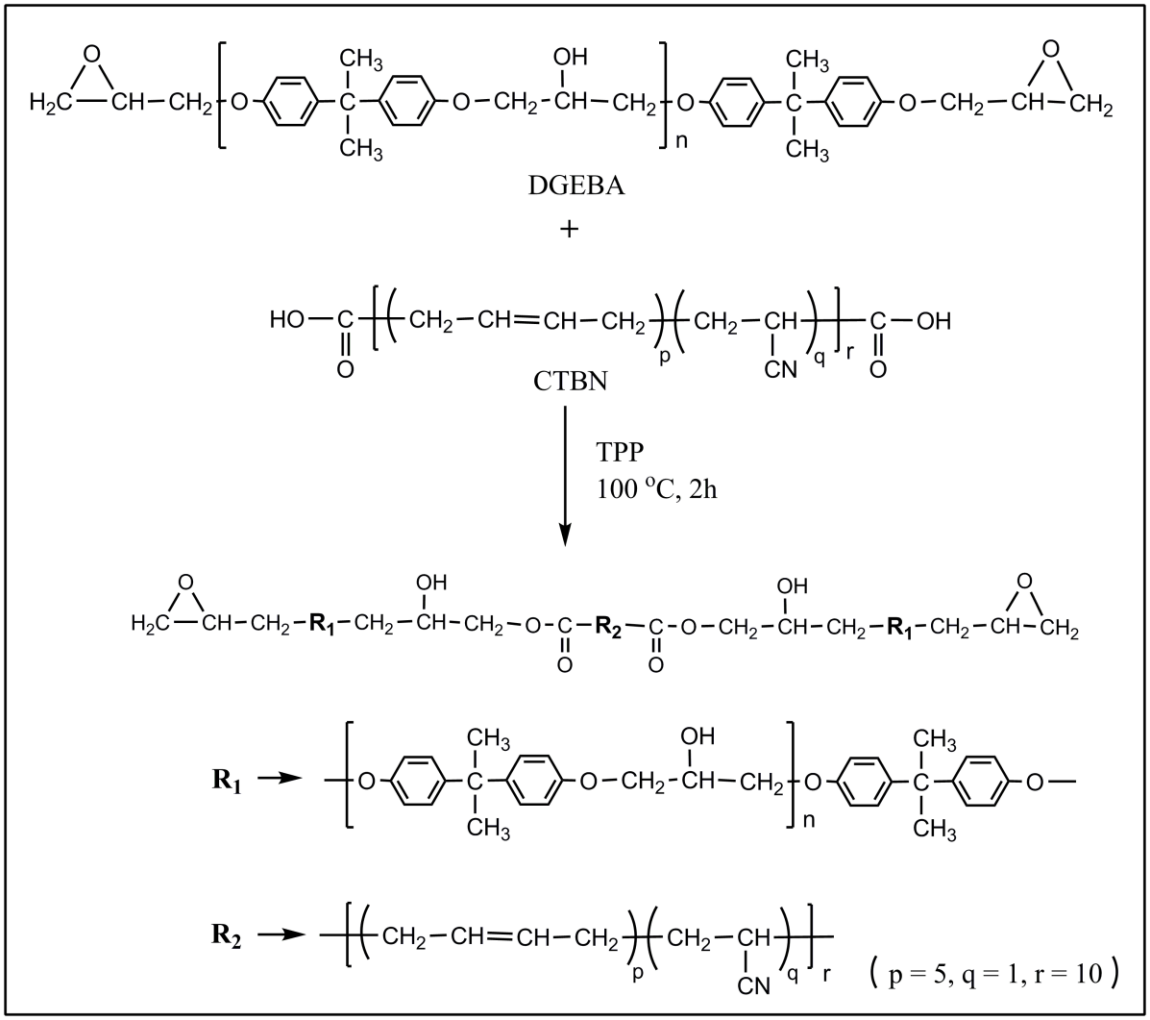

Figure 5.3 *Reaction scheme for the preparation of epoxy-CTBN adduct*

5.2.3 Preparation of adhesive compositions

The epoxy-terminated rubber (epoxy-CTBN adduct) was incorporated into epoxy resin to get various concentrations of rubber in the formulation whereas, ATBN was incorporated as such. All the compositions were cured with 4,4'-dimethyl diaminodicyclohexyl methane hardener (35 phr). Adhesive composition and cure conditions are given in **Table 5.2**. The adhesive system was degassed to remove the air bubbles from the system. The sample codes for example CTEP 15 and ATEP 15 indicates 15% of CTBN and 15% of ATBN in the cured epoxy adhesive respectively.

Table 5.2 *Adhesive composition and cure conditions*

Composition Code	RLP content (Wt %)	Cure condition	
		Curing Temp (^{o}C)/Time (h)	Post curing Temp (^{o}C)/Time (h)
CTEP 0	0	80/1	120/4
CTEP 05	5	80/1	120/4
CTEP 10	10	80/1	120/4
CTEP 15	15	80/1	120/4
CTEP 20	20	80/1	120/4
CTEP 25	25	80/1	120/4
CTEP 30	30	80/1	120/4
ATEP 0	0	80/1	120/4
ATEP 05	5	80/1	120/4
ATEP 10	10	80/1	120/4
ATEP 15	15	80/1	120/4
ATEP 20	20	80/1	120/4
ATEP 25	25	80/1	120/4
ATEP 30	30	80/1	120/4

5.2.4 Preparation of LSS test specimens

For adhesive lap shear strength (LSS) test, metal plates (100mm in length, 25mm in width and thickness of 1.6mm) were used as substrates. Following pretreatment was performed on the metal plates: Metal plates were immersed in ortho-phosphoric acid-ethanol solution (in the ratio of 1:2 by volume) for 10 min at 60°C followed by washing with water and ethanol successively and dried at 120°C for 1h before bonding. About 0.1g of epoxy adhesive (prepared as discussed previously) was spread uniformly on both surfaces of the substrates (surface area 3.175 cm^2). After applying the adhesive on the substrates and forming adhesive layer, clamps were used to hold and to ensure the continuous contact between both the substrates. The test specimens thus prepared, were

kept in the hot air circulated oven at 80°C for 1h for curing and subsequently, post curing at 120°C for 4h.

5.2.5 Preparation of test specimens for DMA analysis

An adhesive formulation after degassing was poured into a PTFE mould and cured in oven as discussed earlier. The cast piece obtained was 1 mm thick, 10 mm in width and 20 mm in length.

5.2.6 Testing and characterization

5.2.6.1 FT-IR spectroscopic analysis

FT-IR studies were done by using a Perkin Elmer Spectrum GX FT-IR spectrometer. Free standing films of cured compositions were cast and used for measurement. The uncured samples were dissolved in chloroform and taken for FT-IR measurements.

5.2.6.2 Thermo gravimetric analysis (TGA)

Thermo gravimetric analysis was performed on the cured, neat and rubber-modified samples using a Perkin Elmer STA 6000 thermo gravimetric analyzer. About 10 mg of sample was taken in a platinum crucible and heated from ambient to 900 °C at a heating rate of 10°C/min in the air with the flow rate of 50 mL/min.

5.2.6.3 Morphological properties

The morphology of cryo-fractured surfaces of all cured adhesive compositions with gold sputtered coating was studied using a scanning electron microscope (SEM Leica-440).

5.2.6.4 Mechanical testing

Dynamic mechanical properties of adhesive compositions were determined using a dynamic mechanical analyzer (Rheometric Scientific DMTA), with a single cantilever bending mode at a heating rate of 5°C/min and at frequency of 10rad/s. The lap shear strength was determined as per ASTM D1002 by using an Instron tensile tester. Tests were carried out at 30°C and 150°C with a speed of 5mm/min and the results were an

average of at least five repetitive measurements. A typical LSS test specimen is shown in **Figure 5.4**.

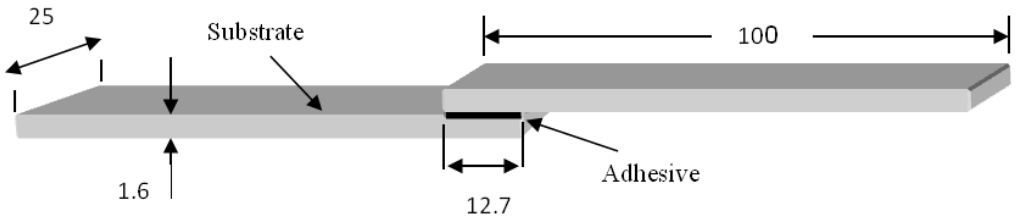

Figure 5.4 *Test specimen used for lap shear strength with adhesive (dimensions in mm)*

5.3. Results and Discussion

5.3.1 FT-IR analysis

In order to elucidate the formation of epoxy-CTBN adduct prepolymer and to study the curing reaction of adhesive, the samples were analyzed by FT-IR spectrophotometer. We show in **Figure 5.5 (a-e)** the FT-IR spectra of a) epoxy resin, b) CTBN, c) ATBN, d) epoxy-CTBN adduct and e) the cured epoxy composition CTEP 15.

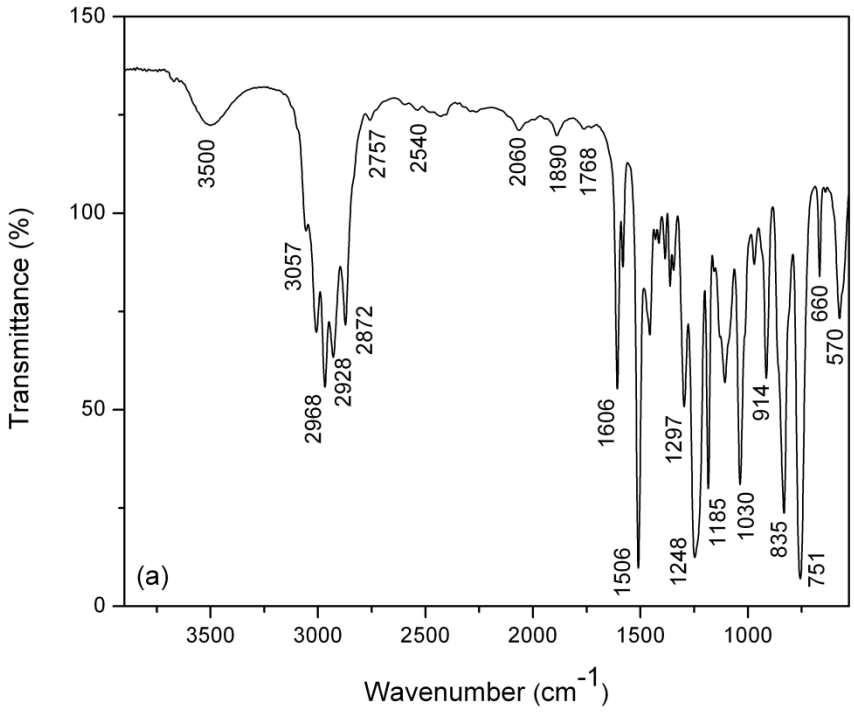

Figure 5.5a *FTIR spectrum of epoxy resin*

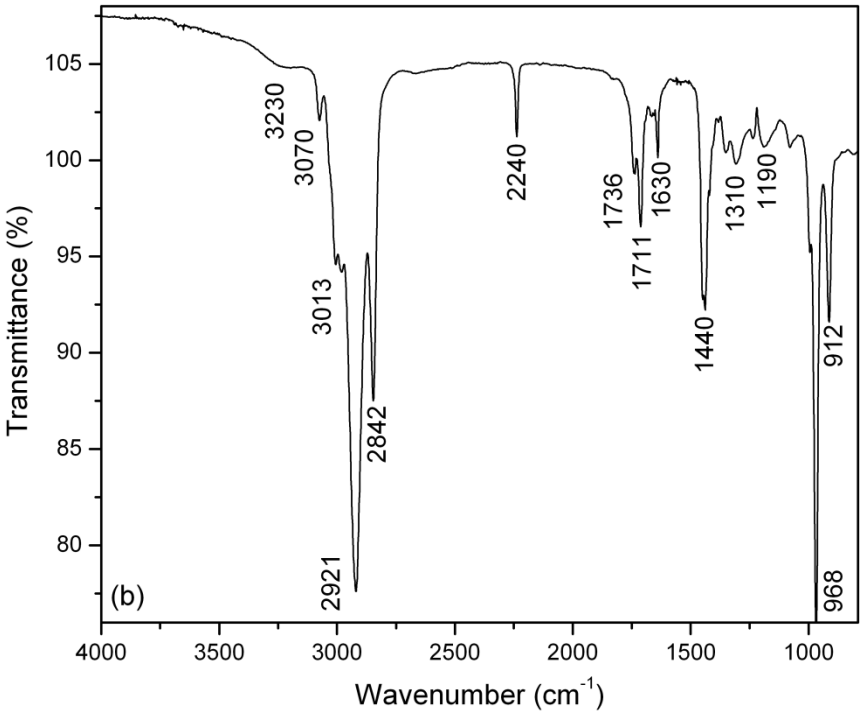

Figure 5.5b *FTIR spectrum of CTBN*

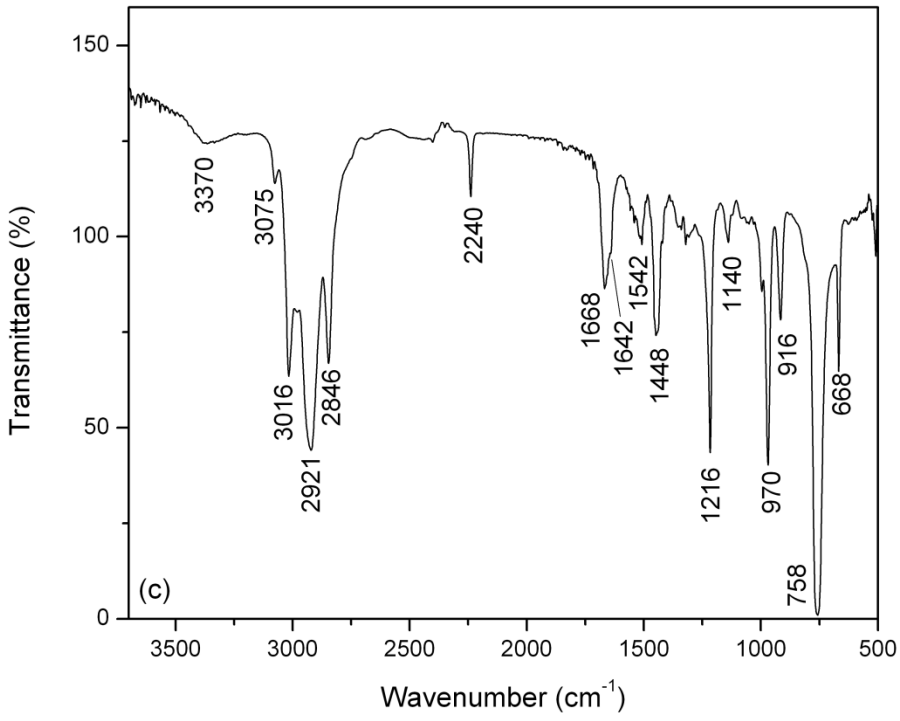

Figure 5.5c *FTIR spectrum of ATBN*

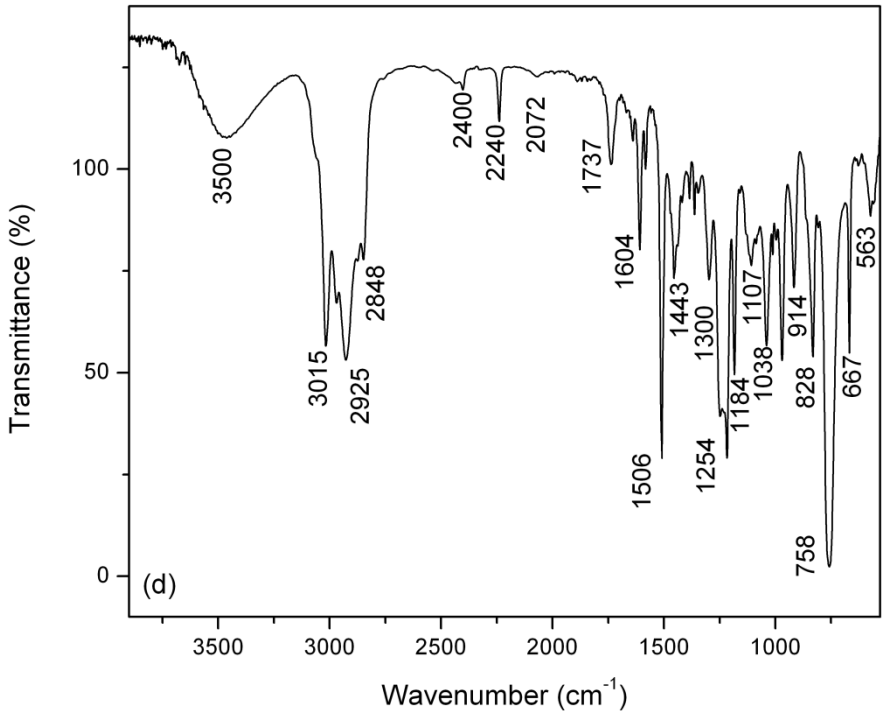

Figure 5.5d *FTIR spectrum of epoxy-CTBN adduct*

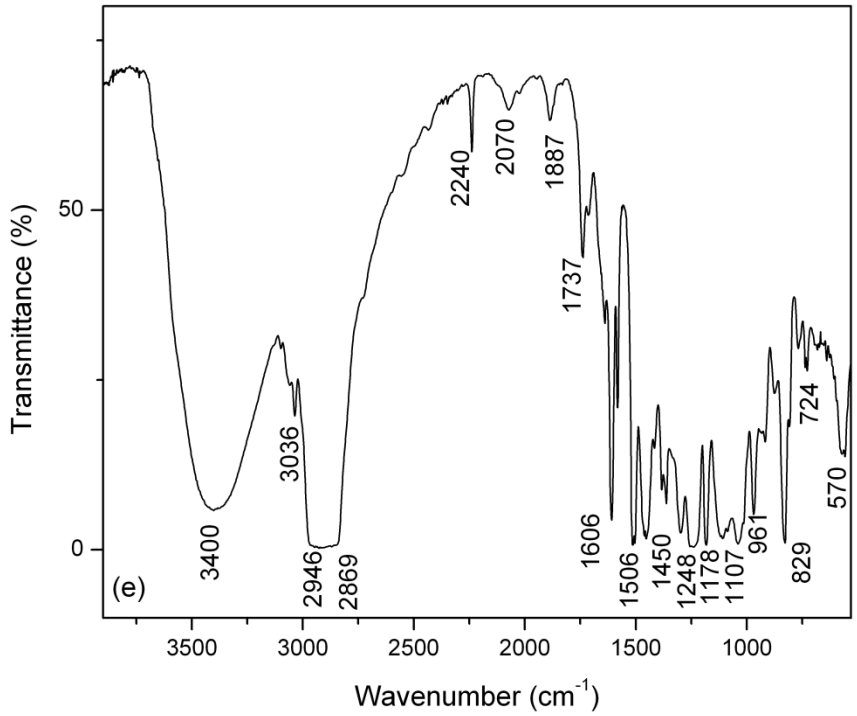

Figure 5.5e *FTIR spectrum of cured CTEP 15*

The absorption band at 914 cm^{-1} (**Figure 5.5a**) can be ascribed to the oxirane group of epoxy resin. The absorption band at 3500 cm^{-1} arises from the –OH groups of epoxy resin. Figure 4b shows the IR spectra of CTBN, where the absorption bands at 912 cm^{-1} due to the vinyl group of CTBN and the absorption band at 1711 cm^{-1} and 1736 cm^{-1} due to stretching vibrations of carboxyl groups of CTBN. A sharp −C≡N peak at 2240 cm^{-1} also appeared in the CTBN spectrum. ATBN spectrum showed broad absorption band centered at 3370 cm^{-1} which can be readily attributed to the NH modes of the amide linkages in the terminal groups. This peak displayed a low frequency component due to hydrogen bonded N-H groups, while high frequency component was due to free N-H. Typical amide absorptions were detected at 1642 cm^{-1} (C=O stretching) and 1542 cm^{-1} (N-H bending). The ATBN spectrum clearly displayed two unresolved components at 1668 cm^{-1} due to free carbonyls and at 1642 cm^{-1} due to hydrogen bonded carbonyls. In the spectrum of epoxy-CTBN adduct (**Figure 5.5d**), the absorption band at 1711 cm^{-1} (due to –COOH group) disappeared and a new absorption band at 1737 cm^{-1} appeared, which indicates the formation of ester group due to the reaction between the carboxyl group of CTBN and the oxirane group of epoxy resin. Finally, in the IR spectrum of cured sample (**Figure 5.5e**), the absorption band at 914 cm^{-1} disappeared indicating the complete reaction of oxirane group with the hardener in the sample (CTEP 15). Furthermore, the presence of absorption band at 2240 cm^{-1} in both the spectra of epoxy-CTBN adduct and cured sample clearly indicates that the −C≡N group remain unaltered during the formation of epoxy-CTBN adduct as well as during the curing process.

5.3.2 Dynamic mechanical analysis (DMA) study

The dynamic mechanical loss factor (tan δ) versus temperature plots of pure epoxy resin and CTBN and ATBN incorporated epoxy resins are shown in **Figures 5.6 - 5.9**. It can be readily seen that there is a single relaxation peak for the neat epoxy (CTEP 0) at around 130^{o}C which can be related to the glass transition temperature of the neat epoxy resin. This is referred to as α-transition. However, upon incorporating CTBN and ATBN into epoxy resin, there was a slight shift in tan δ peak corresponding to α-transition of epoxy along with the appearance of small peak at around -40^{o}C, which could be attributed to β-transition in CTBN and ATBN moiety. The β transition/relaxation peak at about -40°C

becomes more prominent above the 15% of CTBN and above 10% ATBN content as seen from **Figure 5.7** and **5.9** The intensities of β-relaxation peak for the sample containing 25% and 30% of CTBN are greater than with the α relaxation peaks, whereas, the intensities of the β relaxation peaks containing 20%, 25%, and 30% of ATBN were smaller than the α relaxation peaks. This indicates that, CTBN gave more flexibility to the matrix as compared to ATBN. The increase in flexibility of the polymer network and phase inversion with increase in RLP content has been further evidenced in the morphological studies of adhesive composition containing CTBN. Initially, CTBN shows good solubility in base epoxy resin resulting into homogeneous solution. As the curing reaction proceeds, the molecular weight increases and phase separation occurs at some stage, leading to the formation of two phase morphology. In this two phase system, the rubber particles dispersed and bonded to the epoxy matrix act as center for dissipation of mechanical energy by cavitation and shear yielding.

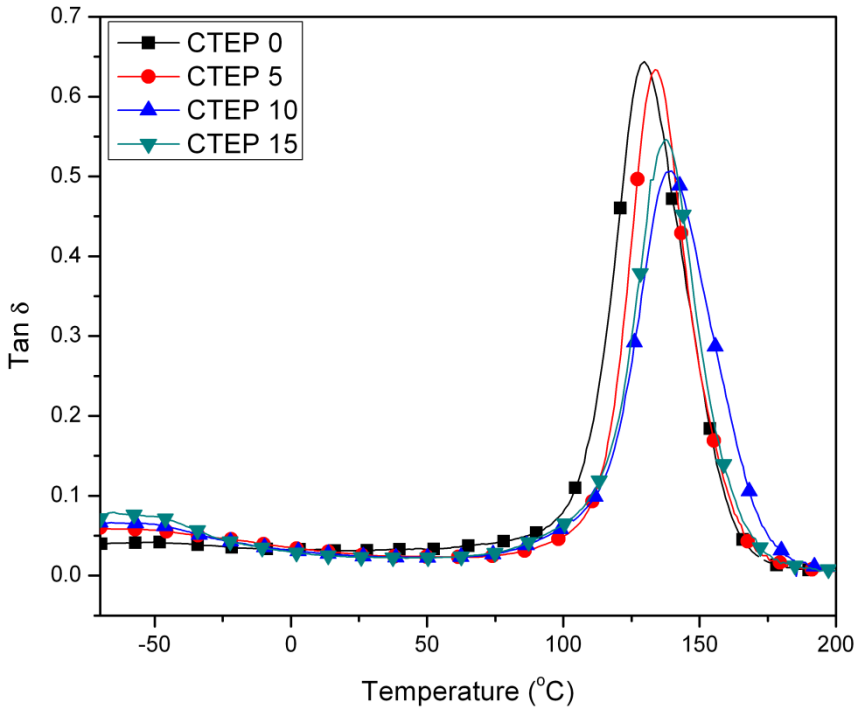

***Figure* 5.6** *Dynamic loss factor, Tan δ versus temperature for cured epoxy compositions containing CTBN*

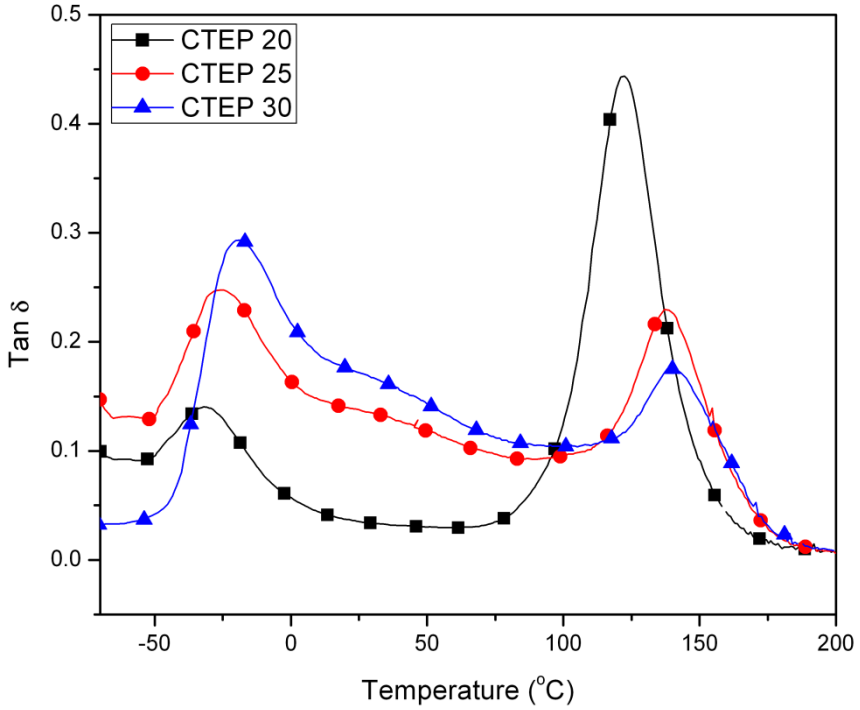

Figure 5.7 *Dynamic loss factor, Tan δ versus temperature for cured epoxy compositions containing CTBN*

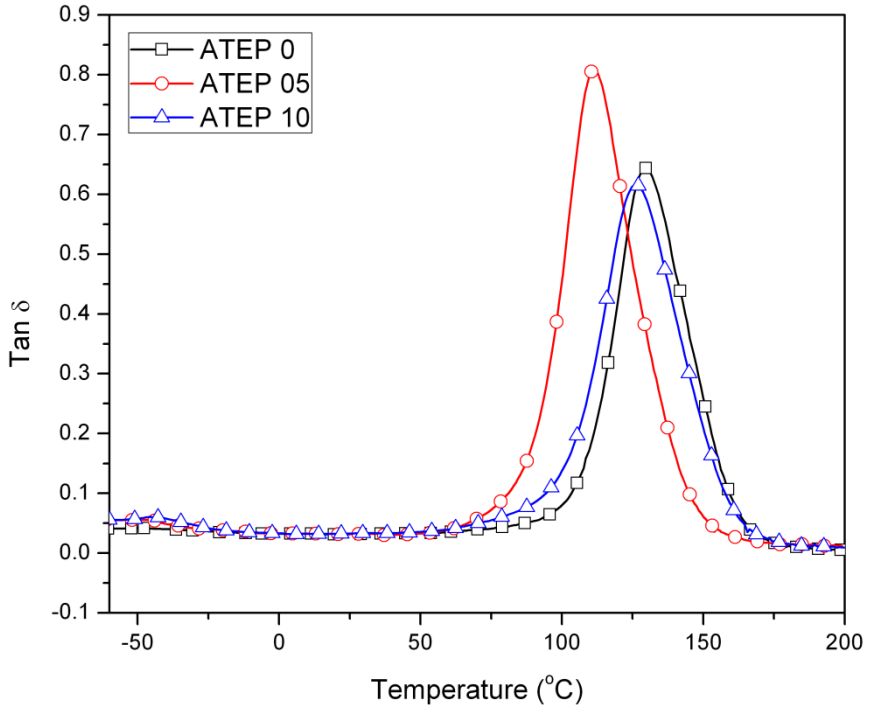

Figure 5.8 *Dynamic loss factor, Tan δ versus temperature for cured epoxy compositions containing ATBN*

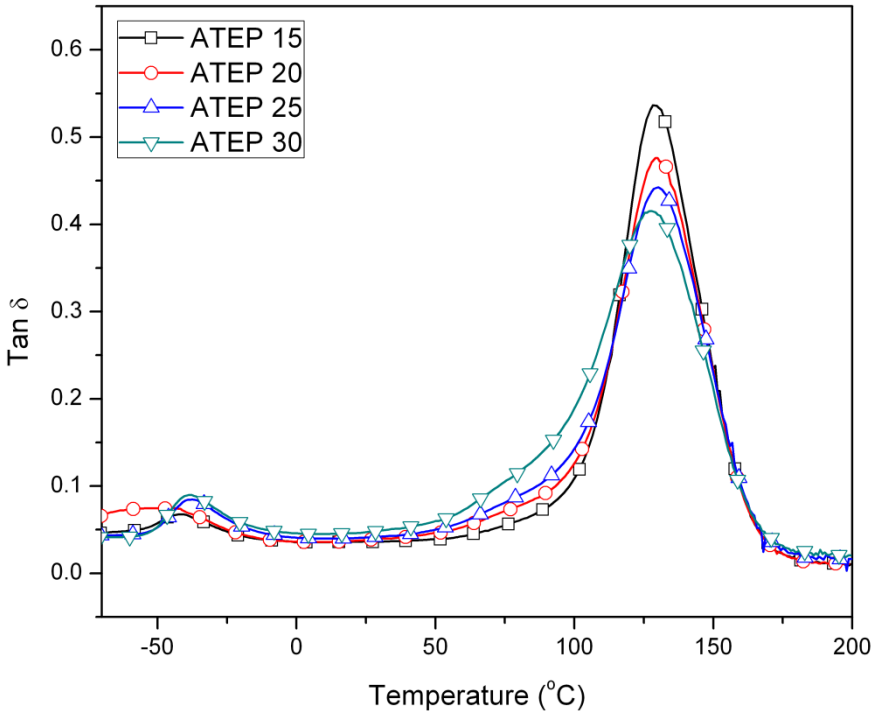

Figure 5.9 *Dynamic loss factor, Tan δ versus temperature for cured epoxy compositions containing ATBN*

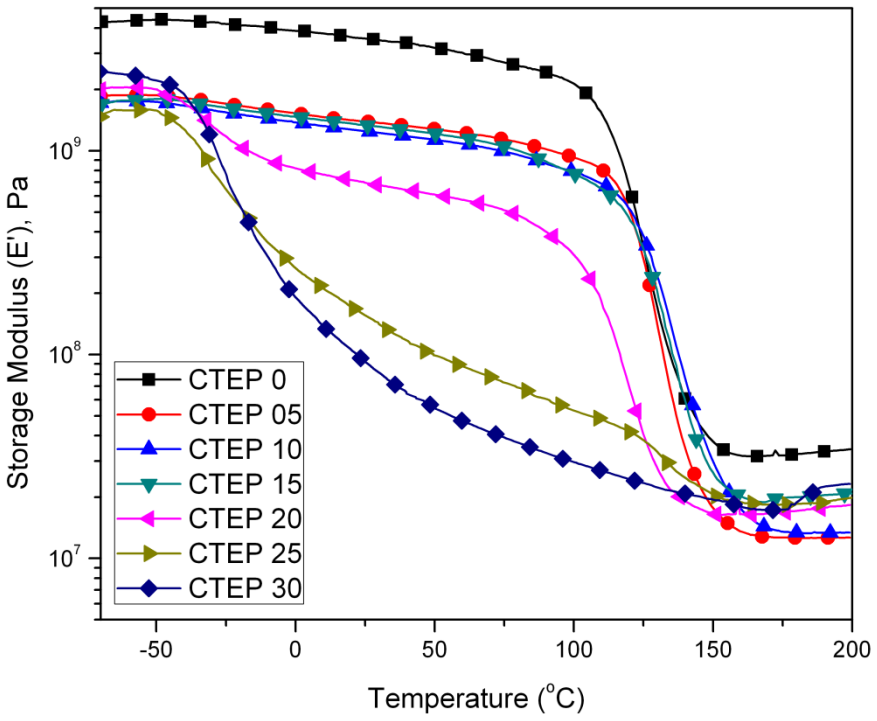

Figure 5.10 *Storage modulus versus temperature for cured epoxy compositions containing CTBN*

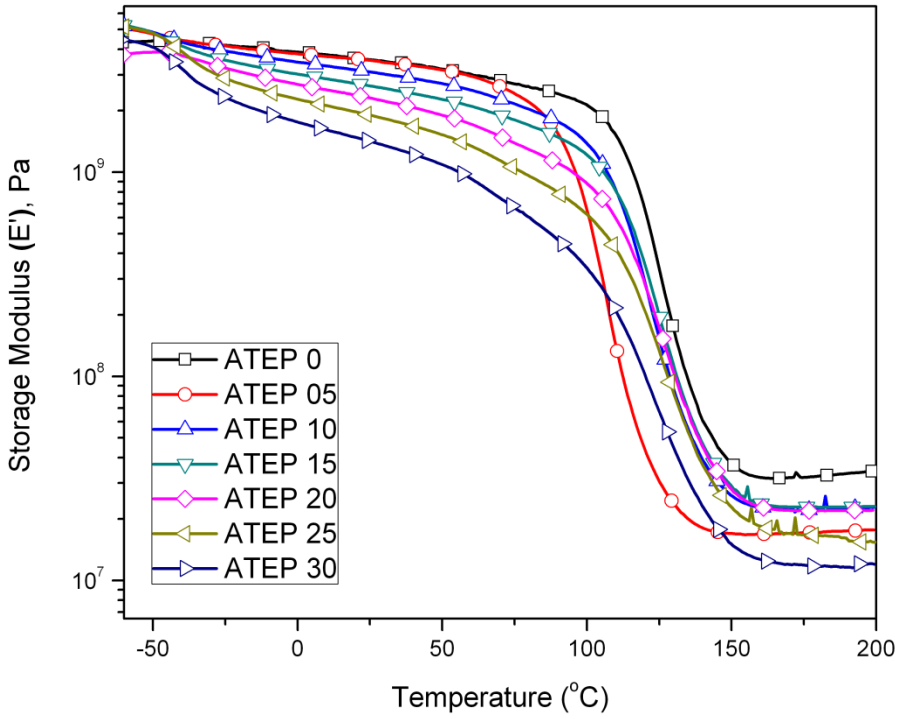

Figure 5.11 *Storage modulus versus temperature curves for cured epoxy compositions containing ATBN*

We show in **Figure 5.10** and **5.11**, the storage moduli of neat epoxy resin along with samples containing different amounts of CTBN and ATBN respectively as a function of temperature. Neat epoxy and samples containing CTBN up to 15% showed gradual decrease in storage modulus w.r.t. temperature up to about 100-120°C and then exhibited abrupt decrease above 120°C. Whereas, **Figure 5.11** showed gradual decrease in storage modulus with an increase in ATBN content. The decrease in modulus can be attributed to the enhancement of flexibility resulting from the incorporation of RLP. However, with high content of CTBN (20 to 30%) the storage modulus decreased sharply at -30 to -40°C which was not observed in the case of ATBN. This may be attributed to the reactions of amine functional groups of ATBN with epoxies resulting into more cross linked structure.

5.3.3 Thermo gravimetric study

Thermal stability and thermal degradation behavior of the neat and modified samples were derived from TGA traces. **Figure 5.12** and **5.13** show the TGA thermograms of the epoxy adhesives modified with CTBN and ATBN respectively. The experiments were performed in the air atmosphere. A neat epoxy sample was observed to be more thermally stable than the modified samples, which can be attributed to the higher cross-linking density and the inherent property of epoxy system. Inclusion of RLPs create domains of rubber particles in between the cross-links which ultimately reduce the cross-linking density and reduces thermal stability. This effect is more dominant in the CTBN modified adhesives. From the TGA curves, it can be clearly seen that the neat and modified systems were found to be thermally stable up to 350°C and the LSS measurements of adhesive compositions could be readily done at 150°C without the thermal degradation of the samples.

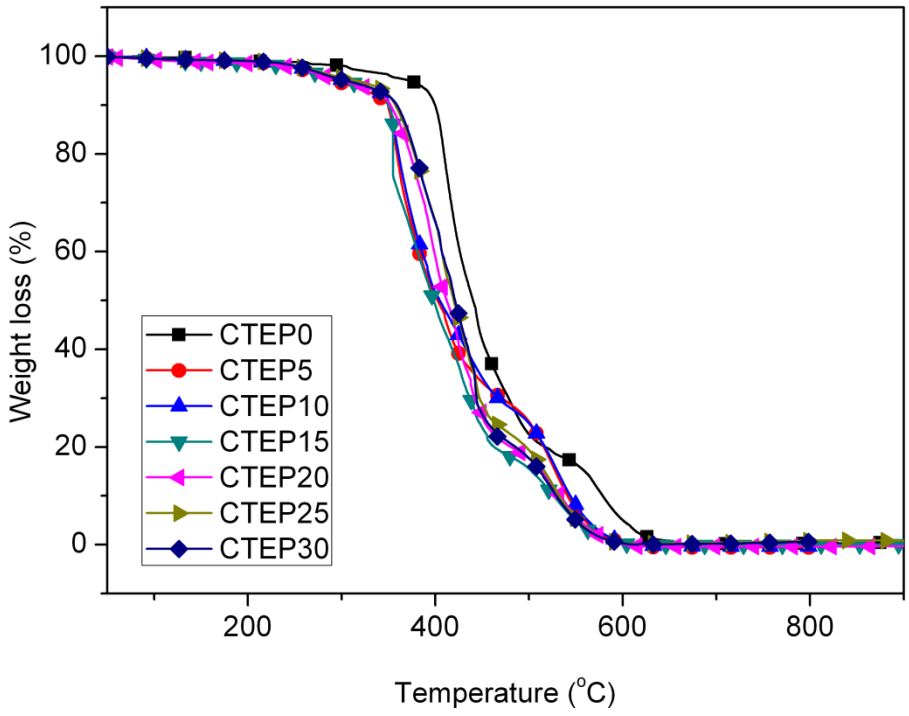

Figure 5.12 *% weight loss versus temperature curves for cured compositions containing CTBN*

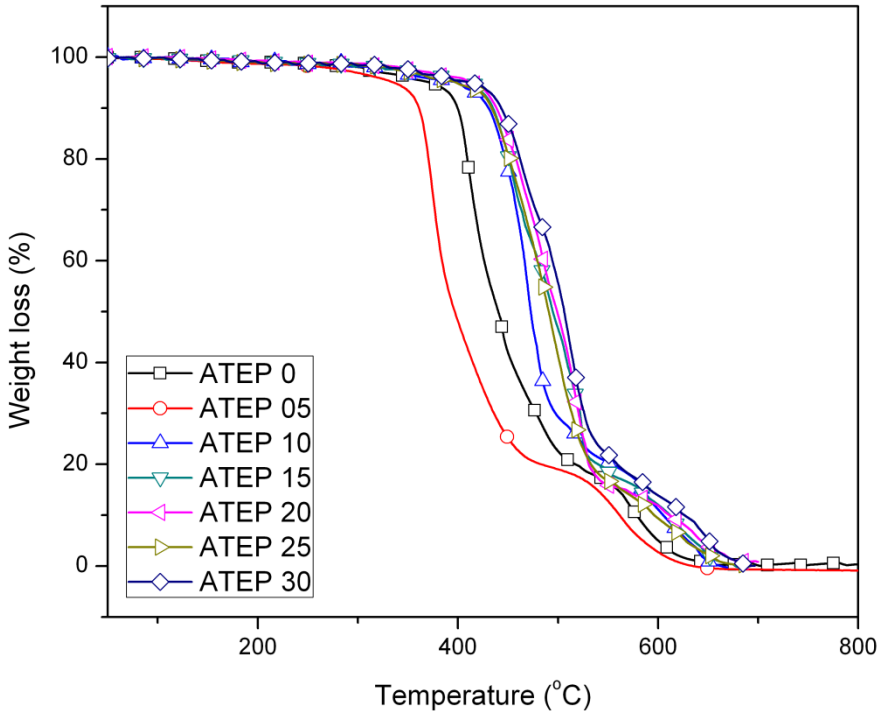

Figure 5.13 *% weight loss versus temperature curves for cured compositions containing ATBN*

5.3.4 Lap shear strength (LSS) study

We show in **Figure 5.14** and **5.15**, the results of LSS of epoxy adhesives modified with different contents of CTBN and ATBN respectively. The measurements were made at room temperature (30°C) and at 150°C. It can be readily seen that the LSS of all the samples are much higher at room temperature (30°C) and are in the range of 80 to 170 Kg/cm^2 with CTBN modified adhesives and in the range of 150-300 Kg/cm^2 for ATBN modified epoxy adhesives. Whereas, at higher temperature (150°C) the LSS decreased significantly to the values ranging from of 10 to 25 Kg/cm^2 with CTBN modified adhesives and to the range of 10-50 Kg/cm^2 for the ATBN modified adhesives. The higher LSS for ATBN modified epoxy adhesive can be explained on the basis of better interaction between epoxy resin and ATBN. Nevertheless, it is interesting to note that, the LSS of epoxy resin increased gradually with the incorporation of RLP, reached maximum at about 15% of CTBN and 20% of ATBN and decreased upon further increase in RLP content. There exists a two-phase microstructure consisting of relatively small rubber particles dispersed in the epoxy matrix flexibilizing the brittle epoxy resin. At higher

concentrations (~20 to 30%) of CTBN, the rubber phase becomes indistinguishable from the epoxy matrix. Hence, the rubber that is not phase separated can lead to softening of the cured epoxy resin resulting into lower values of LSS as observed in our case. These results clearly indicate that the optimum LSS values were obtained at 15% of CTBN and 20% of ATBN for the samples measured at room temperature as well as at 150^{o}C. The higher values of LSS with ATBN modified adhesives were attributed to the reaction between amine functional groups with the epoxy matrix increasing more cross linking as compared to the CTBN.

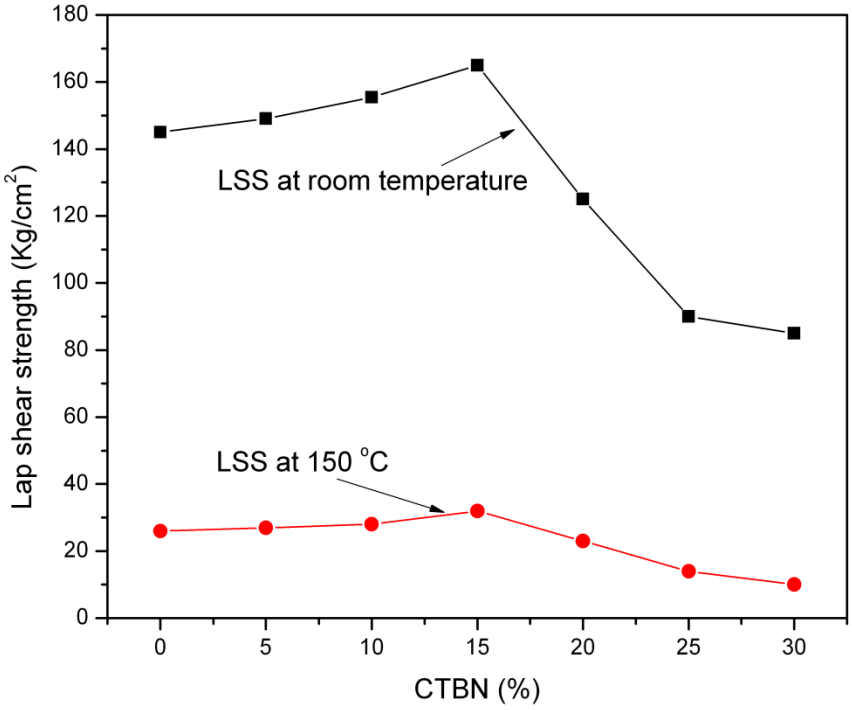

Figure 5.14 *Lap shear strength (LSS) of epoxy adhesive as a function of CTBN content*

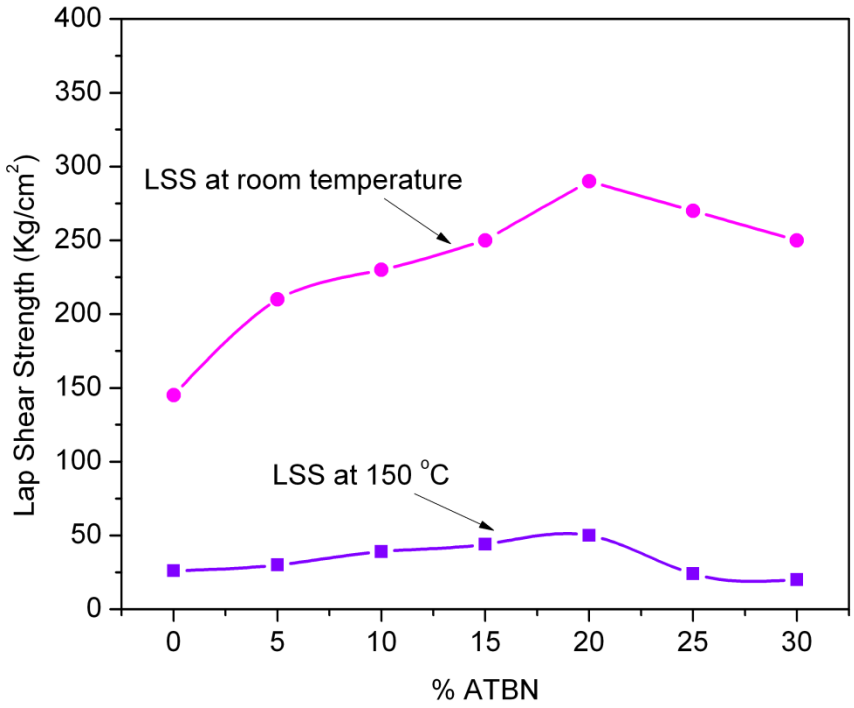

Figure 5.15 *Lap shear strength (LSS) of epoxy adhesive as a function of CTBN content*

5.3.5 Morphological study

The fractured surfaces of cured samples were examined using scanning electron microscopy (SEM). We show in **Figure 5.16** and **5.17** the fracture surfaces of cured epoxy adhesive modified with different contents of CTBN and ATBN respectively. The neat epoxy matrix (**Figure 5.16a**) showed, smooth, glassy and rivery fractured surface with ripples. The ripples arise due to the brittle fracture of the network, which accounts for its poor impact strength, as there is no energy dissipation mechanism operating. Whereas, the cryogenically fractured surface of the CTBN modified epoxies (**Figure 5.16 b-e**) clearly showed two distinct phases consisting of continuous epoxy matrix and the dispersed rubber particles. The size of dispersed rubber particles was found to be around 0.5 µm up to 15% of CTBN content. With an increase in CTBN content (around 20 to 30%) the particle size increased up to 1-2µm, which could be attributed to the coalescence of the dispersed rubber particles. Upon further increase in the concentration of CTBN (CTEP 20 and CTEP 30), the rubber phase becomes indistinguishable. As seen from the **Figure 5.17**, the epoxy adhesive modified with ATBN showed the ductile fracture of the samples. It is also seen that the separation of two phases in the adhesive

modified with ATBN was not clearly distinguishable (phase separation is not complete) [31, 32]. It may be explained by the fact that ATBN was solubilized in epoxy matrix due to the reaction between the amine functional groups and epoxy matrix which in turn increased the interfacial mixing.

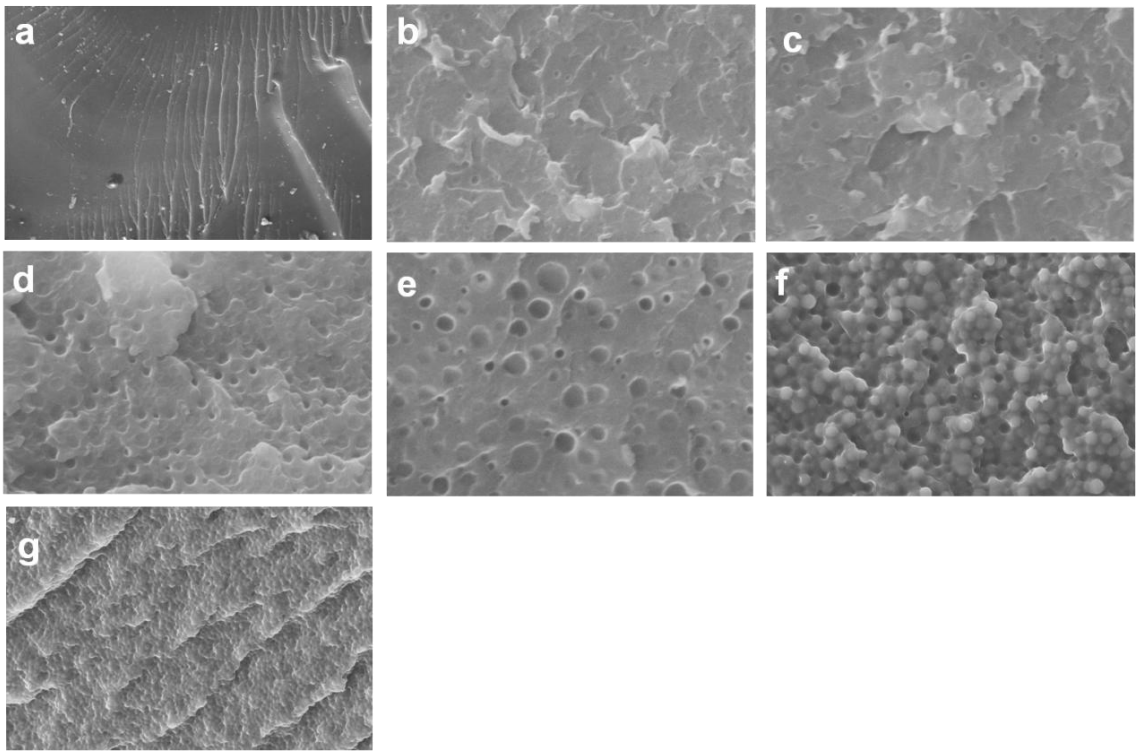

Figure 5.16 *SEM images of cryo fractured surfaces of a) CTEP 0 at 1K, b) CTEP 05 at 5K, c) CTEP 10 at 5K, d) CTEP 15 at 5K, e) CTEP 20 at 10K, f) CTEP 25 at 1K, g) CTEP 30 at 1K*

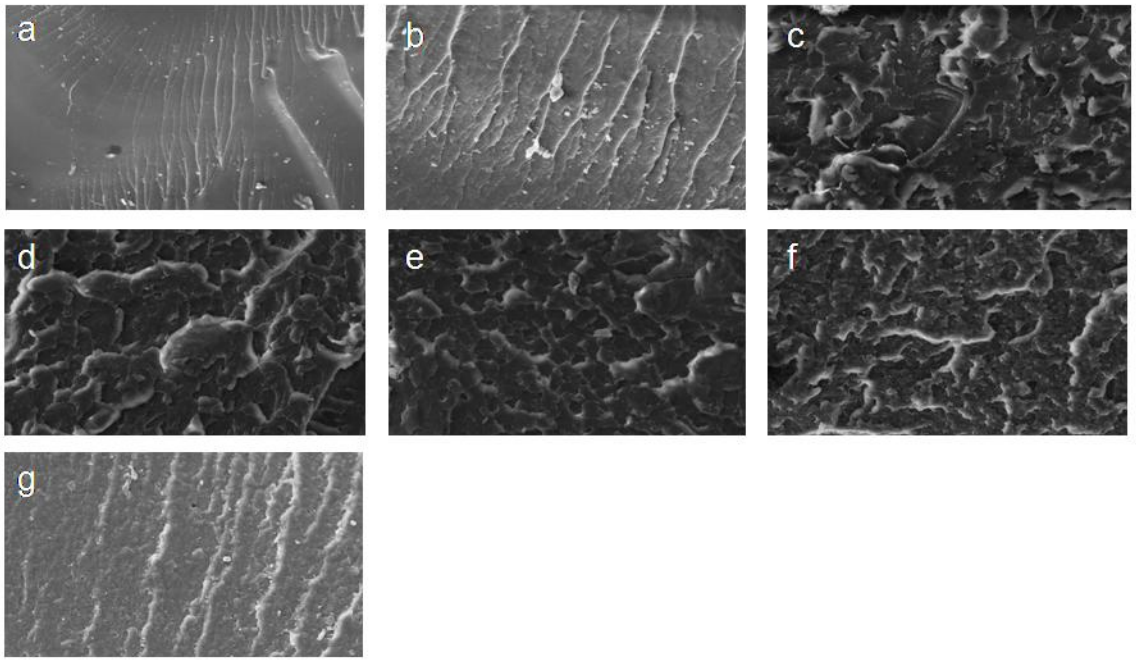

Figure 5.17 *SEM images at 1 K magnification of cryo fractured surfaces of a) ATEP 0, b) ATEP 05, c) ATEP 10, d) ATEP 15, e) ATEP 20, f) ATEP 25, g) ATEP 30*

5.4 Conclusions

In this work CTBN and ATBN modified epoxy adhesives were prepared. Thermal and mechanical properties and LSS were evaluated and compared with neat epoxy resin. In order to increase the compatibility of CTBN with epoxy, an epoxy terminated CTBN i.e. epoxy-CTBN adduct was prepared. The formation of epoxy-CTBN adduct was confirmed by chemical method (acid content) and FTIR spectroscopy. Significant enhancement in the LSS was obtained at room temperature as well as at 150°C upon incorporation RLPs. However, the optimum values of LSS were obtained for the composition CTEP 15 and ATEP 20. ATBN modified adhesives had shown higher LSS as compared to CTBN. This was due to the better interaction between the epoxy resin and ATBN as a result of the reaction between amine functional groups of ATBN with epoxy matrix. It was also observed from DMA study that, the incorporation of CTBN gives more flexibility to the matrix as compared to ATBN. In SEM analysis, the adhesives containing CTBN had clearly shown two distinct phases (i.e. rubber and matrix) whereas, with ATBN modified adhesives the two phases are not clear.

References

1. A. C. Garg and Y. W. Mai, Composites Science and Technology **31**(3), 179-223 (1988).
2. J. Sultan, R. Laible, and F. McGarry, Appl Polym Symp **16**, 127 (1971).
3. R. A. Pearson and A. F. Yee, Journal of Materials Science **26**(14), 3828-3844 (1991).
4. R. A. Pearson and A. F. Yee, Polymer **34**(17), 3658-3670 (1993).
5. D. L. Hunston and W. D. Bascom, Advances in Chemistry Series (208), 83-99 (1984).
6. R. A. Pearson and A. F. Yee, Journal of Materials Science **21**(7), 2475-2488 (1986).
7. A. F. Yee and R. A. Pearson, Journal of Materials Science **21**(7), 2462-2474 (1986).
8. D. J. Hourston and J. M. Lane, Polymer **33**(7), 1379-1383 (1992).
9. M. C. Chen, D. J. Hourston, and W. B. Sun, European Polymer Journal **28**(12), 1471-1475 (1992).
10. R. A. Pearson and A. F. Yee, Journal of Applied Polymer Science 48(6), 1051-1060 (1993).
11. S. J. Wu, N. P. Tung, T. K. Lin, and S. S. Shyu, Polymer International **49**(11), 1452-1457 (2000).
12. F. L. Barcia, B. G. Soares, M. Gorelova, and J. A. Cid, Journal of Applied Polymer Science **74**(6), 1424-1431 (1999).
13. F. L. Barcia, T. P. Amaral, and B. G. Soares, Polymer **44**(19), 5811-5819 (2003).
14. A. Ozturk, C. Kaynak, and T. Tincer, European Polymer Journal **37**(12), 2353-2363 (2001).
15. R. Thomas, D. Yumei, H. Yuelong, Y. Le, P. Moldenaers, Y. Weimin, T. Czigany, and S. Thomas, Polymer **49**(1), 278-294 (2008).
16. R. Bagheri and R. A. Pearson, Journal of Applied Polymer Science **58**(2), 427-437 (1995).
17. P. Bartlet, J. P. Pascault, and H. Sautereau, Journal of Applied Polymer Science **30**(7), 2955-2966 (1985).

18. J. L. Bitner, J. L. Rushford, W. S. Rose, D. L. Hunston, and C. K. Riew, Journal of Adhesion **13**(1), 3-28 (1981).
19. W. L. Bradley, W. Schultz, C. Corleto, and S. Komatsu, Advances in Chemistry Series (233), 317-334 (1993).
20. T. K. Chen and Y. H. Jan, Journal of Materials Science **26**(21), 5848-5858 (1991).
21. Y. Huang, D. L. Hunston, A. J. Kinloch, and C. K. Riew, Advances in Chemistry Series (233), 1-35 (1993).
22. Y. Huang, A. J. Kinloch, R. J. Bertsch, and A. R. Siebert, Advances in Chemistry Series (233), 189-210 (1993).
23. G. Levita, A. Marchetti, and E. Butta, Polymer **26**(7), 1110-1116 (1985).
24. L. T. Manzione, J. K. Gillham, and C. A. McPherson, Journal of Applied Polymer Science **26**(3), 907-919 (1981).
25. L. T. Manzione, J. K. Gillham, and C. A. McPherson, Journal of Applied Polymer Science **26**(3), 889-905 (1981).
26. R. A. Pearson and A. F. Yee, Journal of Materials Science **24**(7), 2571-2580 (1989).
27. C. K. Riew, A. R. Siebert, R. W. Smith, M. Fernando, and A. J. Kinloch, "Toughened epoxy resins: Preformed particles as toughening for adhesives and matrices," in *Toughened Plastics Ii: Novel Approaches in Science and Engineering* (1996), pp. 33-44.
28. R. Thomas, A. Boudenne, L. Ibos, Y. Candau, and S. Thomas, Journal of Applied Polymer Science **116**(6), 3232-3241.
29. R. Yadav and D. Srivastava, Journal of Coatings Technology and Research **7**(5), 557-568.
30. R. Ziraoui, M. Grich, H. Meghraoui, M. Elgouri, A. Mouada, S. Fetouaki, and A. Elharfi, Annales De Chimie-Science Des Materiaux **35**(2), 99-112.
31. B. Mahato and S. Maiti, Colloid and Polymer Science **266**(7), 601-607 (1988).
32. N. Chikhi, S. Fellahi, and M. Bakar, European Polymer Journal **38**(2), 251-264 (2002).

6.1 Introduction

The properties of thermosetting resins, such as an epoxy, depend on the extent of curing reaction and cure kinetics associated with it. The modeling of cure kinetics provides the scientist, engineer or process control manager with valuable information that can be used to optimize processing conditions or to predict the shelf life time of thermosetting resins or composites. The knowledge of the mechanism and cure kinetics is necessary for assigning structure-property relationships and for the usage of the materials as structural adhesives.

Epoxy resins have been widely used in coatings, adhesives, insulating materials, and composites because of their great versatility, low shrinkage, good chemical resistance, adhesion, and high-grade electrical insulation. Epoxy resins cured with amine hardeners mostly suffer from their brittleness, thus limiting their applications in certain areas. Therefore, reactive liquid polymers are introduced as flexibilizer to reduce the brittleness of epoxy resins.

Generally, the curing of the epoxy resin is studied by DSC [1-4]. This calorimetric technique gives a quantitative measurement on the extent of reaction and able to determine the T_g of the material. Cure kinetics of the epoxy-anhydride systems have been studied using various non-isothermal DSC scans, and the activation energies have been calculated by many authors [5, 6]. Some reports have been made on cure kinetics of a DGEBA epoxy resin in the presence of sulfanilamide (SAA) at different heating rates by non-isothermal DSC [7]. Francis et al. have studied the cure kinetics of DGEBA-based epoxy resin modified with an engineering thermoplastic, i.e. poly(ether ether ketone) with diaminodiphenyl sulfone (DDS) as curing agent using isothermal DSC, SEM, and DMTA[8]. Non-isothermal DSC technique was employed by Rosu et al. in a cure kinetic study of DGEBA and diglycidyl ether of hydroquinone (DGEHQ) epoxy resin using triethylenetetramine (TETA) as a curing agent [9]. Near-infrared (NIR) spectroscopy was also employed to analyze the cure kinetics of tetraglycidyl- 4,4′-diaminodiphenyl methane with DDS as a curative [10]. Cure kinetics, using isothermal mode of DSC was employed to study a system composed of o-cresol formaldehyde epoxy resin (o-CFER) using succinic anhydride (SA) as the curative and a tertiary amine as a catalyst [11]. In a

certain study by Raman and Palmese, Fourier transform infrared (FTIR) spectroscopy in the NIR region was used to monitor the cure kinetics of DGEBA epoxy resin and 4,4´-methylenebiscyclohexylamine in the presence of THF as a solvent[12]. DGEBA and aniline modified with a low-Tg poly(ethylene glycol) (PEG) were used as a model system to study the importance of complex formation on the cure kinetics of multicomponent epoxy-amines [13]. In another study, wide-angle X-ray analysis (XRD) was carried out at different stages of cure to monitor the kinetics of di-, tri-, and tetra-functional high-performance, epoxy-layered silicate nano composites [14]. Different techniques including DSC, FTIR, and transmission electron microscopy (TEM) have been used to demonstrate the curing reaction of epoxy thermoset and a block copolymer modifier, synthesized from polystyrene, polybutadiene, and poly(methyl methacrylate) incorporated by an acid-reactive functionality [15].

The inclusion of elastomers in epoxy resin results in a phase separated network on curing. However, there are several reports on DGEBA-based epoxy resin and elastomeric modified blends on immiscibility or miscibility depending on the structure of the curing agent. In a very recent investigation by Kalogeras et al. [16], aromatic amine-cured DGEBA epoxy resin and poly(ethylene oxide) (PEO) blends were analyzed by DSC and dielectric techniques. In another recent work [17], miscibility parameters were analyzed by DSC for ternary thermosetting blends composed of epoxy resin, PEO, and poly(3-caprolactone) (PCL). The epoxy curing generally shows a complex kinetics. Autocatalysis is the reason for initial acceleration. But due to the onset of gelation, the reaction retards in the next stage. The cross-linking leads to an increase in the T_g of the curing matrix. If the curing temperature (T_{cure}) is well above T_g, the kinetics of the reaction between epoxy and hardener is chemically controlled. The resin passes from a flexible rubbery state to a rigid glassy one, when T_g approaches T_{cure}. The reaction, at this stage, becomes very slow and becomes only diffusion controlled, and finally attains vitrification stage and stops.

The important cure kinetics parameters are: the degree of conversion (α), conversion rate ($d\alpha/dt$), and the activation energy (E_a).

The rate of conversion in DSC experiment can be defined as follows:

$$\frac{d\alpha}{dt} = \frac{dH/dt}{\Delta H_{Rxn}} \qquad (1)$$

Where, ΔH_{Rxn} is the heat of reaction.

6.1.1 Kinetic model for curing reaction

The simplest model applied to DSC data was from the mechanism of an n^{th} order reaction. However, this model gave a good fit the experimental data only in a limited range of degree of cure [18]. Whereas, more complicated models for isothermal and dynamic curing process assumed an autocatalytic mechanism [19].

The kinetics of uncatalyzed curing reaction has been established to follow second order autocatalytic model [20] as:

$$\frac{d\alpha}{dt} = k_1\ (1-\alpha)^2 + \ k_2(1-\alpha)^2\alpha \ldots \quad (2)$$

However, in some cases, for both catalyzed and uncatalyzed systems, an n^{th} order reaction has been found to satisfactorily explain the cure profile [21-23]. In the absence of autocatalysis, the reaction can be considered to follow the n^{th} order model as

$$\frac{d\alpha}{dt} = k\ (1-\alpha)^n \ldots \qquad (3)$$

Under nonisothermal conditions, this rate expression takes the form

$$\frac{d\alpha}{dT} = (A/\phi)\ e^{-\frac{Ea}{RT}}\ (1-\alpha)^n \ldots \qquad (4)$$

Where α is the fractional conversion at temperature *T*, following a heating rate ϕ. E_a is the activation energy and *A* the Arrhenius frequency factor. '*n*' is the order of reaction, R is gas constant. With different approximations, the above equation has been reduced to integral form as mentioned bellow:

1. Coats–Redfern Equation [24] (C-R)

$$\ln\{ g\ (\alpha)/T^2\} = \ln\{(AR/\phi Ea)\ (1 - 2RT/Ea)\} - Ea/RT \ldots \quad (5)$$

2. McCallum–Tanner Equation [25] (M-T)

$$\log(AEa/\phi R)\ - 0.483Ea^{0.435}\ -\ (0.449 + 0.217Ea) \times\ 10^3/T \ldots \quad (6)$$

3. Madhusudhanan–Krishnan–Ninan Equation [26] (M-K-N)

$$\ln\{g(\alpha)/T^{1.9215}\} = \ln(AEa/\phi R)\ + 3.7721\ - 1.9215 \ln Ea - 0.12039\ E/T \ldots \quad (7)$$

Where, $g(\alpha) = [1 - (1 - \alpha)^{1-n}]/(1 - n)$;

For n = 1, $g(\alpha) = -\ln(1 - \alpha)$;

In the present study, we have investigated the curing kinetics of a DGEBA based epoxy resin using 3,3´-dimethyl-4,4´-diaminodicyclohexylmethane as a curing agent in the presence of reactive liquid polymers such as CTBN and ATBN. DSC in non-isothermal mode was employed for the calorimetric study and Coats–Redfern equation was used to obtain the kinetic parameters.

6.2 Experimental

6.2.1 Materials

The epoxy resin used was liquid diglycidyl ether of bisphenol A (DGEBA) with an equivalent value of 5.7 eq/Kg, 3,3´-dimethyl-4,4´-diaminodicyclohexylmethane was used as hardener and were obtained from HAL, Bangalore, India. The reactive liquid polymers (RLPs) i.e. carboxyl terminated acrylonitrile butadiene copolymer (CTBN) under the trade name Hypro CTBN 1300X8 and amino terminated acrylonitrile butadiene copolymer (ATBN), were supplied by Emerald Performance Material, U.K. Chemical structures of epoxy resin, CTBN, ATBN and hardener are given in **Figure 6.1.**

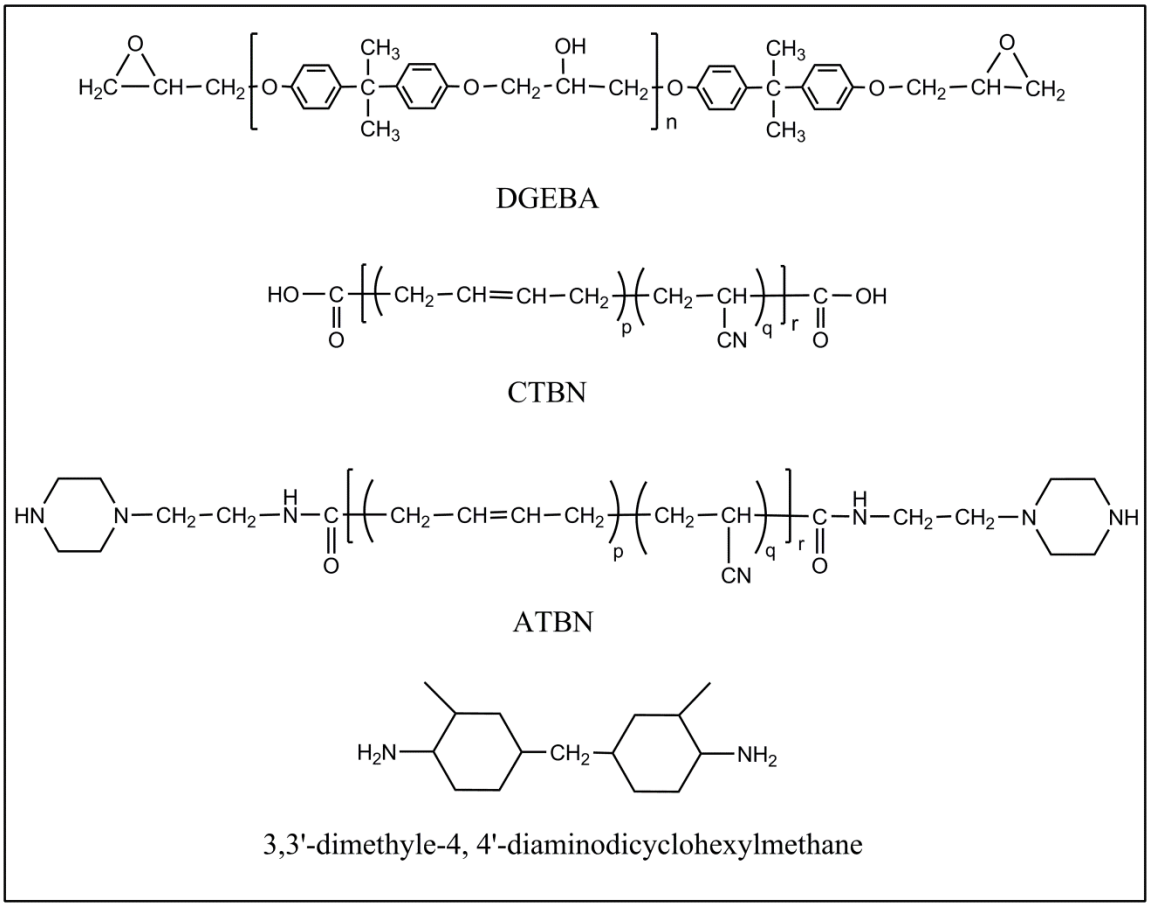

Figure 6.1 *Chemical structures of materials used in this study*

6.2.2 Preparation of adhesive compositions

Samples for DSC analysis were prepared by mixing the components in appropriate ratios as shown in **Table 6.1** and **Table 6.2**. 35 phr of hardener was used in all the compositions. Epoxy-CTBN adduct, terminated with epoxy was synthesized by reacting with DGEBA epoxy. This epoxy-CTBN was incorporated into the epoxy matrix. The liquid epoxy resin, RLPs with varying rubber contents and amine hardener were mixed thoroughly and were immediately loaded into DSC instrument.

6.2.3 DSC measurements

DSC experiments were performed at 10°C/min in static nitrogen, using DSC Q 10 TA Thermal Analyser system. About 9-10 mg of sample was taken in a DSC aluminum pan. Similarly, a reference pan without sample was also made. Nitrogen was used as the purging gas with flow rate of 50ml/min. The sampling time was 0.2 second per point.

Table 6.1 *Adhesive composition containing ATBN*

Sr. No.	Composition Code	ATBN (Wt %)
1	ATEP 0	0
2	ATEP 05	5
3	ATEP 10	10
4	ATEP 15	15
5	ATEP 20	20
6	ATEP 25	25
7	ATEP 30	30

Table 6.2 *Adhesive composition containing CTBN*

Sr. No.	Composition Code	CTBN (Wt %)
1	CTEP 0	0
2	CTEP 05	5
3	CTEP 10	10
4	CTEP 15	15
5	CTEP 20	20
6	CTEP 25	25
7	CTEP 30	30

The temperature and heat flow calibrations were done by the recommended procedure using pure indium metal of melting point 156.4°C and heat of fusion, ΔH_f =6.80 cal/g. The enthalpy of curing, ΔH was determined from the area under the exothermic peak and the mass of the sample. The peak area integration and subsequent fractional conversion (α) temperature calculations were done with software. The integration was done after determining the baseline of the exotherm by joining the temperature of inception of reaction (T_i) and that of completion (T_f). The latter were taken as points where the base line of the thermogram extrapolated to the exotherm starts to deviate. A typical integration is shown in one of the thermograms in **Figure 6.2**. Conversion at any temperature, α_T *was* found from the relation, $\alpha_T = \Delta H_f/\Delta H_T$, where, ΔH_f is the fractional enthalpy at that temperature and ΔH_T, the total heat of reaction. Indirectly these were obtained by the fractional and total areas respectively under the exothermic curve.

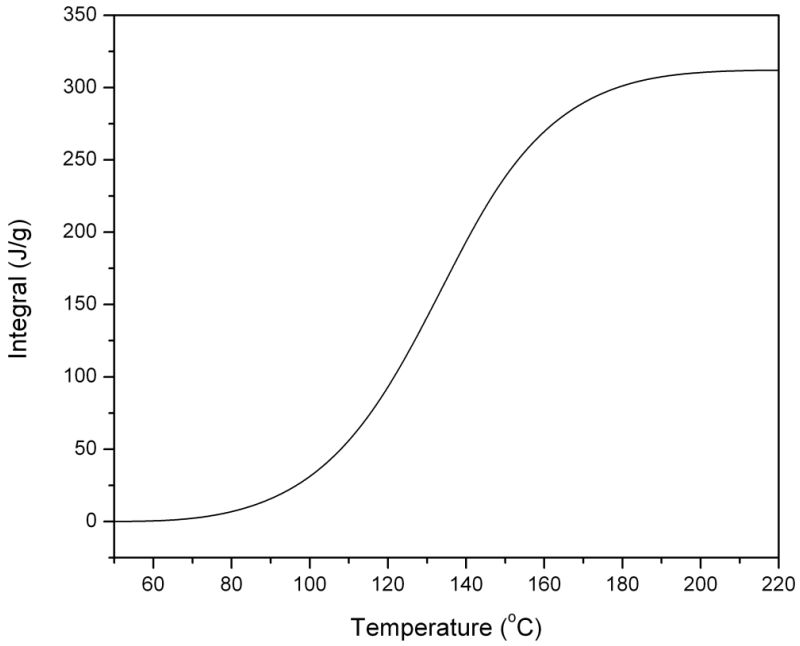

Figure 6.2 *A typical integral of thermogram for the sample CTEP 15*

In this study we have used dynamic method. In this method, the heat flux is recorded when the sample is scanned at a constant heating rate from low temperature to high temperature. The area under the heat flux curve and above baseline is calculated as the heat of reaction.

6.3 Results and discussion

The cure of epoxy groups with amines is an exothermic process that can be monitored by DSC. Small sample size and ease of data gathering are major advantages of DSC in kinetic investigations. Moreover, it can also provide information about thermal transitions such as glass transition temperature (T_g) which can be correlated to the state of cure of resin [27, 28]. A differential scanning calorimeter measures the heat flow required to keep the sample and reference material at the same temperature. DSC can be operated in two basic modes (a) dynamic temperature scanning mode and (b) isothermal scanning mode. In this work dynamic temperature scanning mode is used to study the curing kinetics.

6.3.1 DSC analysis

The adhesive samples as mentioned in **Table 6.1** and **Table 6.2** were analyzed with the heating rate of 10°C/min from 30°C to 250°C and the effect of rubber inclusion on cure kinetics of epoxy was studied. The representative programmed DSC traces of the epoxy adhesive with varying content of CTBN and ATBN in the first heating cycle are shown in **Figure 6.3** and **Figure 6.4** respectively. The cure reaction exotherm is well defined and ends below the degradation temperature of the base epoxy resin. The monomodal distribution confirms the homogeneous distribution of CTBN and ATBN in the epoxy resin. The DSC cell with the sample is then cooled to 30°C at 100°C/min and reheated to 250°C at a heating rate of 10°C/min. The second heating cycle of the epoxy adhesive composition with varying content of CTBN and ATBN are shown in **Figure 6.5** and **Figure 6.6** respectively. It can be readily seen from the figure that, the absence of residual exotherm in the second scan confirms that the cure reaction was completed in the first heating cycle itself.

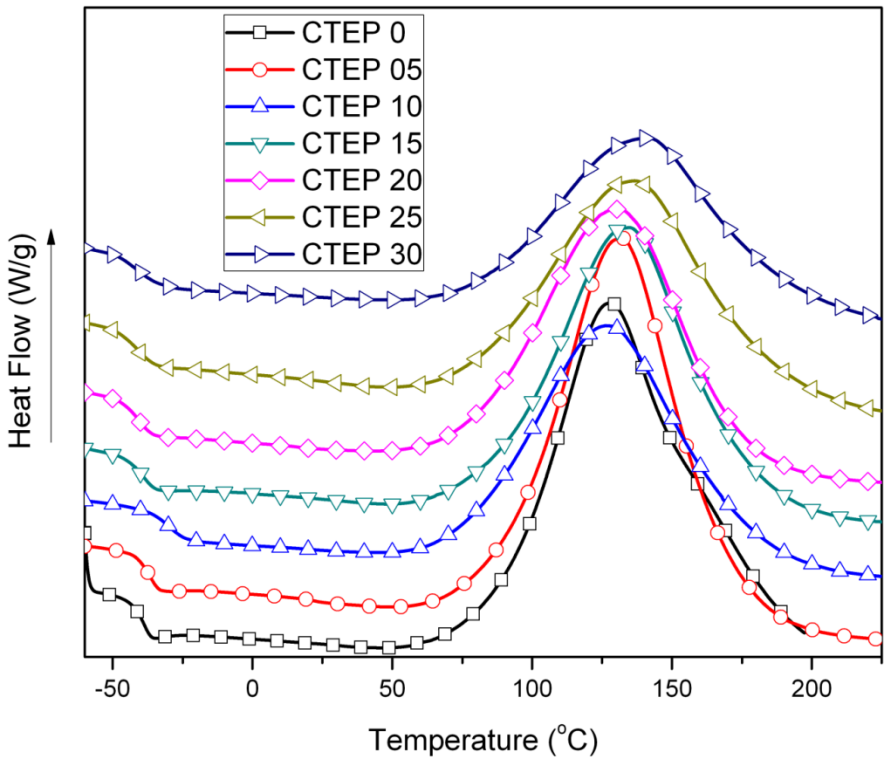

Figure 6.3 *DSC thermograms from first heating cycle for the epoxy adhesives with varying contents of CTBN*

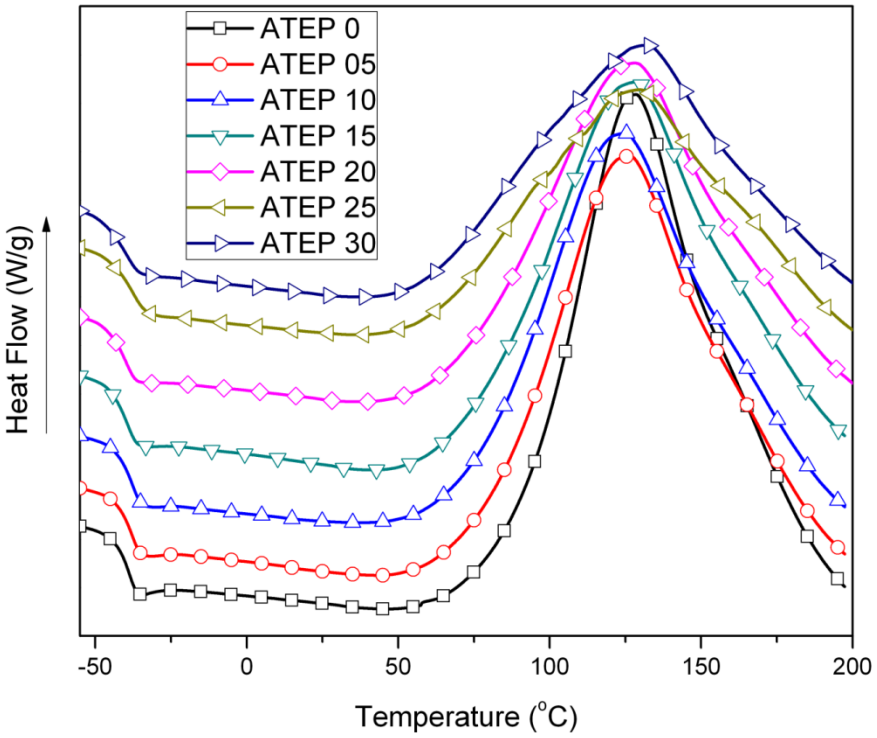

Figure 6.4 *DSC thermograms from first heating cycle for the epoxy adhesives with varying contents of ATBN*

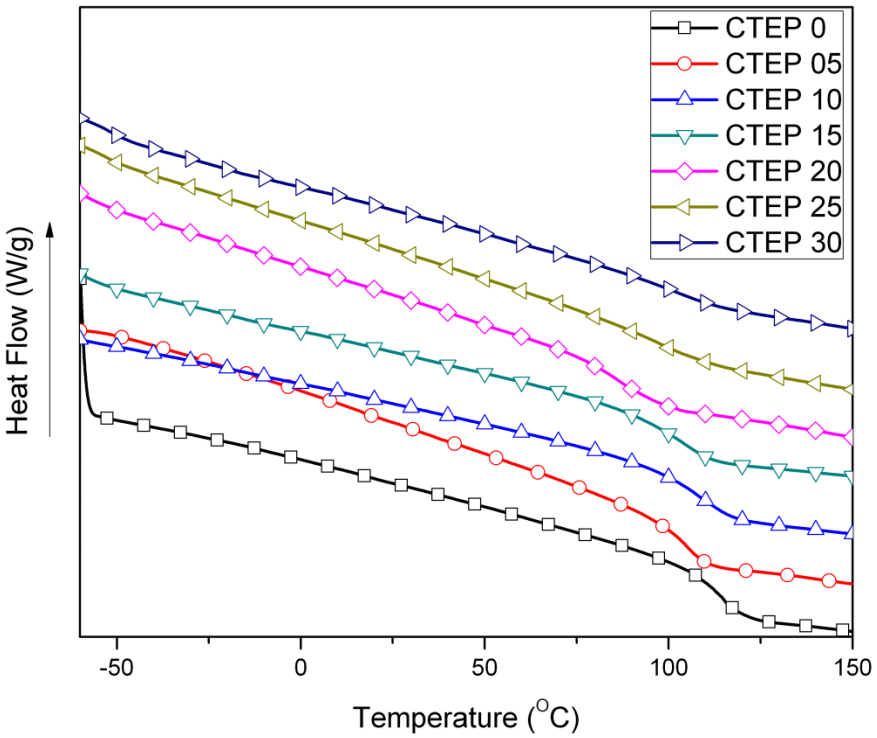

Figure 6.5 *DSC thermograms from second heating cycle for the epoxy adhesives with varying contents of CTBN*

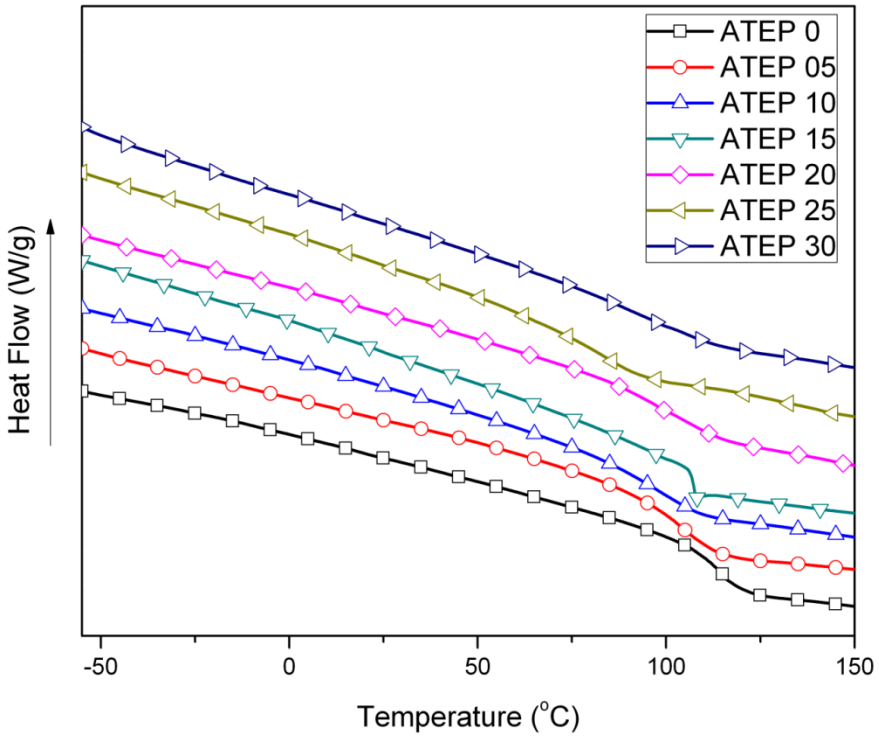

Figure 6.6 *DSC thermograms from second heating cycle for the epoxy adhesives with varying contents of ATBN*

The DSC thermograms show two important regimes: (i) the first regime, is the on-set of curing, which is broad and is predominantly chemically driven process (ii) in the second regime, there is a distinct peak arising due to the combined effect of kinetics and an inherent exothermic reaction.

The overall cure characteristics of epoxy resin cured with hardener in the presence of CTBN and ATBN is given in **Table 6.3** and **Table 6.4** respectively. As tabulated in **Table 6.3**, the exotherm peak was shifted to higher temperature with increase in CTBN content. When the CTBN rubber was added, the curing shifted to higher temperature as observed from a systematic drift in the cure characteristics, such as temperature of onset of cure (*Ti*), peak temperature (*Tp*), conversion at *Tp* (αp) and temperature corresponding to 60% conversion (T_{60}). Whereas with the increase of ATBN content into epoxy matrix as tabulated in **Table 6.4**, there is a decrease in temperature of onset of cure (*Ti*) and increase in the peak temperature (*Tp*) in DSC, conversion at *Tp* (αp) and temperature corresponding to 60% conversion (T_{60}) was observed. The magnitude of temperature

difference between neat epoxy and the composition with 30% CTBN is ~15°C however the magnitude of temperature difference in neat epoxy and composition with 30% ATBN is ~6°C.

Table 6.3 *Effect of CTBN Concentration on Overall Cure Characteristics for DGEBA Cured with BMCHA*

Composition Code	T_i **(°C)**	T_p **(°C)**	**αp (%)**	T_{60} **(°C)**
CTEP 0	64.01	127.91	46.17	136
CTEP 05	59.58	132.44	53	135
CTEP 10	60.32	127.05	49.41	133
CTEP 15	63.68	134.9	53.86	138
CTEP 20	70.67	131.7	54	134
CTEP 25	69.82	137.49	55.66	141
CTEP 30	70.31	141.81	58.35	143

Table 6.4 *Effect of ATBN Concentration on Overall Cure Characteristics for DGEBA Cured with BMCHA*

Composition Code	T_i **(°C)**	T_p **(°C)**	**αp (%)**	T_{60} **(°C)**
ATEP 0	64.01	127.91	46.17	136
ATEP 05	70.91	126.8	46.49	135
ATEP 10	66.22	123.63	43.84	134
ATEP 15	59.98	127.21	47	135
ATEP 20	60.61	128.89	49.78	135
ATEP 25	58.29	130.81	51.11	137
ATEP 30	57.57	132.8	53.49	137

The degree of cure attained at a fixed point in the reaction was calculated as the ratio of the exotherm up to that point to the total area. A set of data (time, temperature and degree of cure) for every composition with varying contents of rubber component was generated. Plots of degree of cure (α) as a function of temperature with different contents of CTBN and ATBN are shown in **Figure 6.7** and **Figure 6.8** respectively.

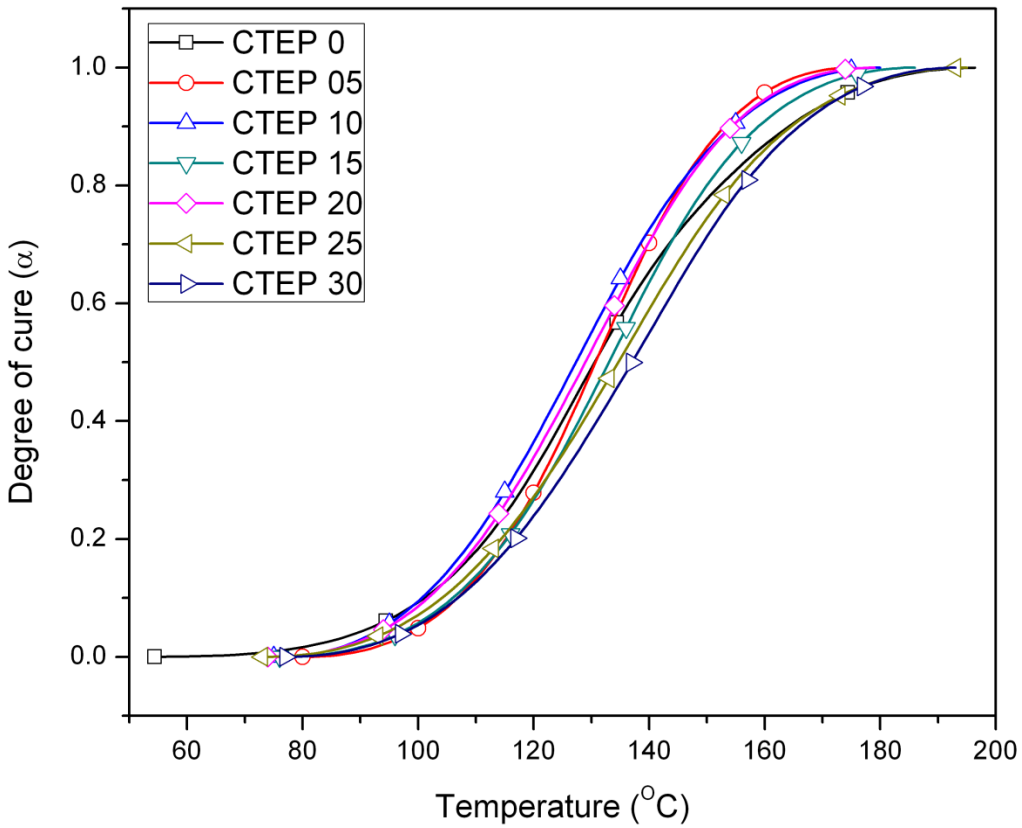

Figure 6.7 *Degree of cure (α) versus temperature over a range of CTBN content*

The curing reaction of a thermoset is a thermally catalyzed and maximum conversion is attained at a higher temperature. As the curing progresses, epoxy resin undergoes polymerization to form three-dimensional network and hence the T_g of the system increases. Complete cure usually occurs at temperatures in the vicinity of the maximum glass transition temperature. This is an indicative of autocatalytic kinetics in the first stage of cure and diffusion controlled reaction as the T_g rises [29].

It can be seen from **Figure 6.7** and **Table 6.3** that, at a particular temperature, there is a slight reduction in conversion for rubber-modified systems which is mainly attributed to the physical changes like dilution effect and/or viscosity increase upon addition of the liquid rubber [30-32] or by the reduction in the density of the reactive groups [33]. The thermoset reactions are accelerated by thermal effect. However, above 50 % of conversion there is an increase in localized viscosity due to Trommsdorff effect and the degree of conversion slightly increases with the increase of CTBN content. It is also noted that, with the higher content of CTBN (~25 and 30%), there was slight reduction in the conversion which could be attributed to the reduction in volume fraction of epoxy resin.

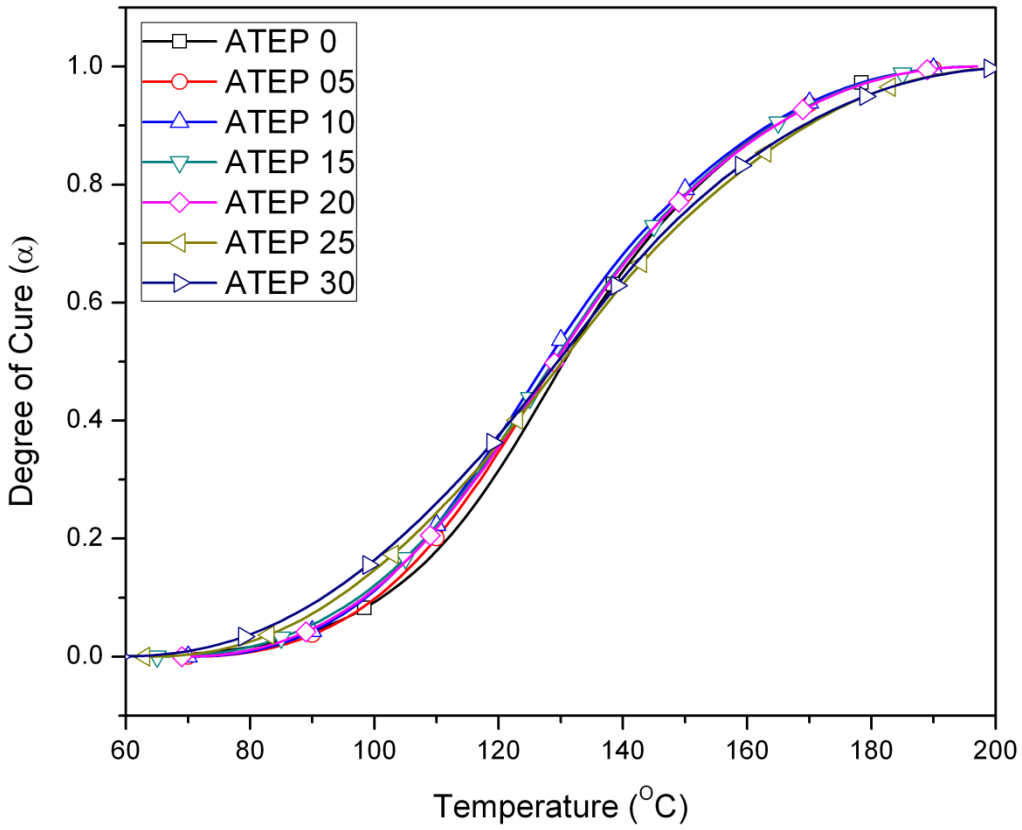

Figure 6.8 *Degree of cure (α) versus temperature over a range of ATBN content*

As seen from **Figure 6.8** and **Table 6.4**, during initial stages of curing, the degree of cure was shifted to the higher side with an increase in ATBN content this may be due to the catalytic effect of amine functional groups of the ATBN during the reaction with epoxy resin. However, during later stage of cure the reaction becomes more diffusion controlled and follows a similar trend of neat epoxy adhesive.

In the present case, the Coats–Redfern equation (equation 5) was applied to derive the kinetic parameters associated with curing process. The order of reaction (*n*) was found from the best linear fit plots of $\ln(g(\alpha)/T^2)$ against 1/T for different values of *n*. Typical plots for determination of *n* containing CTBN and ATBN are given in **Figure 6.9** and **Figure 6.10** respectively.

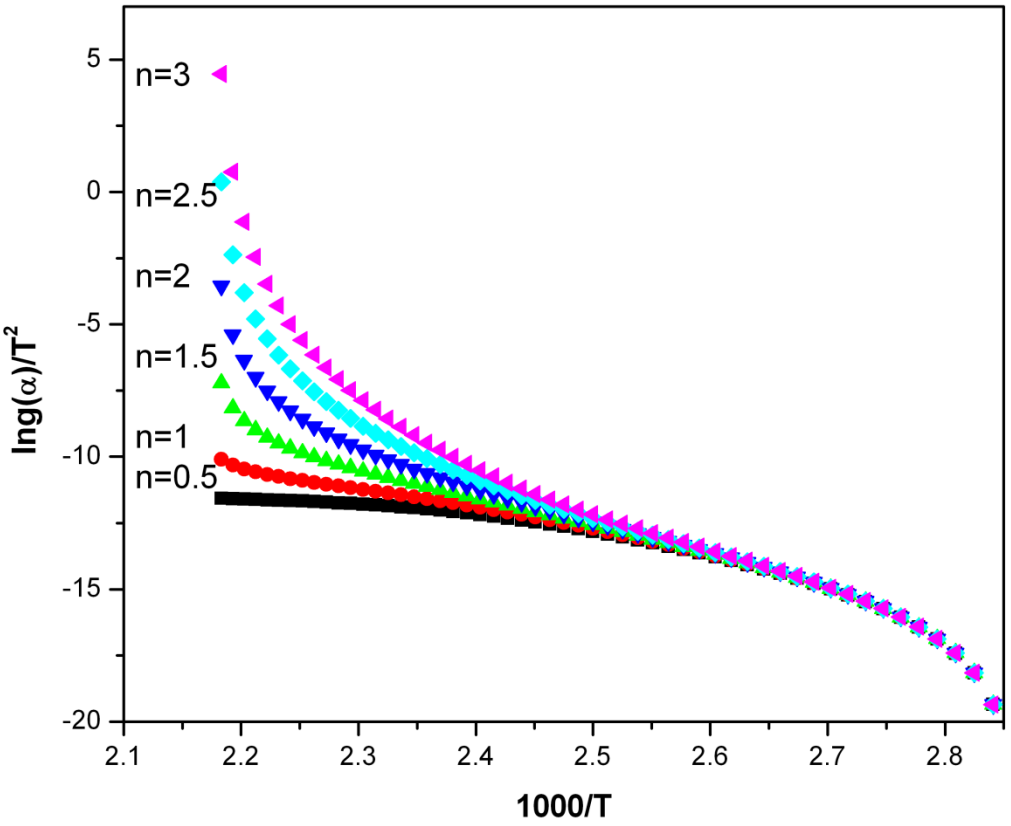

Figure 6.9 *Coats-Redfern plots for adhesive composition containing 15% CTBN for determination of n*

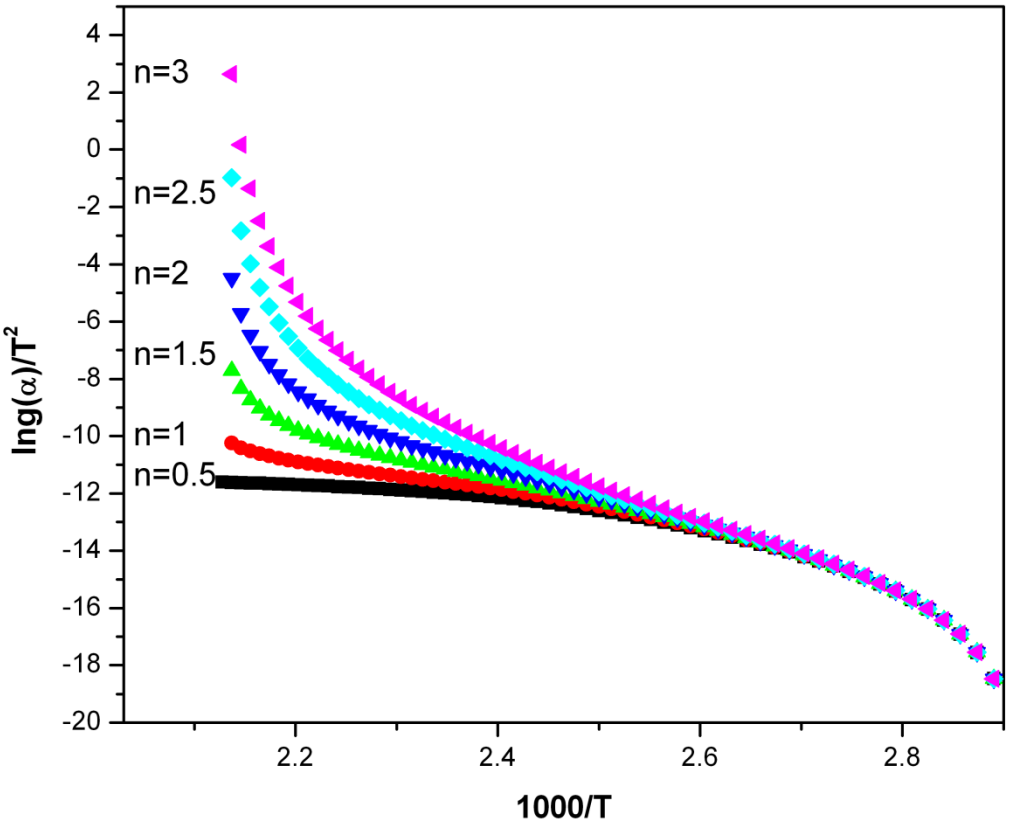

Figure 6.10 *Coats-Redfern plot for adhesive composition containing 20% ATBN for determination of n*

The experimental values of kinetic constants (E_a and A) were determined from the linear plots of ln $g(\alpha)/T^2$ versus 1/T using the predetermined values of *n* and are shown in **Table 6.5** and **Table 6.6**.

Table 6.5 *Effect of CTBN Concentration on activation parameters*

Composition	Activation energy (E_a) (kJ/mol)	Frequency factor (A) (s^{-1})	Order of reaction (n)
CTEP 0	85	$5.x10^5$	1.5
CTEP 05	95	$1. x10^7$	2
CTEP 10	100	$5. x10^7$	1.5
CTEP 15	107	$3. x10^8$	1.5
CTEP 20	107	$5.x10^8$	1.5
CTEP 25	93	$3.9 x10^6$	1.5

Table 6.6 *Effect of ATBN Concentration on activation parameters*

Composition	Activation energy (E_a) (kJ/mol)	Frequency factor (A) (s^{-1})	Order of reaction (n)
ATEP 0	85	$5.5x10^5$	1.5
ATEP 05	104	$2.4 x10^8$	2.0
ATEP 10	86	$7.9 x10^5$	1.5
ATEP 15	81	$1.5 x10^5$	1.5
ATEP 20	84	$4.1 x10^5$	1.5
ATEP 25	60	$1.9 x10^2$	1.5

An increase in the activation energy means the more energy is required for the reaction to complete in addition to the exothermic reaction indicating an acceleration effect. This phenomenon is exhibited in the case of adhesive composition containing CTBN. Whereas, in case of adhesive with ATBN, it was found that the activation energies are close to the values of neat epoxy adhesive with an exception to the composition containing 5% ATBN with order of reaction 2. The increase in E_a with increase of CTBN is due to the increase in the viscosity of the composition and the phase separated CTBN

which hinders the reaction between the epoxide and hardener. In case of adhesive compositions containing ATBN, the amino functional groups present in the ATBN reacts readily with epoxy matrix leading to the lower E_a as compared to the adhesive containing CTBN.

The frequency factor 'A' is the number of collisions of reactants leading to the formation of a product. It was observed that, with the increase in CTBN content in the epoxy matrix, the number of collisions (A) has increased which lead to an increase in activation energies of the compositions. The order of frequency factor (A) of the compositions containing ATBN was 10^5 which is close to the neat epoxy value. This suggests that the compositions containing ATBN requires lesser energies than with the CTBN. In case of adhesive composition containing 5% of CTBN and ATBN the order of reaction was found to be 2. And in all other cases the order of reaction was 1.5 which matches very well with the literature values.

6.4 Conclusion

A DGEBA-based epoxy resin was modified with two reactive polymers, carboxyl terminated butadiene acrylonitrile copolymer (CTBN) and amino terminated butadiene acrylonitrile copolymer (ATBN) using cycloaliphatic hardener 3,3′-dimethyl-4,4′-diaminodicyclohexylmethane. The curing analysis was followed by dynamic DSC. The kinetic analysis was done by Coats-Redfern method (*n*th order kinetic model). The kinetic parameters such as activation energy (E_a), frequency factor (A), order of reaction (n) were examined and predicted. The addition of liquid rubber did not alter the mechanism of cure. However, it was observed that there was an increase in E_a and A with the increase of CTBN content. The extent of reaction decreased after attaining the gelation point. This was due to the phase separation of rubber from the epoxy matrix. Addition of a higher wt% of rubber decreases the rate and conversion. This was due to the dilution effect and increase in viscosity. Whereas, no significant difference in the values of E_a and A was found upon increasing the wt% of ATBN in the matrix. In all the adhesive composition containing ATBN with amine functional groups requires lesser energy as compared to the CTBN.

References

1. ASTM-E698-79, Annual book of ASTM standards **14**, 2 (1996).
2. J. Bouzon and J. M. Vergnaud, Plastics Rubber and Composites Processing and Applications **18**(5), 277-280 (1992).
3. L. Calabrese and A. Valenza, European Polymer Journal **39**(7), 1355-1363 (2003).
4. J. Lange, N. Altmann, C. T. Kelly, and P. J. Halley, Polymer **41**(15), 5949-5955 (2000).
5. J. Galy, A. Sabra, and J. P. Pascault, Polymer Engineering and Science **26**(21), 1514-1523 (1986).
6. W. X. Zukas, Polymer Engineering and Science **29**(22), 1553-1559 (1989).
7. D. Rosu, A. Mititelu, and C. N. Cascaval, Polymer Testing **23**(2), 209-215 (2004).
8. B. Francis, G. V. Poel, F. Posada, G. Groeninckx, V. L. Rao, R. Ramaswamy, and S. Thomas, Polymer **44**(13), 3687-3699 (2003).
9. D. Rosu, C. N. Cascaval, F. Mustata, and C. Ciobanu, Thermochimica Acta **383**(1-2), 119-127 (2002).
10. N. A. Stjohn and G. A. George, Polymer **33**(13), 2679-2688 (1992).
11. Z. G. Ma and J. G. Gao, Journal of Physical Chemistry B **110**(25), 12380-12383 (2006).
12. V. I. Raman and G. R. Palmese, Macromolecules **38**(16), 6923-6930 (2005).
13. S. Swier, G. van Assche, W. Vuchelen, and B. van Mele, Macromolecules **38**(6), 2281-2288 (2005).
14. O. Becker, Y. B. Cheng, R. J. Varley, and G. P. Simon, Macromolecules **36**(5), 1616-1625 (2003).
15. V. Rebizant, A. S. Venet, F. Tournilhac, E. Girard-Reydet, C. Navarro, J. P. Pascault, and L. Leibler, Macromolecules **37**(21), 8017-8027 (2004).
16. I. M. Kalogeras, A. Vassilikou-Dova, I. Christakis, D. Pietkiewicz, and W. Brostow, Macromolecular Chemistry and Physics **207**(10), 879-892 (2006).
17. M. Yin and S. Zheng, Macromolecular Chemistry and Physics **206**(9), 929-937 (2005).

18. J. M. Barton, D. C. L. Greenfield, and K. A. Hodd, Polymer **33**(6), 1177-1186 (1992).
19. K. Horie, H. Hiura, M. Sawada, I. Mita, and H. Kambe, Journal of Polymer Science Part A-1-Polymer Chemistry **8**(6), 1357-1372 (1970).
20. S. L. Simon and J. K. Gillham, Journal of Applied Polymer Science **47**(3), 461-485 (1993).
21. M. C. Lu and J. L. Hong, Polymer **35**(13), 2822-2827 (1994).
22. A. Oseiowusu, G. C. Martin, and J. T. Gotro, Polymer Engineering and Science **32**(8), 535-541 (1992).
23. A. Osei-Owusu, G. C. Martin, and J. T. Gotro, Polymer Engineering & Science **31**(22), 1604-1609 (1991).
24. A. W. Coats and J. P. Redfern, Nature **201**(491), 68-69 (1964).
25. Maccallu.Jr and J. Tanner, European Polymer Journal **6**(7), 1033-1039 (1970).
26. P. M. Madhusudanan, K. Krishnan, and K. N. Ninan, Thermochimica Acta **97**, 189-201 (1986).
27. J. M. Barton, Advances in Polymer Science **72**, 111-154 (1985).
28. J. M. Barton and W. W. Wright, Thermochimica Acta **85**(APR), 411-414 (1985).
29. J. G. Gao and Y. F. Li, Polymer International **49**(12), 1590-1595 (2000).
30. I. Martinez, M. D. Martin, A. Eceiza, P. Oyanguren, and I. Mondragon, Polymer **41**(3), 1027-1035 (2000).
31. G. Cracknell and M. Akay, Journal of Thermal Analysis **40**(2), 565-573 (1993).
32. B. S. Kim, T. Chiba, and T. Inoue, Polymer **34**(13), 2809-2815 (1993).
33. W. Jenninger, J. E. K. Schawe, and I. Alig, Polymer **41**(4), 1577-1588 (2000).

Summary and Conclusions

Due to environmental concern, water borne coatings based on polyurethanes are attracting increasing attention recently. Therefore, there is a great scope in designing and developing new and improved polyurethane dispersions with excellent coating properties such as, gloss, scratch, and abrasion resistance.

In this context, stable dispersions of the blends of two polymers namely; polyurethane dispersion (PUD) and acrylic emulsion (AE) were successfully prepared by the combination of both in different ratios. The dispersion properties such as particle size and viscosity of all the combinations were examined. The FTIR study indicated the decrease in H-bonding interactions with an increasing amount of AE. The mechanical properties, such as tensile strength and storage modulus of the films obtained from the blends showed decreasing trend, which was attributed to the decrease in H-bonding interactions between the two components of the blends. Therefore, it was concluded that, the physical mixing of PUD and AE did not show synergistic effect in the scratch and abrasion resistance of coatings. However, all the blends gave smooth and glossy finish coatings.

In order to improve the scratch and abrasion resistance of coatings, a new approach of making PUDs by reacting mixtures of polyols i.e. polyester polyol (PEP) and acrylic polyol (ACP) with diisocyanate was explored. The viscosity of the PUDs decreased with increase of ACP content due to increase in particle size of the dispersion. The scratch resistance of the coatings increased with increase in ACP content which was attributed to increase in the modulus of the films contributed from the acrylic hard segment in the polymer. Synergistic effect was observed at equal equivalent ratios of PEP/ACP and the film exhibited maximum tensile strength. The abrasion resistance of the films decreased with increase in ACP content which may be due to the decrease in the compatibility between PEP and ACP.

The films were unaffected by water which was evidenced by the absence of blisters, haziness and resistance to delamination in the water immersion test. The study clearly indicates that one can take the advantage of properties of PEP and low cost of ACP to obtain PUDs with synergistic properties.

The combination of organic and inorganic moieties on a molecular scale to achieve synergistic properties in coatings is another important approach. In this work, water-borne organic-inorganic hybrid PUDs based on PEP, isophorone diisocyanate, dimethylolpropionic acid and silica were prepared. The properties such as scratch and abrasion resistance and mechanical strength of the coatings were examined with an increasing amount of nano-silica.

It was found that the scratch resistance of coatings was increased with increase in silica content which may be due to reinforcing effect of silica particles in the PU matrix. It was also noted that, there was no loss of abrasion resistance of coatings with respect to increase in silica content which could be attributed to hydrogen bonding interactions between the surface silanol groups of silica and PU matrix. But the gloss values of the coatings were found to decrease above 3% of silica loading. This may be due to the roughening of surface as a result of densification of silica particles at the surface upon increasing the loading.

Therefore, in order to maintain the gloss and to improve the scratch and abrasion resistance, the silica particles were modified with amino functional silane and incorporated (up to 3%) in to PU matrix.

The ^{29}Si NMR studies confirmed the modification of silica nano particle. The hybrid coating with modified silica (G-silica) exhibited improved scratch and solvent scrub resistance over PUD coating while the gloss and abrasion resistance remained unaffected. The hybrid films also showed higher tensile strength with the incorporation of G-silica which attributed to the better reinforcement of modified silica (G-silica) with PU matrix. Thus, these organic-inorganic hybrid systems studies show promising applications in glossy, scratch and abrasion resistant coatings.

The second part of the thesis work was focused on the epoxy resin based adhesives modified with reactive liquid polymers (RLPs).

Glassy and crosslinked epoxy resins have been extensively used for formulating structural adhesives because of their properties such as, good wetting and formation of strong bond with many polar high energy substrates, superior mechanical strength and

environmental stability. However, epoxy resins are found to be brittle and undergo catastrophic failure at adhesive joints. Therefore, toughening of epoxies has become a necessity to ensure the feasibility of these materials for practical applications. In order to toughen epoxy resins, RLPs such as carboxyl-, amino-, epoxy-, and vinyl- butadiene-acrylonitrile (CTBN, ATBN, ETBN and VTBN) have been used. Most of the studies using the RLPs and applications of toughened epoxy resins at room temperature have been reported.

In this work, we have studied the influence of CTBN and ATBN incorporation in to epoxy resin and examined their properties at room temperature as well as at elevated temperature (150°C). DGEBA based epoxy resin was cured with a cycloaliphatic hardener namely 3,3′-dimethyl-4,4′-diaminodicyclohexylmethane in the presence of different amounts of CTBN and ATBN.

Lap shear strength (LSS), thermal and mechanical properties were evaluated and compared with neat epoxy resin. In order to increase the compatibility of CTBN with epoxy, an epoxy terminated CTBN i.e. epoxy-CTBN adduct was prepared from the DEGEBA and CTBN. The formation of epoxy-CTBN adduct was confirmed by chemical method (acid content) and FTIR spectroscopy. Significant enhancement in the LSS was obtained at room temperature as well as at 150°C upon incorporation of CTBN. However, the optimum value of LSS was obtained for the composition containing 15% CTBN. The SEM micrographs showed the homogeneous dispersion of rubber particles in the epoxy matrix. The increase in LSS with the increase in CTBN was attributed to the cavitation of rubber phase with the inclusion of CTBN and chemical bond formation between the CTBN and the epoxy resin. The LSS of adhesive composition containing 20% ATBN was found to be higher than that of an adhesive with 15% of CTBN. This was attributed to the more reactivity of amine functional groups in ATBN with epoxy matrix which in turn increases the crosslinking and better mixing with the matrix which is evidenced by SEM analysis.

The kinetics of curing of DGEBA with the hardener, 3,3′-dimethyl-4,4′-diaminodicyclohexylmethane in the presence of RLPs, CTBN and ATBN, was investigated using differential scanning calorimeter (DSC) in the non-isothermal mode.

The analysis of curing kinetics was done by Coats-Redfern method (*n*th order kinetic model). The kinetic parameters such as activation energy (E_a), frequency factor (A) and order of reaction (n) were evaluated.

It was observed that there was an increase in E_a and A with increase in CTBN content. The extent of reaction decreased after attaining the gelation. This can be attributed to the phase separation of rubber from the epoxy matrix towards the end of gelation. The reaction kinetics was found to be faster with ATBN since the amine functional groups can readily react with the epoxy resin.

Directions for the future work

In the present work, water borne coatings based on polyurethanes, polyurethane acrylates and organic-inorganic hybrids were prepared from organically modified nano silica and PUD for their applications in scratch and abrasion resistant glossy coatings. Similarly, the influence of modified fillers such as clays (natural and synthetic clays) on the coating properties can be explored.

Further, this study explored CTBN and ATBN modified epoxy adhesives for their elevated temperature applications. This work can be extended by incorporating nano fillers such as silica and clays in reactive liquid polymer modified epoxy adhesives which may find their applications in industry.

Synopsis of the thesis entitled

"Organic-Inorganic Hybrids: Preparation, Characterization and Applications in Adhesives and Coatings"

By

Vivek V. Kodgire

Polymer Science and Engineering Division, National Chemical Laboratory (NCL)

Dr. Homi Bhabha Road, Pune – 411 008

Introduction

The fundamental concept behind the development of organic-inorganic hybrid materials is the combination of organic and inorganic moieties on a molecular scale to achieve synergistic combination of the properties, typical of each of the constituents. The possibility of gaining improved performance by combining organic and inorganic components in coatings and adhesives is well known and is largely practiced. For example, inorganic pigments or fillers are dispersed in organic components/binders (solvent, surfactant, polymers etc) to improve optical, mechanical and thermal properties of coatings.

In the past, solvent borne polyurethane (PU) coating systems have been extensively used in the coating industry due to their excellent solvent and chemical resistant properties along with good weather stability[1]. With the ease of formulating both clear coats and pigmented topcoats, the films also exhibit high gloss finish and very good mechanical properties. The wide applicability of PU coatings is due to versatility in the selection of monomeric raw materials from a huge list of macrodiols, diisocyanates and chain extenders (CE). The chemical structure of PU consists of soft segment and hard segment which can be controlled to tailor-make properties to suite end applications.

Besides several advantages of solvent-borne PU coatings, environmental concerns have driven the coatings researchers to explore new and efficient organic coatings with minimum volatile organic components (VOC). In view of this, water-borne coating systems are becoming increasingly important. Particularly, aqueous polyurethane dispersions (PUDs) have become prominent[2].

The polyurethane dispersions (PUD) are binary colloidal systems having PU particles (size 0.01 to 1 μm) dispersed in continuous aqueous phase. In order to enhance the dispersibility in aqueous media, ionic groups are introduced along the polymer chain by using hydrophilic monomers or hydrophilic internal emulsifiers. The dispersions obtained using internal emulsifier, such as dimethylol propionic acid (DMPA) have fine particle size, better stability and give films with good water resistance. Most of the work on aqueous PUDs has been done in industrial laboratories and is patented. These patents have been well revised and documented by Dieterich[3], Rosthauser and Nachtkamp[4]. These dispersions can be formulated into coatings and adhesives containing little or no solvent and can be applied on to plastics or other substrates, which are sensitive to solvent attack. The viscosity of dispersion is independent of molecular weight of the polyurethane but dependent on average particle size, particle size distribution and solids content. Therefore, PUDs can be prepared at high molecular weight with low viscosity and can be easily coated on to the substrates. The coating properties of PUDs such as gloss, water resistance are comparable to those of conventional solvent-borne polyurethane lacquers and two component polyurethanes coatings[5-8]. The basic building blocks used for the preparation of aqueous PUDs are the same as those used for conventional solvent borne polyurethanes.

Polymeric/organic clear coats have gained widespread usage as the final coat in many diverse manufactured goods, car bodies, mobile phones, furniture lacquers, safety helmets, writing pens, etc., just to mention a few[9]. However, their aesthetic appearance and durability is rapidly impaired through constant use. Therefore, these coatings need to be improved in mar, scratch and abrasion resistances. These new waterborne systems are expected to have improved coating properties like scratch resistance and abrasion resistance to fulfill the property profile of similar solvent-borne systems.

Therefore, the first objective of this research work was to prepare water-borne coatings with improved scratch and abrasion resistant properties using organic-organic/inorganic hybrid approach, where polyurethane and acrylates are organic polymers and nano silica is an inorganic filler.

Secondly the work was also focused on toughening of epoxy resins using reactive liquid polymers (RLP).

Glassy, highly crosslinked thermoset epoxy resins have been used for formulating structural adhesives because of their properties such as, good wetting and formation of strong bonds with many polar high-energy substrates, low cure shrinkage without evolution of low molecular weight substances, superior mechanical properties, and environmental stability. For structural adhesives with good elevated temperature capability, high glass transition temperature (T_g) is an essential requirement to retain the adhesive strength at high temperature. All the unmodified and cured epoxy resins with relatively high T_g have drawback, i.e., brittleness, which can produce catastrophic failure of the adhesive joint. Therefore, it is necessary to toughen epoxy resins without reduction in thermal and mechanical properties. Sultan et al.[10,11] were the first one to show that, the fracture toughness of epoxies can be improved by an introduction of a dispersed rubber phase.

Barcia et al.[12] employed hydroxyl terminated polybutadiene (HTPB) as a surface modifier in carbon fiber (CF) reinforced, epoxy matrix composites. The surface of carbon fibers (CFs) was grafted with HTPB, which formed a flexible interface between CF and epoxy matrix and eventually improved the mechanical properties of the system. In an interesting study, the DGEBA based epoxy resin was modified with block copolymers from isocyanate terminated polybutadiene[13]. Ozturk et al.[14] employed modified HTPB rubbers to improve thermal and mechanical properties by toughening an epoxy matrix.

Several studies have been reported on the enhancement of toughness of cured epoxy resins without significant reduction in the thermal and mechanical properties, by the addition of low levels of a reactive liquid polymer[15,16]. However, only scanty reports are available on elevated temperature service capabilities of adhesives prepared from them. In view of this, work was undertaken to incorporate RLP in epoxy resins and properties were studied using DMA, UTM, rheology and SEM.

The thesis comprises of following chapters:

Chapter 1: *Introduction and Literature Review*

The introductory chapter addresses some of the basic concepts of coatings and adhesives and also gives a comprehensive review of the literature on the organic-inorganic hybrid systems for the application in polymeric coatings. The importance of water-borne coatings and toughening of epoxy resins have been discussed. The techniques for the evaluation of coating properties such as scratch resistance, abrasion resistance and gloss have been discussed. This chapter also covers the use of dynamic mechanical analyzer (DMA) and universal tensile testing machine (UTM) for the understanding the mechanical behavior of coatings and adhesive systems.

Chapter 2: *Scope and Objectives*

This chapter highlights the objectives and scope of the present work

Objectives of the present research work

- To prepare silane modified silica nano particles using functional silane coupling agents
- To develop high performance Organic-Inorganic hybrid polymeric coatings with improved scratch and abrasion resistance
- To understand and correlate the structural attributes, which are responsible for exhibiting the scratch and abrasion resistant properties to the coatings
- To prepare epoxy adhesives using reactive liquid polymers (RLPs) such as carboxyl terminated acrylonitrile butadiene rubber (CTBN) and amine terminated acrylonitrile butadiene rubber (ATBN)
- To study the curing kinetics of toughened epoxy adhesives
- To study structure property relationship in toughened epoxy resin

Chapter 3: *Water borne polyurethane dispersion (PUD) coatings*

In this chapter, the process for the preparation of water-borne PUD and its blends with acrylic emulsion (AE) is discussed. The new approach for making PUD by reacting two polyols in one step has been explained. The mechanical properties of dried films were investigated by using UTM, and the coating properties such as, scratch resistance and abrasion resistance were evaluated.

Chapter 4: *Organic-inorganic hybrid coatings*

In this chapter, the process for the preparation of water-borne organic-inorganic hybrid coatings has been discussed. Polyurethane was used as an organic matrix and nano silica was used as an inorganic filler. The mechanical properties of the dried films were investigated by using UTM and DMA, whereas film properties such as scratch and abrasion resistance were evaluated.

Chapter 5: *Epoxy resin based adhesives*

This chapter describes the process for toughening of epoxy resin with reactive liquid polymers (RLP). The cured epoxy adhesive compositions were analyzed by DMA and UTM for their improvement in toughening and adhesive strength respectively.

Chapter 6: *Curing kinetics of epoxy adhesives*

This chapter deals with the curing kinetics of epoxy adhesives toughened with RLP. Non isothermal kinetics technique was used to study the curing kinetics of the uncured adhesive compositions to obtain activation energies (E_a) and frequency factor (A).

Chapter7: *Summary and Conclusions*

This chapter summarizes the important conclusions of the work.

References

1. Hommer, D.; Garbett, I., Paint Ink Int **May/June**, 6 1996.
2. Vogt-Birnbrich, B., Progress in Organic Coatings **29**, 31 1996.
3. Dieterich, D., Progress in Organic Coatings **9**, 281 1981.
4. Rosthauser, J. W.; Nachtkamp, K., Advances in Urethane Sci. and Tech. **10**, 121 1987.
5. Ganss; Helmut. BASF **WO/2004/003045** 2004.
6. Lu, M. G.; Lee, J. Y.; Shim, M. J.; Kim, S. W., Journal of Applied Polymer Science **86**, 3461 2002.
7. Ramanathan, L. S.; Raut, K. G.; Srinivasan, S. R.; Sivaram, S.; Council of Scientific & Industrial Research, **US 6239213**: 2001.
8. Zhou, S.; Wu, L.; Sun, J.; Shen, W., Progress in Organic Coatings **45**, 33 2002.
9. Barna, E.; Bommer, B.; Kursteiner, J.; Vital, A.; von Trzebiatowski, O.; Koch, W.; Schmid, B.; Graule, T., Composites Part a-Applied Science and Manufacturing **36**, 473 2005.
10. Sultan, J.; Laible, R.; McGarry, F., Appl Polym Symp **16**, 127 1971.
11. Sultan, J.; McGarry, F., Polym Eng Sci **13**, 29 1973.
12. Barcia, F. L.; Soares, B. G.; Gorelova, M.; Cid, J. A., Journal of Applied Polymer Science **74**, 1424 1999.
13. Barcia, F. L.; Amaral, T. P.; Soares, B. G., Polymer **44**, 5811 2003.
14. Kaynak, C.; Ozturk, A.; Tincer, T., Polymer International **51**, 749 2002.
15. Bartlet, P.; Pascault, J. P.; Sautereau, H., Journal of Applied Polymer Science **30**, 2955 1985.

16. Manzione, L. T.; Gillham, J. K.; McPherson, C. A., Journal of Applied Polymer Science **26**, 907 1981.

Mr. Vivek V Kodgire (Research student)

Dr. M. V. Badiger (Research guide)

Publications

1. "Comparing and contrasting the properties of blends of urethane dispersion and acrylic emulsion with those of individual polymers" at "Polymer 2008", Chennai
2. "Thermal and mechanical properties of Epoxy resin: Influence of reactive liquid polymer (RLP) modification" at "PSE 2010", Chandigarh
3. "Development of Adhesive Formulation for Automotive Clutch Disc Applications," at "Material Science and Technology Showcase Event" (2012), NCL, Pune
4. "High Temperature Lap Shear Strength Study of Epoxy Resins Modified with Amine Terminated Butadiene Acrylonitrile Copolymer" Communicated to the journal for publication (2012)

करुणानिधे! प्रभो! नो दोषान् क्षमस्व भगवन।
सुचिरात् प्रसुप्तदेशं परिबोधयाशु भगवन्।।
भुवि भूतसर्वभाषा परिपूरिताभिलाषा।
श्वसितीव देवभाषा, तां पालयस्व भगवन्।।
आसीत् कदाचिदेषा, वाणी विशुद्धवेषा।
अधुना लवावशेषा, तामाश्रयस्व भगवन्।।
देशे स्वतंत्रतायाः प्राचीनसभ्यतायाः।
समयं समर्घतायाः पुनरानयस्व भगवन्।।
करुणानिधे प्रभो.....